

NOTICE OF FILING

Details of Filing

Document Lodged: Expert Report
Court of Filing: FEDERAL COURT OF AUSTRALIA (FCA)
Date of Lodgment: 19/12/2023 9:50:50 AM AWST
Date Accepted for Filing: 19/12/2023 9:50:54 AM AWST
File Number: WAD37/2022
File Title: YINDJIBARNDI NGURRA ABORIGINAL CORPORATION RNTBC ICN
8721 AND STATE OF WESTERN AUSTRALIA & ORS
Registry: WESTERN AUSTRALIA REGISTRY - FEDERAL COURT OF AUSTRALIA



Sia Lagos

Registrar

Important Information

This Notice has been inserted as the first page of the document which has been accepted for electronic filing. It is now taken to be part of that document for the purposes of the proceeding in the Court and contains important information for all parties to that proceeding. It must be included in the document served on each of those parties.

The date of the filing of the document is determined pursuant to the Court's Rules.



No. WAD37 of 2022

Federal Court of Australia
District Registry: Western Australia
Division: General

Yindjibarndi Ngurra Aboriginal Corporation RNTBC (ICN 8721)

Applicant

State of Western Australia and others

Respondents

APPLICANT'S EXPERT HYDROLOGIST'S REPORT

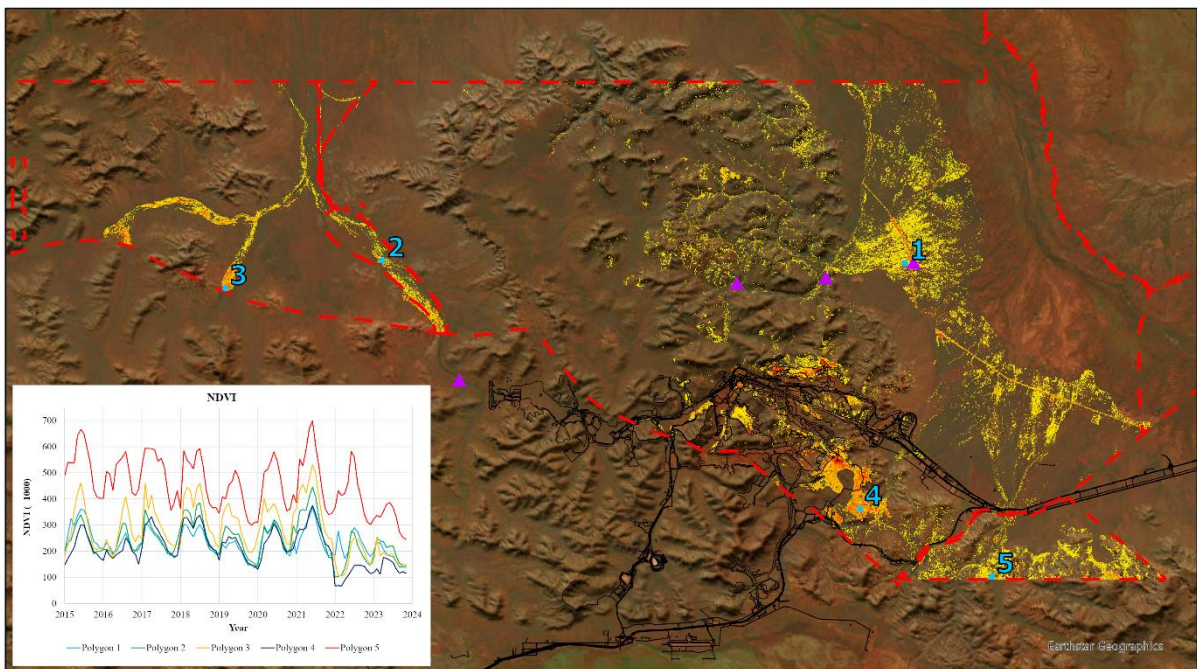
Filed on behalf of (name & role of party) The Applicant
Prepared by (name of person/lawyer) Simon Blackshield
Law firm (if applicable) Blackshield Lawyers
Tel (08) 9288 4515 / 0414257435 Tel (08) 9288 4515 / 0414257435
Email simon@blackshield.net
Address for service Level 28, AMP Tower, 140 St Georges Terrace PERTH WA 6000
(include state and postcode)

[Form approved 01/08/2011]

Assessment of Groundwater-Dependent Terrestrial Vegetation Surrounding the Solomon Mine

Dr Huade Guan

National Centre for Groundwater Research and Training, &
Ecology, Evolution and Environment, College of Science and Engineering
Flinders University, Australia



19th December 2023

Executive Summary

1 I, as a hydrologist by training, have expertise in mountain block hydrology and hydrogeology, remote sensing vegetation cover, terrestrial ecohydrology and hydrometeorology. I was requested by the Yindjibarndi Ngurra Aboriginal Corporation Applicant to provide an assessment of the impacts of the Solomon Hub iron ore mine project (SHP) on vegetation and water. I have undertaken remote sensing NDVI trend analysis over the Yindjibarndi Ngurra Compensation Application Area, particularly on the potential groundwater-dependent terrestrial vegetation, and reasoned on the connections between the observed vegetation degradation and the SHP, as well as the impacts of the SHP on groundwater and surface water.

2 I conclude that FMG' mining activities at the Solomon Hub have very likely caused vegetation degradation in the reach of both Kangeenarina Creek and Weelumurra Creek as follows:

- the degradation in Kangeenarina Creek has occurred mostly in the alluvial fan where the creek enters Lower Fortescue Valley, and in a few riparian sections within Hamersley Range. The degradation appears to have developed gradually since 2015; and
- the degradation in Weelumurra Creek has occurred in three valleys to the northwest of the SHP. The degradation appears to have become more serious since 2021 shortly after groundwater abstraction in Valley of the Queens increased.

3 I also conclude that the SHP area is a groundwater recharge zone. Groundwater abstraction in the SHP has very likely disturbed regional, intermediate, and local flow paths in the Hamersley Range as follows:

- the disturbance in the regional and intermediate flow paths very likely has reduced groundwater replenishment in the areas where degradation of groundwater-dependent terrestrial vegetation occurred in the reach of Kangeenarina Creek;
- the disturbance in Weelumurra Creek appears to be more serious on the local and intermediate flow paths, very likely resulting in a falling groundwater table in the three valleys of Weelumurra Creek to the northwest of the SHP; and
- it is difficult to assess any changes to the connectivity of surface flows due to a lack of surface water monitoring data. However, given that the creeks only flow episodically, surface water connections are maintained by shallow groundwater-



dependent pools (or waterholes). It is very likely that the SHP has changed connectivity of surface flows as well due to its impacts on shallow groundwater inferred from degraded terrestrial GDEs.

4 Lastly, I expect that groundwater levels have decreased at the locations where degradation of groundwater-dependent terrestrial vegetation has occurred. These changes are very likely to have resulted from dewatering in the SHP area.

5 In preparing this report I agree to be bound by the Federal Court Expert Evidence Practice note, which I have read, understood and endeavored to comply with in setting out my opinions and the evidence on which they are based. All opinions I have expressed in this report derive wholly or substantially from my specialized knowledge. I discuss my professional experience and relevant training immediately below and have attached a Curriculum Vitae at Appendix 1 setting out the basis for this specialized knowledge in more detail.

A handwritten signature in black ink, appearing to read "Huade Gu". The signature is written in a cursive, flowing style.

Table of Contents

| | |
|--|----|
| Executive Summary | 2 |
| 1. Introduction | 7 |
| 2. Hydrogeology and groundwater-dependent terrestrial vegetation in the SHP area | 11 |
| 3. Detecting changes of vegetation cover from satellite remote sensing..... | 13 |
| 4. NDVI degradation of selected vegetation quadrats | 16 |
| 5. Spatially distributed NDVI trends in and surrounding the SHP area | 20 |
| 6. Is this remotely sensed vegetation degradation related to the SHP? | 28 |
| 7. Conclusions | 29 |
| References..... | 31 |
| Appendices..... | 32 |

List of Figures

| | | |
|-----------|---|----|
| Figure 1 | The regional geographic context of the SHP area, showing that the SHP is located in the Hamersley Range which is bounded by the Lower Fortescue Valley to its north (copied from CSIRO 2015, Appendix 4a) | 10 |
| Figure 2 | The geographic locations of Valley of the Kings, Valley of the Queens, Trinity Valley, and Firetail Valley in the SHP area adopted from Golder Associates 2012). | 12 |
| Figure 3 | Distribution of groundwater table elevations before the start of mine operation, indicating two groundwater divides (adopted from Golder Associates 2012). | 12 |
| Figure 4 | Spectral reflectance of three objects (pinon, juniper, and soil) in a woodland in New Mexico, USA based on measurement using a portable hyperspectral radiometer, and calculated NDVI of three objects (Zhou et al. 2009). | 14 |
| Figure 5 | Monthly NDVI (x 1000) time series of a randomly selected pixel (longitude: 117.8683593 °, latitude -22.1230784 °) in a mine pit of the SHP, showing that the vegetation cover was removed in 2012. | 15 |
| Figure 6 | Monthly Landsat (blue) and Sentinel-2 (orange) NDVI (x1000) time series for a selected <i>M. argentea</i> occurrence quadrat (#220 in Ecologia 2014, longitude: 117.8660053°, latitude: -22.1181386°) in the SHP area, showing an abrupt degradation of vegetation cover during 2019, followed by a rapid recovery of greenness in 2021 . Here the orange data points from 2015 to 2018 are adjusted Landsat NDVI towards Sentinel-2 NDVI, as shown in Figure 7. | 16 |
| Figure 7 | Distribution of selected vegetation quadrats of Ecologia (2014) which have <i>M. argentea</i> , <i>E. camaldulensis</i> , and/or <i>E. Victrix</i> , in relation to moderate terrestrial GDE coverage, the Compensation Application Area, and the terrain modification due to mine operation of the SHP. | 17 |
| Figure 8 | Interannual variation of annual precipitation surrounding the SHP area, based on four Bureau of Meteorology weather stations (5001: Coolawanyah, 34.5 km away from the study area, 5014: Mount Florance, 35.9 away, 5005: Hamersley, 28.7 km away, and 5026: Wittenoom, 48.5 km away). | 17 |
| Figure 9 | Monthly Landsat (blue) and Sentinel-2 (orange) NDVI (x1000) time series for a selected <i>M. argentea</i> occurrence quadrat (#26) in the SHP area, showing slightly different NDVI values for the common period (shaded in yellow) two sources, and the high correlation between the two NDVI sources shown in the right. This correlated relationship is then used to adjusted two NDVI products toward each other. The grey dots and lines show adjusted Landsat NDVI to match Sentinel-2 NDVI for that period. | 18 |
| Figure 10 | Monthly NDVI time series harmonized from Landsat and Sentinel-2 datasets for vegetation quadrat # 127, showing a decreasing trend from 2015 through to 2023. | 20 |
| Figure 11 | Spatially distributed NDVI trends (0.001*NDVI/yr) for the five-year period of 12/2018 - 11/2023, positive values (green) indicating vegetation improvement, and negative values | |

| | |
|--|----|
| (red) indicating vegetation degradation. The Compensation Application Area and potential GDE coverage are shown on the map. | 21 |
| Figure 12 Annual precipitation time series of (a) Yalleen, WA (BOM ID 5029, 21.68 °S, 116.39 °E), (b) Newman Aero, WA (BOM ID 7176, 23.42 °S, 119.80 °E). zoom-in view of Figure 15 to Zalamea gorge. | 21 |
| Figure 13 A zoomed-in view of Figure 11 to Kangeenarina Creek. | 22 |
| Figure 14 A zoomed-in view of Figure 11 to Weelumurra Creek. | 22 |
| Figure 15 A zoomed-in view of Figure 11 to Zalamea gorge. | 23 |
| Figure 16 Spatially distributed NDVI decreasing trends ($0.001 * NDVI/yr$) for the five-year period of 12/2018 - 11/2023 for the common area of the Native Title and the moderate potential GDEs, with an inset showing monthly NDVI time series for five one-hectare polygons. | 25 |
| Figure 17 A zoomed-in view of Figure 16 to Kangeenarina Creek. | 25 |
| Figure 18 A zoomed-in view of Figure 16 to Weelumurra Creek. | 26 |
| Figure 19 A zoomed-in view of Figure 16 to Zalamea gorge. | 26 |
| Figure 20 A conceptual diagram showing different groundwater flow paths along a transect from the mountain range to the basin floor (copied from Bertrand et al. 2011). | 27 |
| Figure 21 (a) Annual groundwater abstraction from the SHP (calculated from Fortescue 2014, 2017, 2020, and 2023), and (b) Daily groundwater abstraction and injection from the zone of Valley of Queens (adopted from Fortescue 2022). | 27 |

1. Introduction

6 This report has been requested by the Yindjibarndi Ngurra Aboriginal Corporation (YNAC) Applicant as per to the Brief dated on 13th October 2023 which is attached to this report as Appendix 2. I was asked to provide an assessment on the impacts of the Solomon Hub iron ore mine project (SHP) by reviewing the materials provided to me together with the Brief and conducting further research, on the following aspects:

- (a) changes to vegetation richness, extent and any other markers of ecological health caused by the mining activities in the SHP to groundwater-dependent terrestrial vegetation through analysis of remote sensing data;
- (b) changes to connectivity of surface flows, particularly at Kangeenarina and Weelumurra Creeks, and groundwater flows;
- (c) any observed or predicted impacts to groundwater levels as a result of dewatering, including after mine closure, and associated long-term ecological impacts related to changes in the water table, through a literature review of reports provided by FMG; and
- (d) any other hydrogeological or ecological impacts, at or surrounding the SHP.

7 I accepted the brief from YNAC as it relates to my expertise area. I obtained my PhD degree from New Mexico Institute of Mining and Technology in 2005, with a dissertation entitled “Water above Mountain Front – Assessing Mountain-Block Recharge in Semiarid Regions”. My postdoctoral research at the University of Texas at San Antonio was on remote sensing terrestrial vegetation cover. I am now an Associate Professor at Flinders University, South Australia, with nearly 20 years of research experience in ecohydrology and hydrometeorology. I published over 120 peer-reviewed articles with an h-index of 34 in Scopus (39 in Google Scholar). My research in groundwater recharge mainly focuses on mount-block recharge using environmental tracers. My ecohydrological research covers from field-based investigation of vegetation water use and water stress, numerical modelling of plant transpiration and drought responses, and to remote sensing analysis of large-scale interactions of climate, vegetation and soil moisture. I have served as an Associate Editor for Journal of Hydrology since 2015, and for Frontiers in Climate (Climate, Ecology and People) since 2021. At Flinders University, I have taught two topics – *Ecohydrology* and *Catchment Hydrology* since 2015. A copy of my resume is included at Appendix 1 of this Report.

8 For this project, I started reviewing the literature from 24th September 2023. In order to address the above questions specified in the brief, I realized new investigation in addition to reviewing the reports provided were required. A list of the materials I have been briefed with forms Appendix 3. Additional materials I have considered are also listed at Appendix 4. Given the short time frame, I decided to prioritise my time in reviewing most relevant materials and in undertaking remote sensing analysis as there has not been sufficient time to conduct field investigation. As a result, my literature review were focusing on reading the reports (or part of the reports) based on observations .

9 Most of the reports provided by FMG are about the conditions within the SHP area or in its close proximity. They do not provide sufficient information to assess the potential impacts of the SHP via groundwater flow paths in the mountain range (explained later in this report). A few reports provided cover a bigger area, however, they do not provide continuous monitoring data over the years. Here I adopt a satellite remote sensing-based approach to reveal temporal and spatial patterns. From my specialised experience, this is more likely to see the connections (if there are any) between the SHP and the environment.

10 Remote sensing investigation requires a large amount of data handling, visualisation, analysis, and graphing. Two PhD students under my supervision from Flinders University and one undergraduate student from Australia National University (ANU) have provided me with assistance. They are Wenjie Liu, Zhongli Liu, and Hansen Guan. CVs for each of these persons are included at Annexure 1. Wenjie has been using Google Earth Engine in his PhD research, with one peer-reviewed article recently published partly based on this method (Liu et al. 2023). Wenjie Liu assisted Hansen Guan to use Google Earth Engine. Zhongli Liu has used the groundwater-dependent ecosystems (GDEs) atlas (Data source: Bureau of Meteorology, retrieved October 2023) for his PhD research. The assistance these persons have provided me is as follows. Zhongli Liu cropped the GDEs maps for the project area which I have prepared and included in this Report. Hansen Guan is a third-year Earth Science student from ANU. Under my supervision, Hansen Guan downloaded remote sensing data via Google Earth Engine, conducted data analysis in Google Earth Engine, using Python and EXCEL, and produced maps using ArcGIS Pro.

11 The SHP is operated by the Fortescue Metals Group Limited (FMG). The SHP is located within the Hamersley Ranges, with the Lower Fortescue Valley to its north (Figure 1). The mine has been in production since late 2012 (Fortescue, 2014). From 2011 to 2022, about 23 million square meters of the land has seen an increase in topography and a similar area of surface has seen a decrease in topography due to mining. This was based on the analysis of LiDAR data provided with my brief. Groundwater is extracted for mining progression, dust suppression, ore processing, construction and

camp supply. It is estimated that about 160 GL groundwater has been extracted from 2011 to 2022, based on the data provided in FMG's triennial review reports (Fortescue 2014, 2017, 2020, 2023).

12 According to my brief, the Yindjibarndi People, the traditional owners of the SHP site and its surrounding areas, noticed diminished water flows, loss of vegetation and fewer fauna for hunting in recent years. My brief provides that the reported environmental degradation in Kangeenarina Creek and Weelumurra Creek, flowing from or surrounding the SHP site, is of particular concern for the Yindjibarndi People.

13 My brief requires me to consider whether or not this apparent environmental degradation is physically related to the SHP operations. In the area of the SHP and its surrounding, the climate is dry. The rainfall deficit (defined as pan evaporation - rainfall) exceeds 2300 mm/year (CSIRO, 2015, provided at Appendix 4a). Flora and fauna are highly dependent on water availability in the environment. This can be seen from the fact that trees often distribute along the drainage lines where water accumulates from the landscapes during rainfall events. Based on my specialised knowledge in ecohydrology as a hydrologist, I know that in areas where groundwater is shallow, ecosystems may develop fully or partly based on groundwater, which are called groundwater-dependent ecosystems. If the SHP has changed the level of water supply in the environment, it is most likely to impact groundwater storage and consequently groundwater-dependent ecosystems.

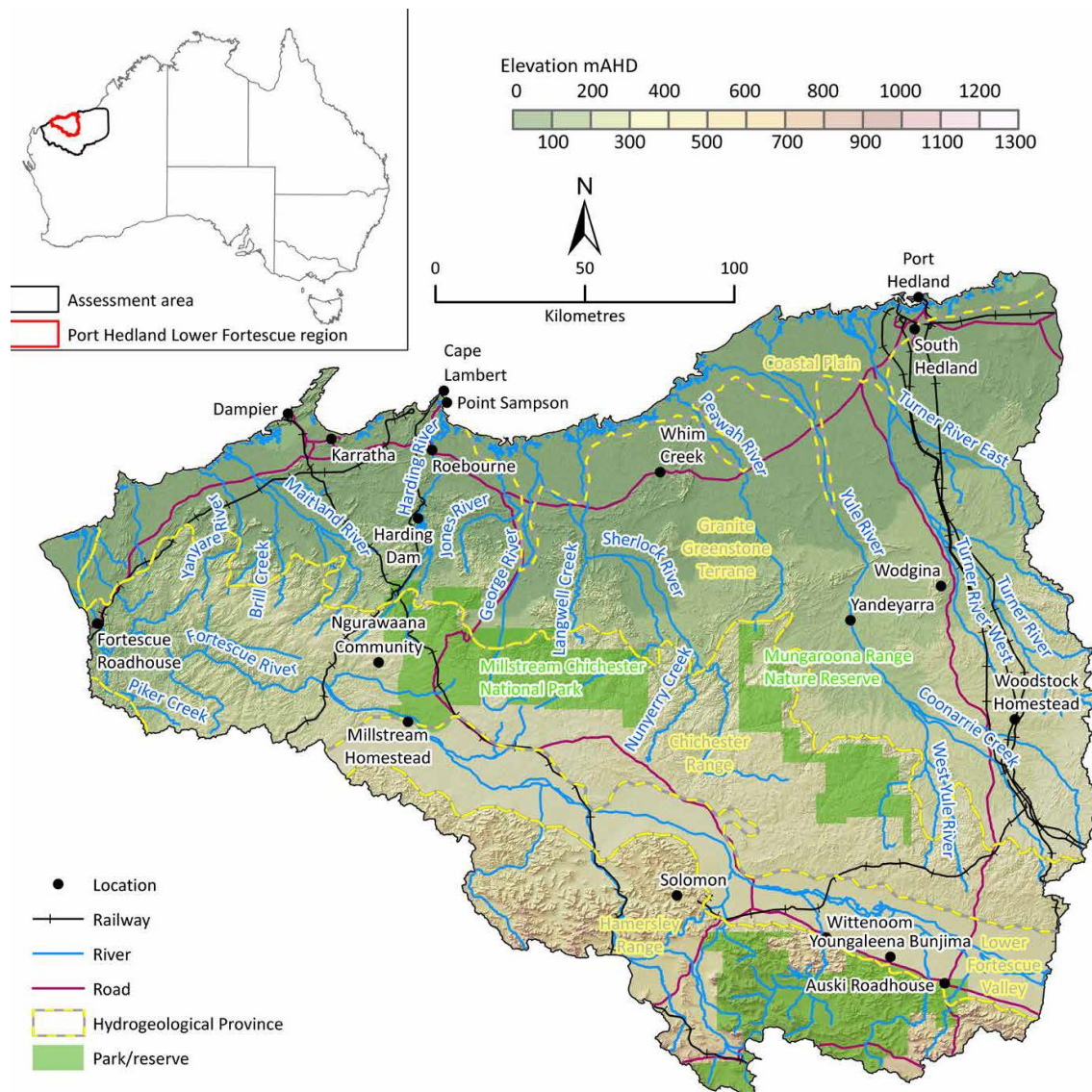


Figure 1 The regional geographic context of the SHP area, showing that the SHP is located in the Hamersley Range which is bounded by the Lower Fortescue Valley to its north (copied from CSIRO 2015, Appendix 4a)

14 Groundwater-dependent ecosystems (GDEs) are categorized into spring GDEs, aquatic GDEs, terrestrial GDEs, and subterranean GDEs. Among them, terrestrial GDEs (primarily the vegetation components) often have a coverage large enough to be observable from satellites (Doody et al. 2017, Brim Box et al. 2022, Fildes et al. 2023). Terrestrial GDEs conserve biodiversity by providing habitats for animals, regulate microclimate, provide aesthetic pleasantness, and house cultural and spiritual resources particularly for the First Nations people (Murray et al. 2006).

15 As part of my brief, I have investigated whether the terrestrial GDEs have experienced degradation in the Yindjibarndi Ngurra Compensation Application Area (the Compensation Application Area) surrounding the SHP, and determine if the degradation is linked to the SHP operation.

2. Hydrogeology and groundwater-dependent terrestrial vegetation in the SHP area

16 The hydrogeological system of the SHP area is defined as the Hamersley Province in CSIRO (2015). In this area, groundwater of high yield occurs in shallow paleochannels and deep karstified dolomites in the Wittenoom Formation. Groundwater recharge primarily occurs through streambeds following heavy rainfall (daily rainfall exceeding 38 mm). Diffuse recharge may occur to localized fractured rock aquifers when daily rainfall exceeds 20 mm (CSIRO, 2015).

17 The Wittenoom karstified dolomites extend regionally into the Lower Fortescue Valley, overlain by the paleochannel aquifers. The paleochannels here are wider and deeper than those in the Hamersley Range. The aquifers in the Lower Fortescue Valley receive recharge from the river and the valley aquifers in the Hamersley Range (CSIRO 2015). Thus, any change in the river discharge and Hamersley valley aquifers can impact groundwater balance in the Lower Fortescue Valley.

18 The SHP mines iron ore in Valley of the Kings, Firetail Valley, Trinity Valley, and Valley of the Queens (Fortescue 2012). Three Fortescue tributaries flow through or surrounding the project area. They are Kangeenarina Creek, Weelumurra Creek, and Zalamea Gorge (Figure 2). Kangeenarina Creek flows from south to north through Valley of the Kings and Trinity Valley. Weelumurra Creek flows towards the northwest; and drains water from Valley of the Queens in the western part of the SHP. Zalamea Gorge flows northeast in the east of the SHP area, and drains part of the Firetail Valley. The creeks only flow following heavy rainfall. Most of time, they are filled with waterholes which are supported by groundwater (CSIRO 2015, AQ2 2019).

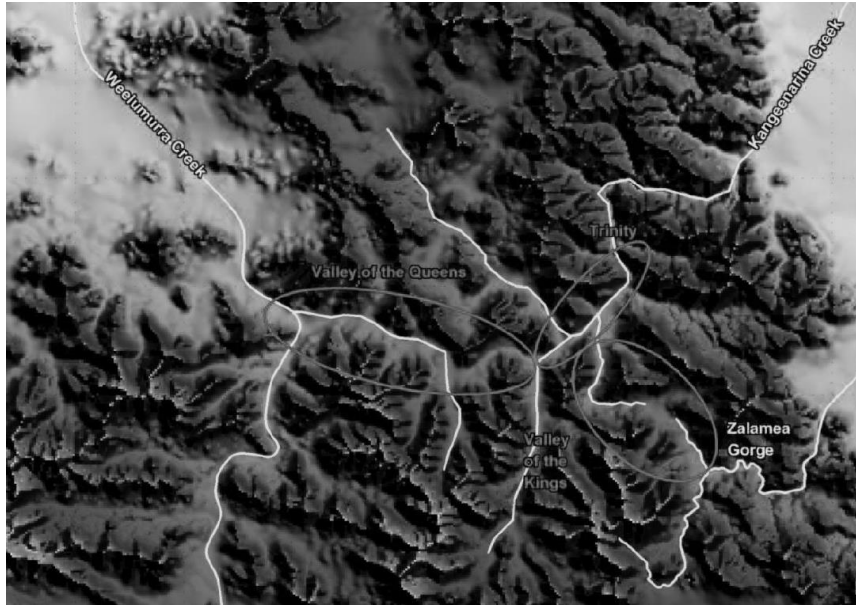


Figure 2 The geographic locations of Valley of the Kings, Valley of the Queens, Trinity Valley, and Firetail Valley in the SHP area (adopted from Golder Associates 2012).

19 Based on groundwater table depth observation before ore production, two ‘soft’ groundwater divides were inferred in the SHP area (Golder Associates 2012). One occurred between Valley of the Kings and Valley of the Queens, the other occurred near the top of the Valley of Kings (Figure 3). This situation suggests that the SHP area happens to be groundwater recharge zones. Groundwater recharged in different zones across the divides in mountain ranges (e.g., Hamersley Range in this case) very often has different flow paths to replenish the aquifers in the basin floor (e.g., Lower Fortescue Valley here) (Wilson and Guan 2004 provided at Appendix 4b).

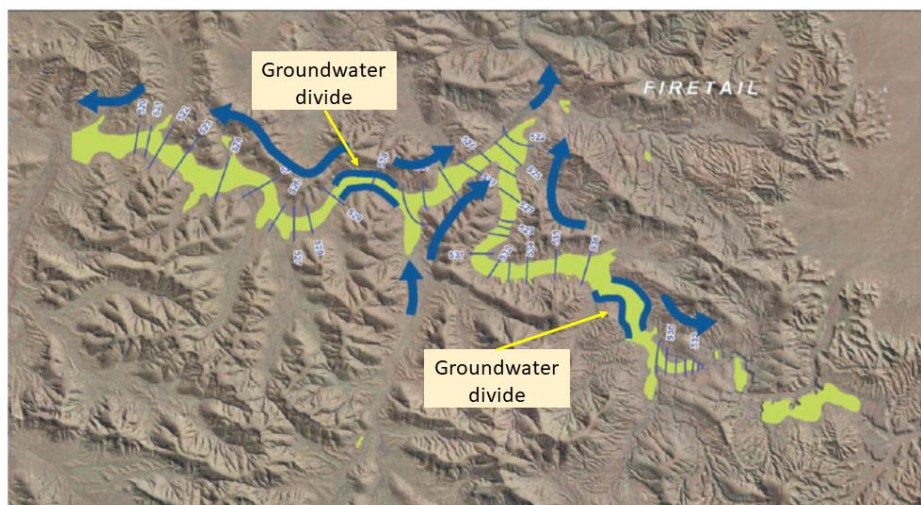


Figure 3 Distribution of groundwater table elevations before the start of mine operation, indicating two groundwater divides (adopted from Golder Associates 2012).

20 Groundwater in the riparian zone is shallow; and varies in a range of 0.8-1.8 m in Kangeenarina Creek based on five observation bores from 2009-2018, 1.7-4.6 m in Zalamea Gorge based on three bores, and 4.3-6.1 m in Weelumurra Creek based on three bores. In some sections, groundwater is exposed to the surface forming waterholes (AQ2 2019).

21 Vegetation surveys are often conducted over individual small squared (or rectangle) areas of land surface. Each of the areas is called a quadrat. Over 281 quadrats (mostly 50 m x 50 m) were surveyed in 2014 by several botanists documented in Ecologia (2014). The surveys identified several vegetation units in and surrounding the SHP area which are either groundwater-dependent or of potential groundwater dependence (Ecologia 2014). Typical GDE species in the area include *Melaleuca argentea* and *Eucalyptus camadulensis*. *Eucalyptus victrix* is common in the vegetation units of potential groundwater dependence. The quadrats with these species are chosen in this study to examine whether terrestrial GDE has experienced degradation in recent years. These quadrats are later shown in Figure 7.

3. Detecting changes of vegetation cover from satellite remote sensing

22 Just as our eyes can see objects in our field of view, the sensors onboard satellites can see objects on the Earth's surface under the flight path of the satellites. Based on my knowledge of optical remote sensing which I gained from my PhD study, I know that human beings see objects primarily based on the colour and brightness of light received by his/her eyes. The remote sensors on a satellite function similarly, except that they may see light which is invisible to our eyes, for example, the near infrared light.

23 I am aware from my knowledge of optical remote sensing that the human eye tells vegetation apart from other objects in the environment primarily based on its colour because most vegetation reflects more green light than red and blue light. Vegetation also reflects a lot more near infrared light than any visible light (Figure 4). The human eye would be able to see vegetation a lot better if eyes were able to sense near infrared light. There is no such limitation for remote sensors because they can be designed to sense both visible and near infrared light. Thus, with remote sensing, we can utilise the vegetation's characteristic high reflectance in the near infrared band and low reflectance in the red band by combining them in a spectral index.

24 I am aware from my study, training and experience as a hydrologist that the Normalized Difference Vegetation Index (NDVI) is the most commonly used index for investigating vegetation

distribution and change on the Earth’s surface. In the woodland shown in Figure 4, trees have an NDVI of 0.7-0.8 while the soil NDVI is only 0.14. Thus, NDVI allows us to differentiate vegetation from other properties on the land surface, and detect change of vegetation cover at individual locations.

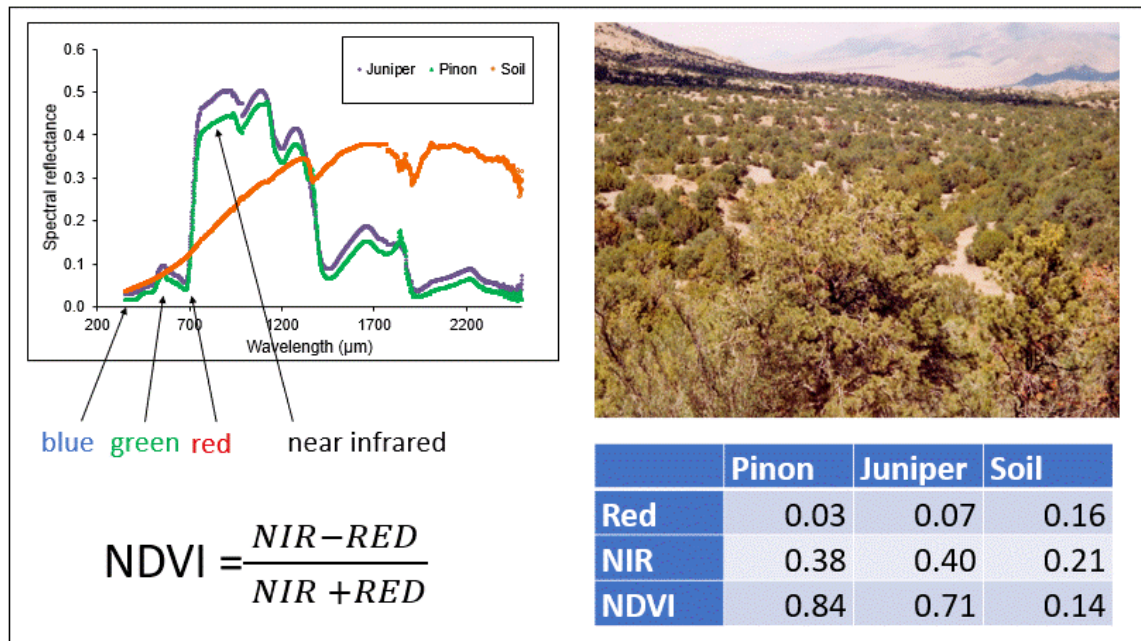


Figure 4 Spectral reflectance of three objects (pinon, juniper, and soil) in a woodland in New Mexico, USA based on measurement using a portable hyperspectral radiometer, and calculated NDVI of three objects (Zhou et al. 2009).

25 Another difference between how the human eye observes surroundings and how satellites remotely sense land surfaces is the spatial resolution. We can see individual trees, or even individual leaves if we are close enough. Due to the long distance, most sensors onboard satellites cannot resolve individual trees. What they “see” are individual pixels of which everything within each pixel is combined. A pixel of the surface shown in Figure 4 would have an NDVI value between those of individual trees and the soil. A pixel of more tree cover would have a larger NDVI than a pixel of less tree cover. If the vegetation cover condition of a pixel has changed, the change can be detected by comparing the pixel NDVI values obtained at different times.

26 In addressing this brief, I have used two types of satellite remote sensing NDVI products – Landsat and Sentinel-2. Landsat data were obtained from a series of Earth-observation satellite missions jointly managed by NASA and U.S. Geological Survey, dated back to 1972. Sentinel-2 mission is managed by the European Space Agency. Both Landsat and Sentinel-2 missions provide red band and near infrared band reflectance data, from which NDVI can be calculated. I obtained Landsat and Sentinel-2 NDVI data from Google Earth Engine, with assistance from Hansen Guan. The Landsat

NDVI pixel has a size of 30 m x 30 m. The Sentinel-2 NDVI pixel has a size of 10 m x 10 m, which has been available since 2018.

27 The NDVI of a pixel reflects its vegetation cover condition. If, for example, the vegetation of a woodland is disturbed by wildfire, the NDVI of individual pixels in the burnt area would decrease abruptly. Recently, a team I worked with demonstrated that Landsat NDVI is even better than a commonly used burn index for mapping burnt areas of historical bushfires for national conservation parks in Eyre Peninsula of South Australia (Liu et al. 2023).

28 Figures 4 and 5 are two examples of monthly NDVI time series for two pixels in the SHP area. The NDVI values shown on the graphs are 1000 times of real NDVI data, inherited from what is stored in Google Earth Engine to avoid decimal numbers so as to save storage space. Thus a value of 300 on the graphs which Hansen Guan has prepared below represents an NDVI value of 0.3. Figure 5 clearly shows that NDVI is very sensitive to mining related vegetation clearance. Figure 6 shows an abrupt decrease and recovery of NDVI within two years. This is most likely due to a bushfire in the area.

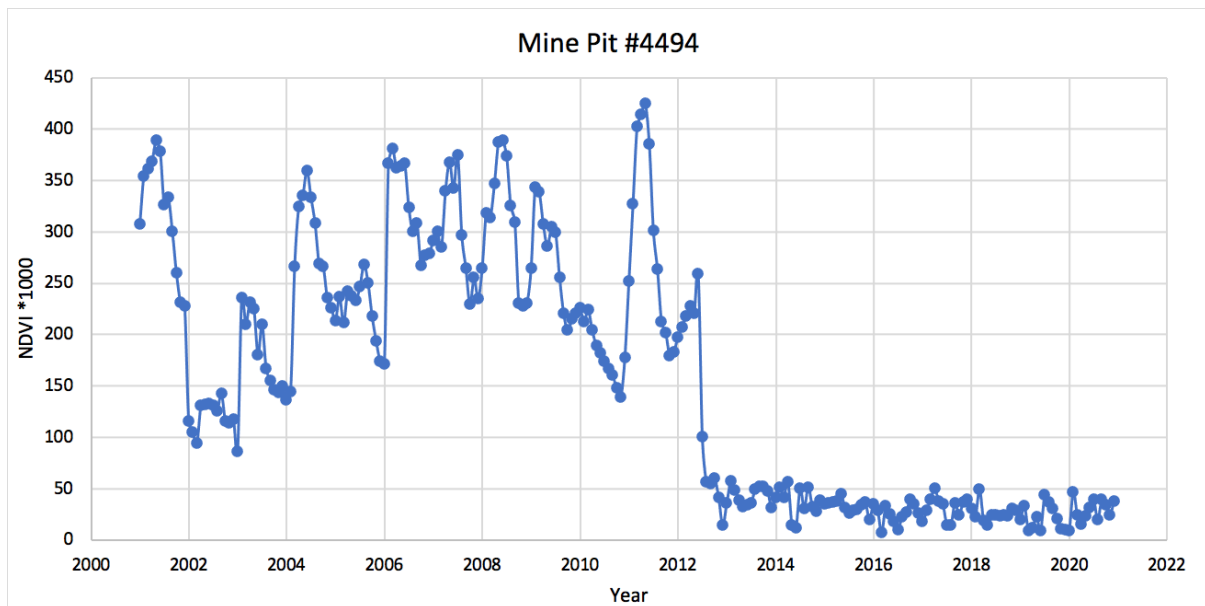


Figure 5 Monthly NDVI (x 1000) time series of a randomly selected pixel (longitude: 117.8683593°, latitude -22.1230784°) in a mine pit of the SHP, showing that the vegetation cover was removed in 2012.

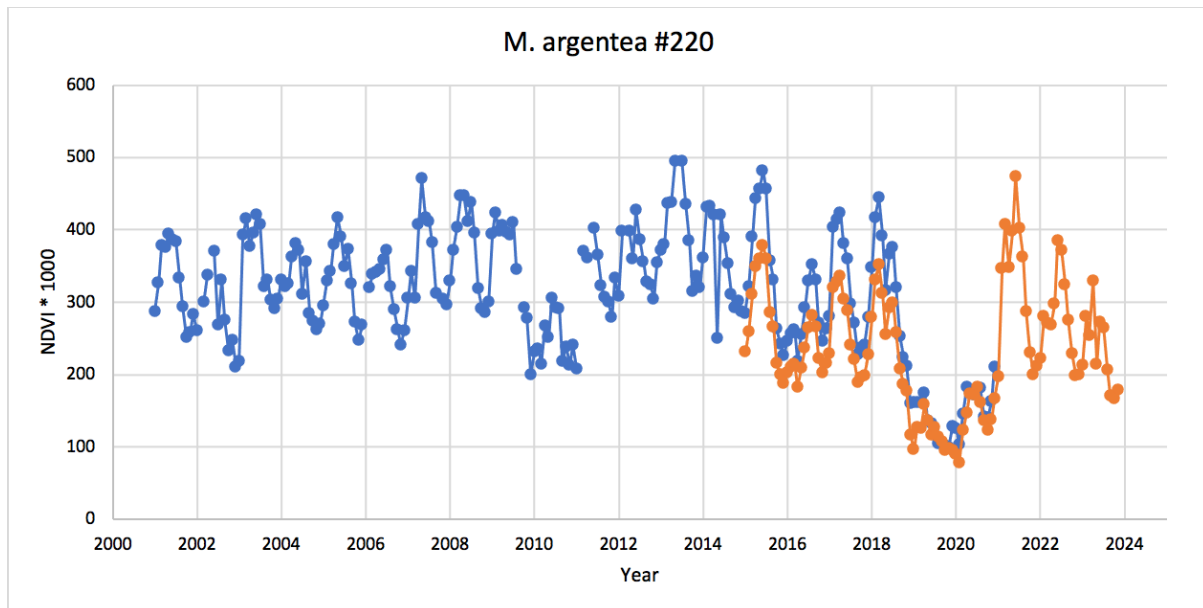


Figure 6 Monthly Landsat (blue) and Sentinel-2 (orange) NDVI ($\times 1000$) time series for a selected *M. argentea* occurrence quadrat (#220 in Ecologia 2014, longitude: 117.8660053°, latitude: -22.1181386°) in the SHP area, showing an abrupt degradation of vegetation cover during 2019, followed by a rapid recovery of greenness in 2021. Here the orange data points from 2015 to 2018 are adjusted Landsat NDVI data towards Sentinel-2 NDVI, as shown in Figure 7.

4. NDVI degradation of selected vegetation quadrats

29 As part of my brief, I chose the vegetation quadrats of GDEs or of potential groundwater dependency to examine any NDVI degradation in recent years. Hansen Guan assisted me to map the locations of these quadrats, including all vegetation quadrats with *M. argentea* or *E. camaldulensis* occurrence, and nearly all quadrats with *E. victrix* occurrence. They are shown in Figure 7, including six quadrats with both *M. argentea* and *E. camaldulensis*, seven with *E. camaldulensis*, and 27 with *E. victrix* occurrence. The quadrat IDs cited here follow those in Ecologia (2014). Almost all of these vegetation quadrats are distributed in the area of moderate potential terrestrial GDEs or in the riparian zone of the Lower Fortescue River.

30 Unlike bushfires or mine vegetation clearance which can cause abrupt changes of pixel NDVI, changes of vegetation cover due to soil moisture and/or groundwater depletion are generally gradual. Here linear regression of NDVI versus time is adopted to identify any gradual changes of vegetation cover in and surrounding the SHP area. Interannual variation of precipitation sometimes may lead to NDVI trends for a couple of years, which generally would not continue for several years. Annual rainfall time series of four nearby weather stations of long data records are shown in Figure 8. No extreme wet conditions have occurred since 2011, which in my view, based on my training and experience as a hydrologist, provides reasonable climatic context to examine potential problems of terrestrial groundwater-dependent vegetation. Here the period from January 2015 to November

2023 was chosen to evaluate the NDVI trends, to avoid potential effects of relative wet conditions in 2013 as shown in Figure 8.

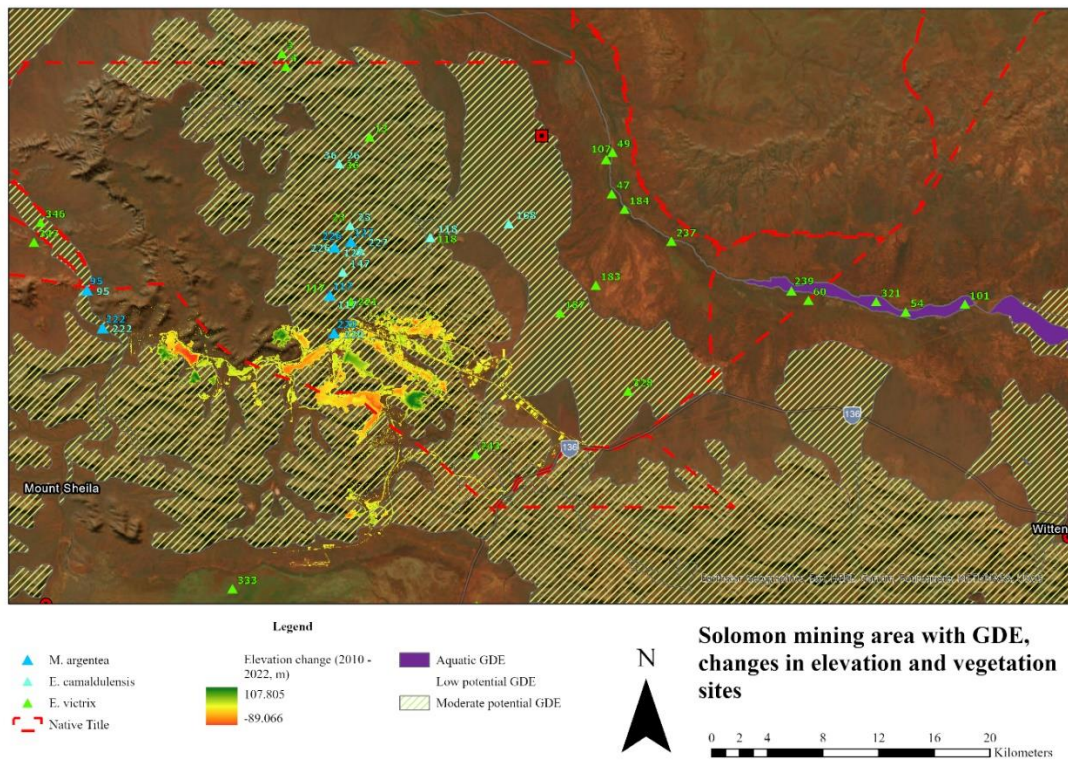


Figure 7 Distribution of selected vegetation quadrats of Ecologia (2014) which have *M. argentea*, *E. camaldulensis*, and/or *E. Victrix*, in relation to moderate terrestrial GDE coverage, the Compensation Application Area, and the terrain modification due to mine operation of the SHP.

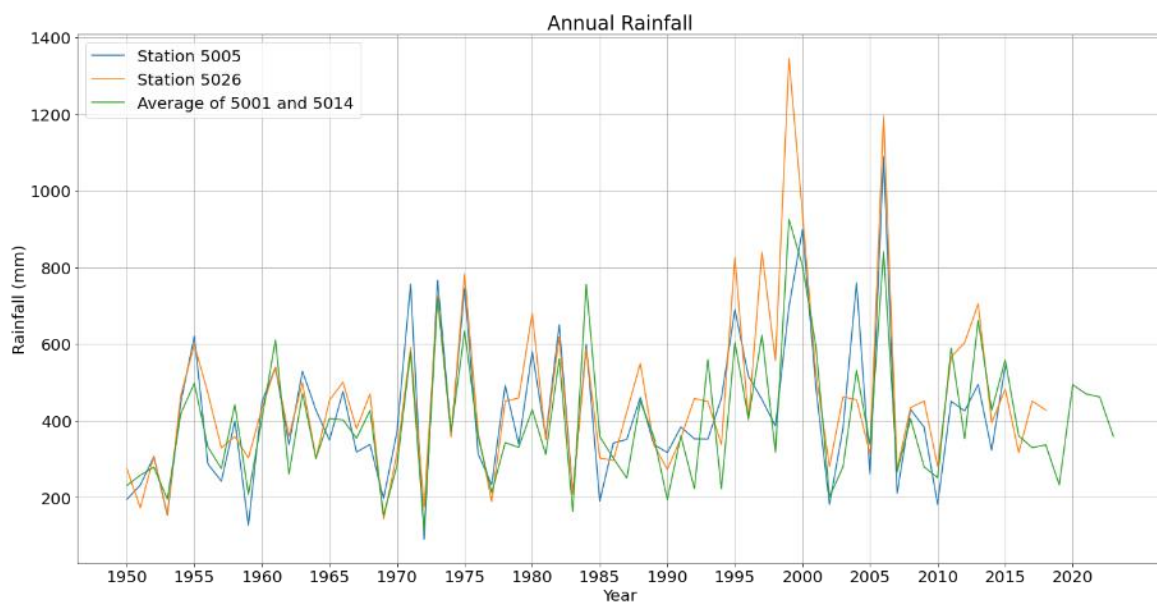


Figure 8 Interannual variation of annual precipitation surrounding the SHP area, based on four Bureau of Meteorology weather stations (5001: Coolawayah, 34.5 km away from the study area, 5014: Mount Florance, 35.9 away, 5005: Hamersley, 28.7 km away, and 5026: Wittenoom, 48.5 km away).

31 In the current Google Earth Engine, Landsat NDVI time series covers the period up to 2021 with most recent data missing, and Sentinel-2 data starts only from 2018. I, with assistance from Hansen Guan, connected the two datasets in order to have continuous NDVI dataset for trend analysis. The two satellite missions do not capture information from the same surface area (a Landsat pixel is nine times that of a Sentinel-2 pixel). They do not take images on the same days either. I note that the NDVI values from the two sources are not exactly the same (Figure 9 left panel: blue vs. orange in the yellow shaded period). This could cause a problem if the NDVI trend is examined for a period with NDVI coming from two sources, for example from 2015 to 2023.

32 Here I have joined the two NDVI sources by a commonly used data-harmonisation method in my area of expertise. This harmonisation method is as follows. Hansen Guan and I first found the relationship between Landsat and Sentinel-2 NDVI (Figure 9 right panel), which is then applied to adjust Landsat NDVI to match Sentinel-2 NDVI (Figure 9 left panel: grey dots). After this adjustment, the NDVI trend (if any) between 2015 and 2023 can be reliably examined and accurately estimated.

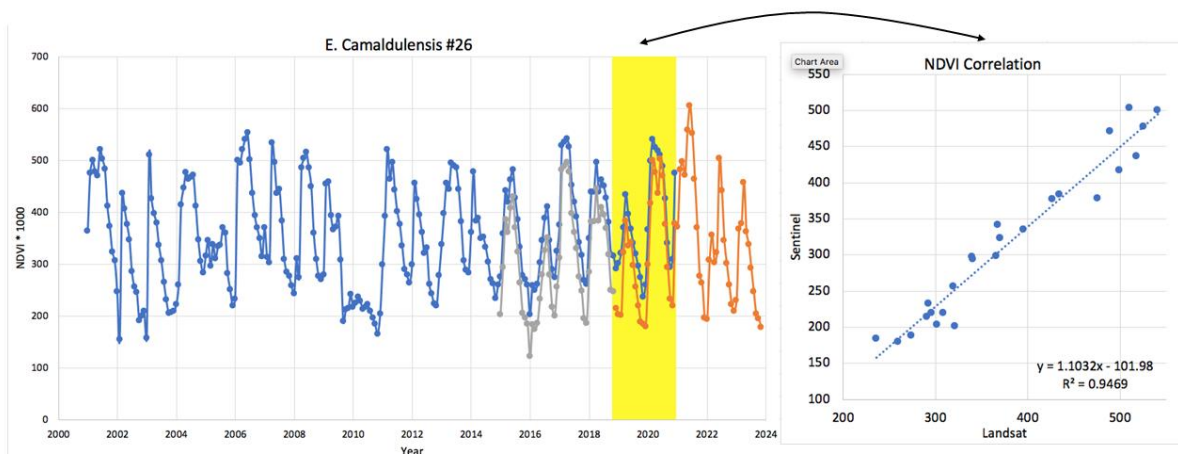


Figure 9 Monthly Landsat (blue) and Sentinel-2 (orange) NDVI (x1000) time series for a selected *M. argentea* occurrence quadrat (#26) in the SHP area, showing slightly different NDVI values for the common period (shaded in yellow) two sources, and the high correlation between the two NDVI sources shown in the right. This correlated relationship is then used to adjusted two NDVI products toward each other. The grey dots and lines show adjusted Landsat NDVI to match Sentinel-2 NDVI for that period.

33 Of six quadrats with both *M. argentea* and *E. camaldulensis* occurrence, two of them (#127, #222) show statistically significant negative NDVI trends during 2015-2023. Of seven quadrats with *E. camaldulensis* occurrence, two (#118, #168) appear to have significant negative NDVI trends. Due to time limitation, not all 27 quadrats with *E. victrix* have been examined for NDVI changes. Nine quadrats within the mapped area of the moderate potential GDEs were selected. Of them, three show significant NDVI trends, including two negative trends (#243, #347), and one positive trend

(#221). Details of these NDVI trends are summarized in Table 1. In the table, a negative trend coefficient means a decreasing NDVI trend, and a p value smaller than 0.05 indicates that the trend is statistically significant. An example of the trend on #127 is shown in Figure 10, which has a p value of 0.000002.

34 These results suggest that the terrestrial GDEs appear to have degraded during the period from 2015 to 2023 at some locations surrounding the SHP area. They are related to Kangeenarina Creek, Weelumurra Creek, and Zalamea Gorge. Vegetation at one location (quadrat #221) in Kangeenarina Creek appears to have improved. The fact that not all vegetation quadrats investigated here show decreasing NDVI trends suggest that the decreasing NDVI trends observed at some locations were not caused by the climate.

Table 1 Summary of NDVI trends in 2015-2023 and their statistics of the NDVI pixels co-located with seven vegetation quadrats in Ecologia (2014)

| Quadrats ID | GDE species | Related creeks | Trend coefficient 0.001 NDVI /year | Statistical significance p values |
|-------------|--------------------------------------|----------------|---------------------------------------|---|
| 127 | <i>M. argentea, E. camaldulensis</i> | Kangeenarina | -13.8 | 0.000002 |
| 222 | <i>M. argentea, E. camaldulensis</i> | Weelumurra | -8.3 | 0.006 |
| 118 | <i>E. camaldulensis</i> | Kangeenarina | -6.8 | 0.0004 |
| 168 | <i>E. camaldulensis</i> | Kangeenarina | -10.3 | 0.0002 |
| 243 | <i>E. victrix</i> | Zalamea | -17.2 | 0.000004 |
| 347 | <i>E. victrix</i> | Weelumurra | -26.3 | 0 |
| 221 | <i>E. victrix</i> | Kangeenarina | 9.3 | 0.005 |

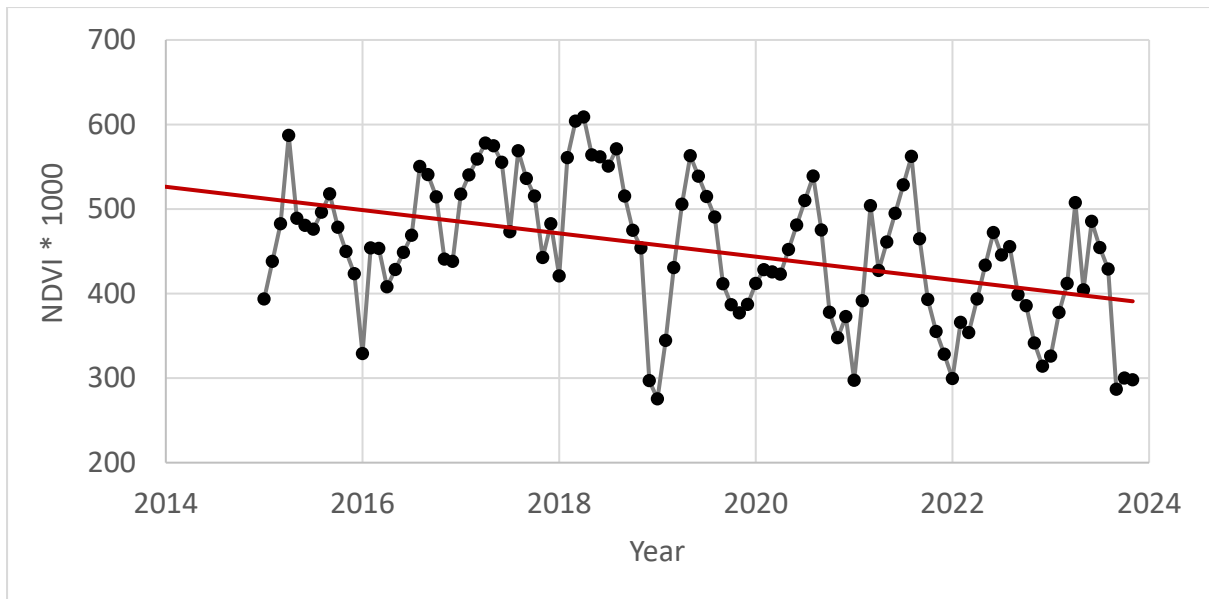


Figure 10 Monthly NDVI time series harmonized from Landsat and Sentinel-2 datasets for vegetation quadrat # 127, showing a decreasing trend from 2015 through to 2023.

5. Spatially distributed NDVI trends in and surrounding the SHP area

35 The investigation presented in Section 4 is constrained to the selected vegetation quadrats. It does not provide the whole picture of NDVI decreasing or increasing trends in the area. Here I examined the NDVI trends in and surrounding the SHP area based on Sentinel-2 data (12/2018-11/2023).

36 The results of Sentinel-2 NDVI trends are shown in Figure 11. A large proportion of the region shows improving vegetation cover (shown as green areas on the map) particularly near and to the north of the SHP area. It is noted that some green areas on the map, for example, the northeast and northwest parts of the map, are not marked as moderate potential terrestrial GDEs. This suggests that vegetation improvement in those areas is most likely due to an increase in precipitation in the past five years (Figure 12).

37 The zoomed-in map of Kangeenarina Creek (Figure 13) shows that vegetation degradation tends to occur in the alluvial fan and some sections of the Kangeenarina valley. Having said that, there is a section about 1 km long immediately downstream of the SHP area showing improved vegetation conditions on Kangeenarina Creek. The zoomed-in map of Weelumurra Creek (Figure 14) shows that vegetation degradation has occurred more seriously in the valleys and the hilly areas between the

valleys, which are not far from the SHP. Vegetation degradation in the Zalamea catchment primarily occurs within the SHP area (Figure 15).

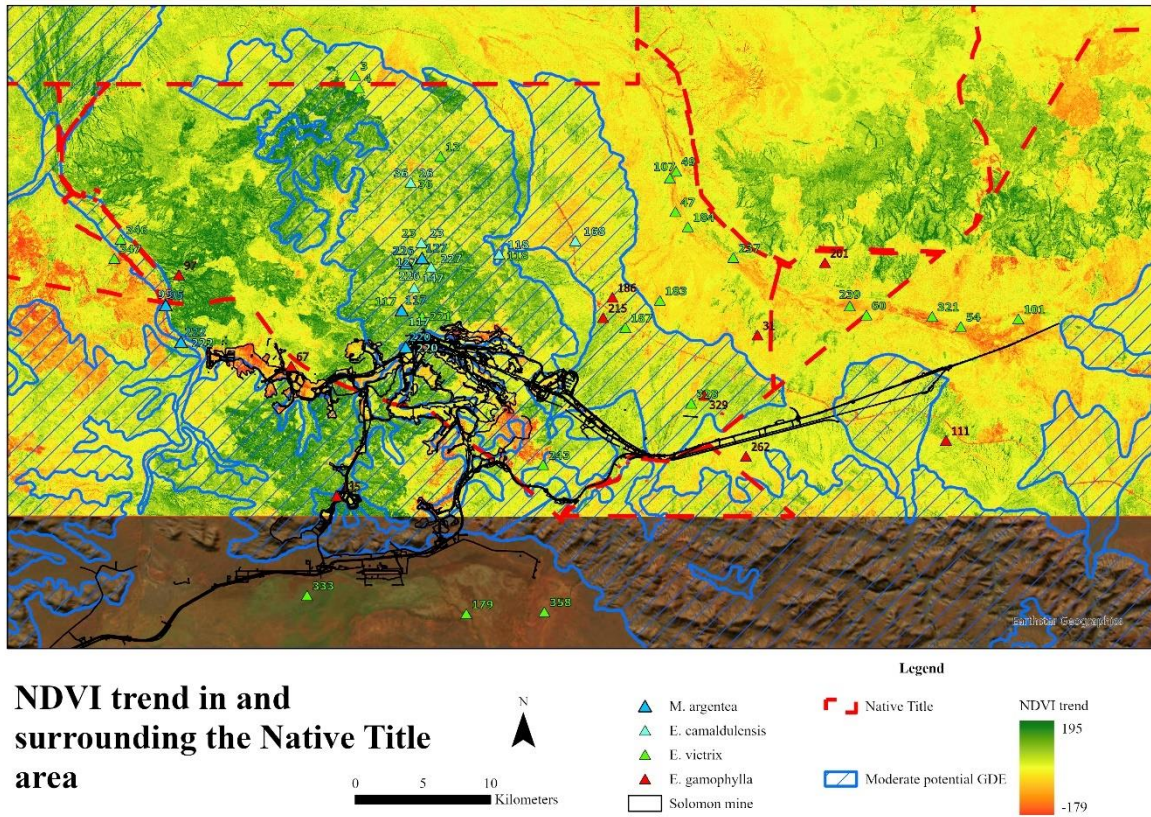


Figure 11 Spatially distributed NDVI trends ($0.001 * NDVI/yr$) for the five-year period of 12/2018 - 11/2023, positive values (green) indicating vegetation improvement, and negative values (red) indicating vegetation degradation. The Compensation Application Area and potential GDE coverage are shown on the map.

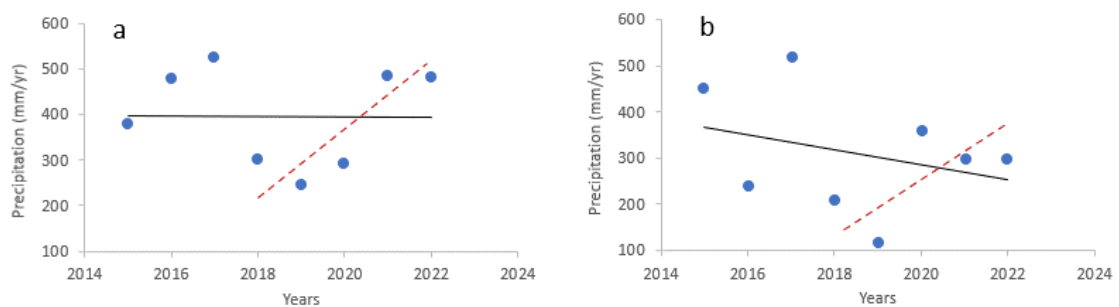


Figure 12 Annual precipitation time series of (a) Yalleen, WA (BOM ID 5029, 21.68 °S, 116.39 °E), (b) Newman Aero, WA (BOM ID 7176, 23.42 °S, 119.80 °E). zoom-in view of Figure 15 to Zalamea gorge.

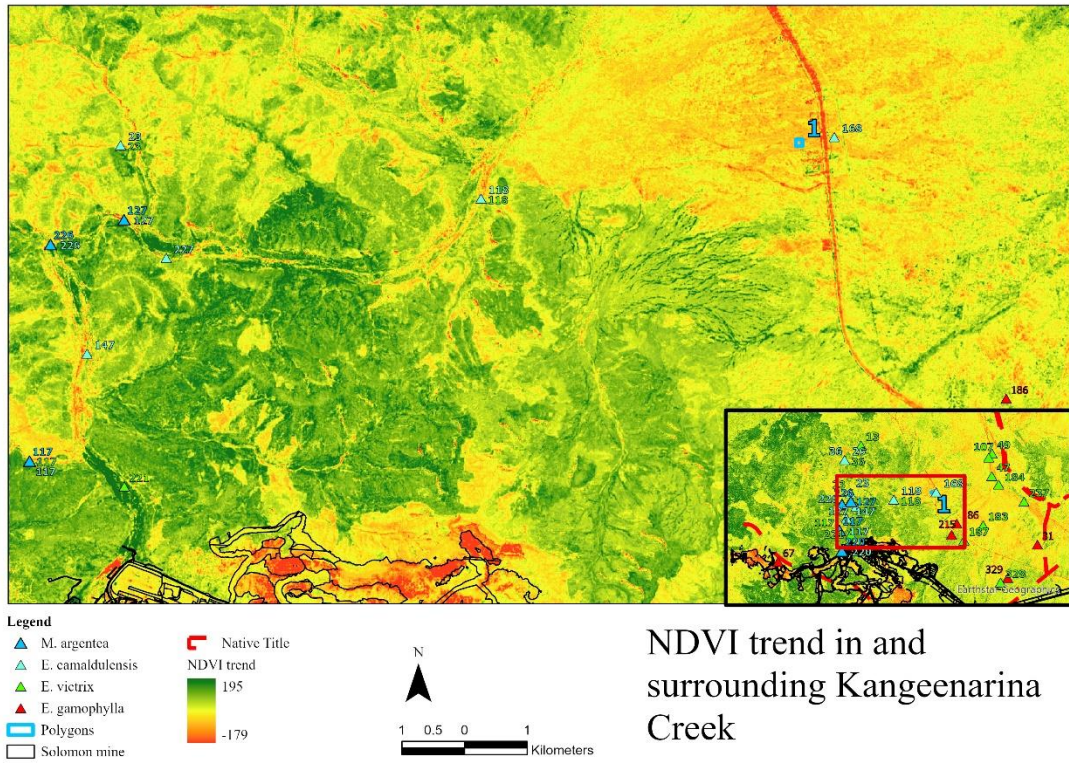


Figure 13 A zoomed-in view of Figure 11 to Kangeenarina Creek.

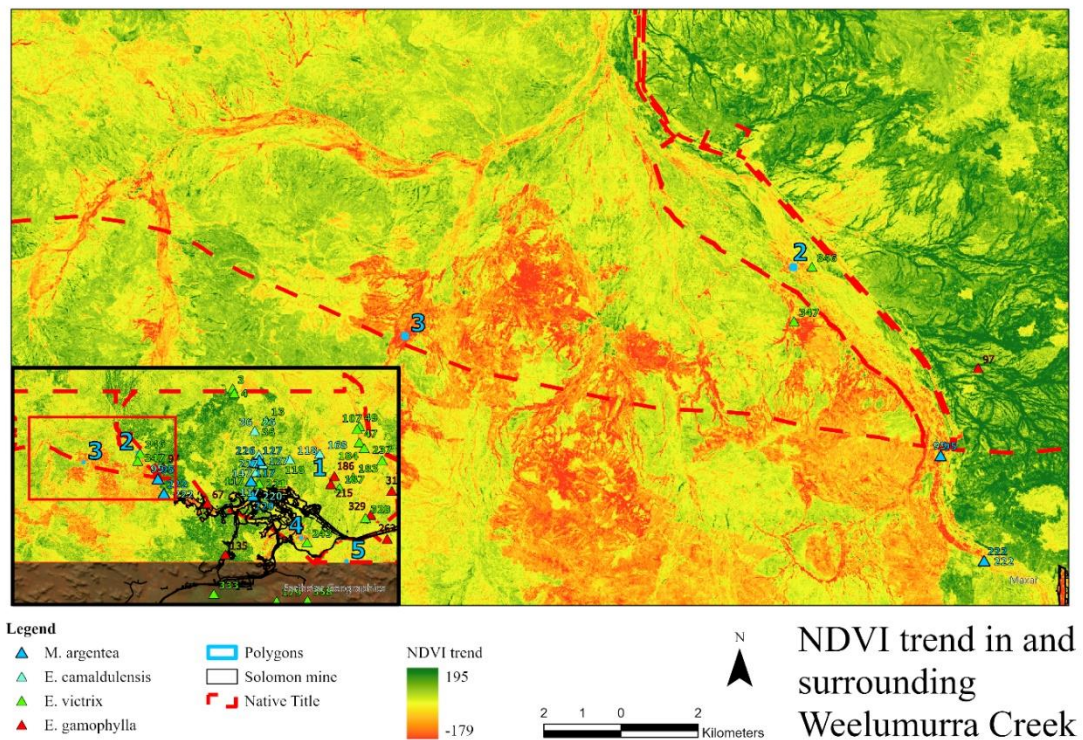


Figure 14 A zoomed-in view of Figure 11 to Weelumurra Creek.

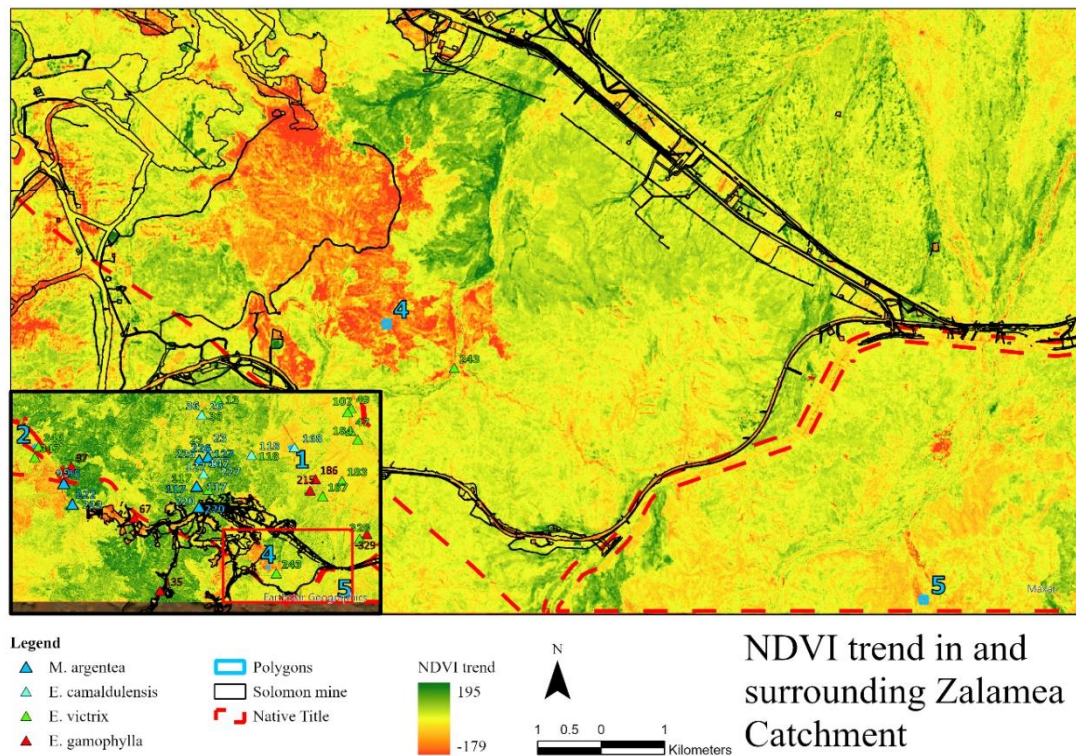


Figure 15 A zoomed-in view of Figure 11 to Zalamea gorge.

38 To examine terrestrial GDE degradation in the Compensation Application Area, decreasing NDVI trends for the pixels in common between the moderate potential terrestrial GDEs and the Compensation Application Area are shown in Figure 16, with three zoomed-in maps shown in Figures 17, 18 and 19 for Kangeenarina Creek, Weelumurra Creek, and Zalamea Gorge, respectively. Although the decreasing NDVI trends shown in these maps are not all statistically significant, the spatial coherence of those decreasing-trend pixels suggests they have occurred.

39 Figure 17 shows that the GDE degradation in Kangeenarina Creek mostly occurs in the alluvial fan where the Creek enters Low Fortescue Valley, about 10 km downstream from the SHP area. The NDVI degradation occurred gradually according to the details at one polygon (100 m x 100 m) and three vegetation quadrats as shown in the inset graph of Figure 17. Based on my hydrogeological knowledge from my PhD degree and my research in mountain-block hydrology and mountain-front recharge (e.g., Wilson & Guan 2004), the GDE degradation in the alluvial fan of Kangeenarina Creek is very likely linked to the disturbance of the groundwater recharge zone in the SHP area via regional groundwater flow paths (Figure 20). Groundwater flows from the recharge zone in the mountain range to the valley at the mountain front. This flow is driven by the hydraulic gradient between the two ends. Continuous groundwater abstraction (Figure 21) in the SHP area, the recharge end, has

reduced this gradient, which must have reduced groundwater replenishment at the mountain front via the regional flow paths. This possible mechanism explains the NDVI gradual decreasing trends in the alluvial fans.

40 Similarly, groundwater in the recharge zone flows via local and intermediate paths which can support GDEs in the mountain ranges. The SHP groundwater abstraction (Figure 21) should have also reduced groundwater replenishment via these flow paths. This possibility explains remote-sensing data inferred NDVI gradual decreasing trends at vegetation quadrats #127 and #118 (Figure 17 inset graph).

41 I also note that NDVI increasing trends have occurred over a section of Kangeenarina Creek immediately next to the SHP. Based on my hydrogeological knowledge, this is very likely due to the effectiveness of a grout barrier and water supplementation to maintain pool water levels in Kangeenarina Creek (Fortescue 2021).

42 GDE degradation in Weelumurra Creek has occurred in the valleys within the Hamersley Range downstream from the Valley of the Queens (Figure 18). The change at Weelumurra Creek occurred in 2021-2022 according to the inset graphs of polygons #2 and #3, and the NDVI has not recovered since then. This timing coincides with an increase of groundwater abstraction in the Valley of the Queens (Figure 21). This coincidence supports that the GDE degradation in Weelumurra Creek (Figure 18) is linked to groundwater abstraction in the Valley of the Queens. The widespread distribution of degraded NDVI in Figure 18 and Figure 14 suggests that the supplementation for Weelumurra Creek has not functioned as it was expected to. Having said that, they may help to some extent the locations very close to the injection wells, because in 2021-2022 no abrupt NDVI degradation occurred in vegetation quadrat #222 as shown in the inset of Figure 18.

43 GDE degradation in Zalamea Gorge is not obvious (Figure 19). The degradation has primarily occurred in the SHP operation area. However, some vegetation degradation may be occurring in the downstream alluvial fan (Figure 16), which may develop into what appears now in the Kangeenarina alluvial fan if the current condition continues. An alluvial fan is an accumulation of sediment that fans outwards from a concentrated source of sediments.

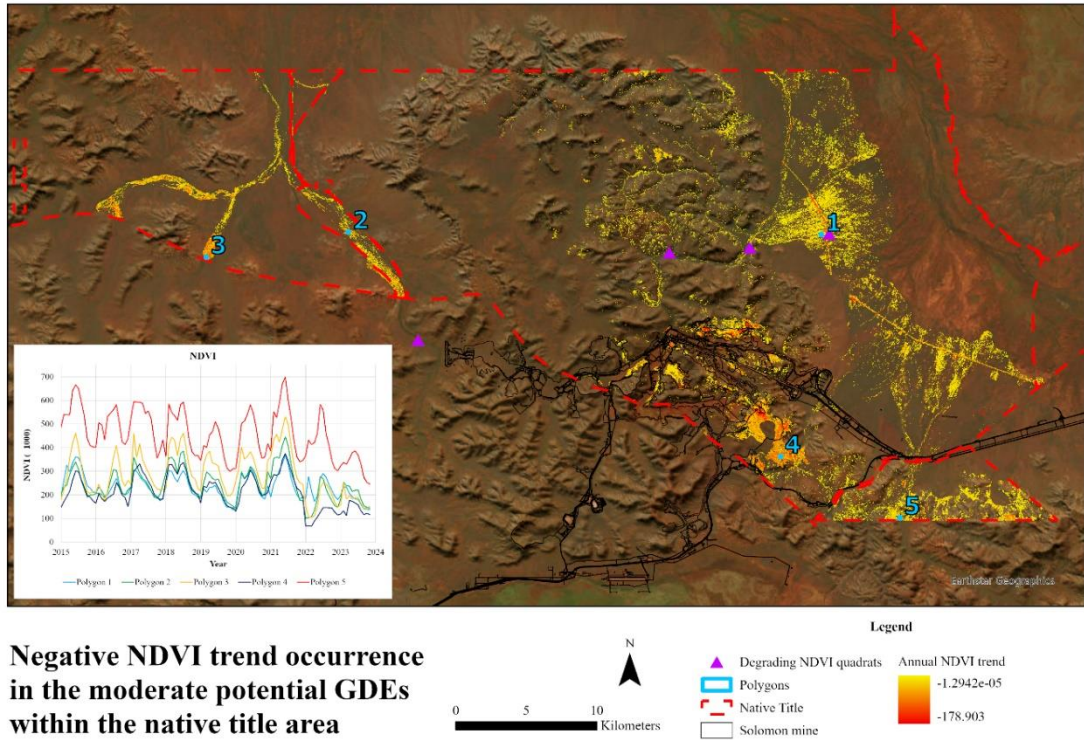


Figure 16 Spatially distributed NDVI decreasing trends ($0.001 * NDVI/yr$) for the five-year period of 12/2018 - 11/2023 for the common area of the Native Title and the moderate potential GDEs, with an inset showing monthly NDVI time series for five one-hectare polygons.

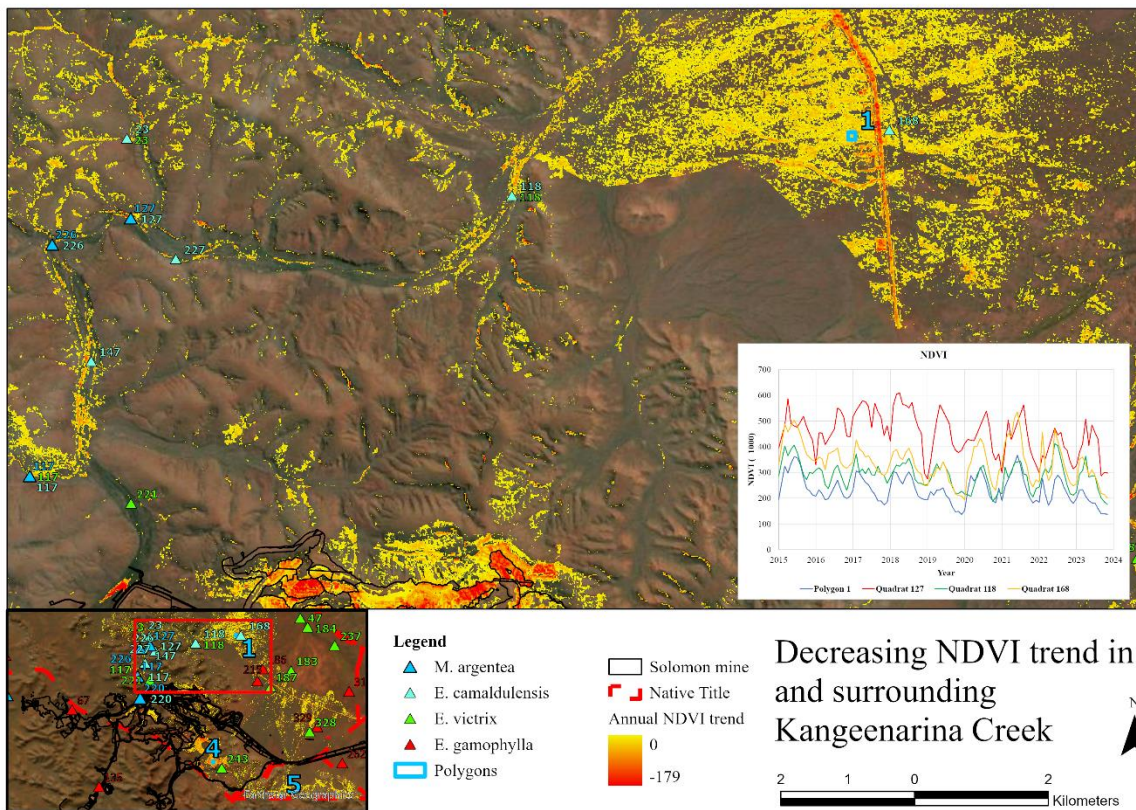


Figure 17 A zoomed-in view of Figure 16 to Kangeenarina Creek.

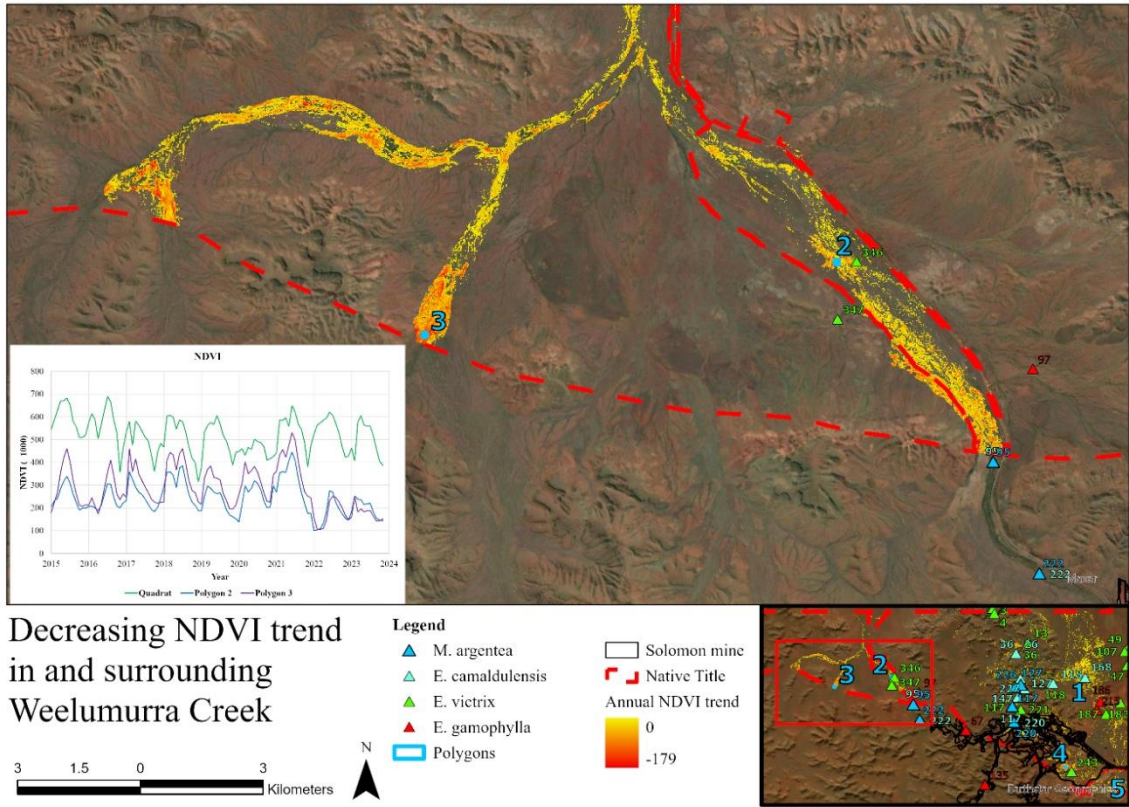


Figure 18 A zoomed-in view of Figure 16 to Weelumurra Creek.

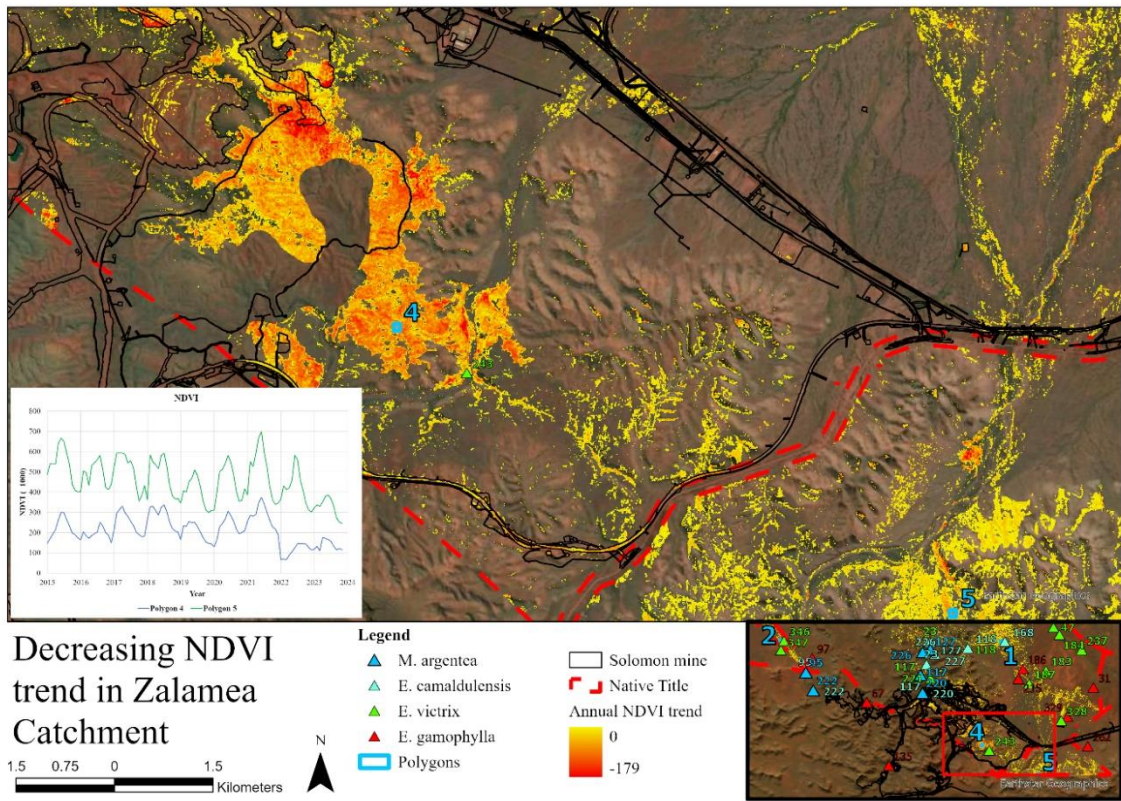


Figure 19 A zoomed-in view of Figure 16 to Zalamea gorge.

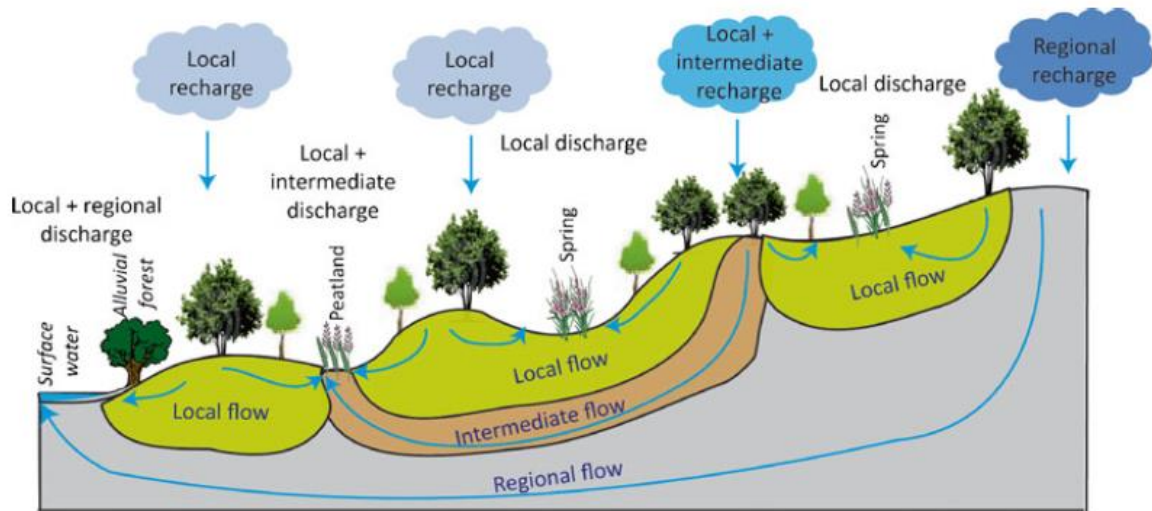


Figure 20 A conceptual diagram showing different groundwater flow paths along a transect from the mountain range to the basin floor (copied from Bertrand et al. 2011).

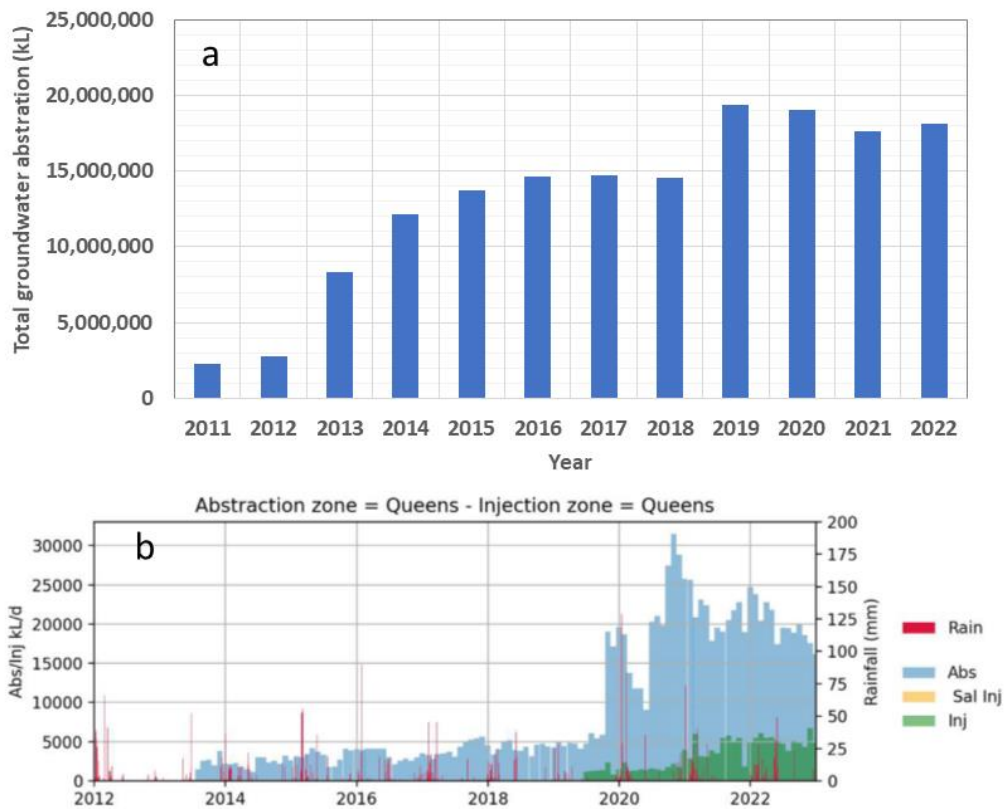


Figure 21 (a) Annual groundwater abstraction from the SHP (calculated from Fortescue 2014, 2017, 2020, and 2023), and (b) Daily groundwater abstraction and injection from the zone of Valley of Queens (adopted from Fortescue 2022).

6. Is this remotely sensed vegetation degradation related to the SHP?

44 Vegetation degradation is observed for six vegetation quadrats (Table 1), and in sections of both Kangeenarina and Weelumurra Creeks (Figure 16). It is almost certain that this vegetation degradation has been caused by the SHP operation. My opinion is based on the following facts and/or understandings arising from my study, training and experience as a hydrologist:

- a) the degradation occurs in groundwater-dependent ecosystems. All six quadrats with degrading vegetation (Table 1) have typical groundwater-dependent species, including *M. argentea*, *E. camaldulensis*, and/or *E. Victrix*.
- b) the mapped vegetation degradation (2019-2022) (Figure 16) cannot be explained by precipitation variability in the period when precipitation actually increased (Figure 12). The increasing precipitation in recent years explains NDVI improvement for areas where no terrestrial GDEs are considered to be present (Figure 11). Thus, the mapped vegetation degradation in Figure 16 must have been due to groundwater depletion at those locations.
- c) the timing of vegetation degradation matches groundwater abstraction in the SHP area. For the spots with vegetation degradation related to Kangeenarina Creek, the degradation has occurred gradually since 2015 (the inset in Figure 17), which is consistent with the groundwater abstraction in the SHP area (Figure 21). For the spots with vegetation degradation related to Weelumurra Creek, the degradation has occurred since 2015 for quadrat 222 which is close to the mine site, and occurred more abruptly in 2021-2022 as shown from the inset of Figure 18. This abrupt change is very likely in response to the fact that more groundwater abstraction shifted to the Valley of the Queens in recent years (Figure 21).
- d) the NDVI series in vegetation quadrat #221 (Table 1) and the nearby section of Kangeenarina Creek (Figure 17) shows vegetation improvement, suggesting the positive effect of a combination of the supplementation injection and the grout wall for Kangeenarina Creek. However, vegetation downstream along the creek, and particularly in the alluvium fan, has degraded, suggesting that groundwater within a distance from the SHP has depleted, mostly likely due to a reduction of groundwater recharge from the SHP area via intermediate/regional flow paths to the degraded areas; and
- e) vegetation degradation in Weelumurra Creek in proximity of SHP suggests that the supplementation wells have not functioned as well as expected.

7. Conclusions

45 Based on the analyses of NDVI trends for the Compensation Application Area surrounding the SHP, and investigating a possible linkage with the SHP, I conclude as follows:

(a) FMG' mining activities at the SHP have very likely caused vegetation degradation in the reach of both Kangeenarina Creek and Weelumurra Creek as follows:

- i. the degradation in Kangeenarina Creek has occurred mostly in the alluvial fan where the creek enters the Lower Fortescue Valley, and in a few riparian sections within the Hamersley Range. The degradation appears to have developed gradually since 2015; and
- ii. The degradation in Weelumurra Creek has occurred in three valleys to the northwest of the SHP. The degradation appears to have become more serious since 2021 shortly after groundwater abstraction in the Valley of the Queens increased; and

(b) the SHP area is a groundwater recharge zone. Groundwater abstraction in the SHP has very likely disturbed regional, intermediate, and local flow paths in the Hamersley Range as follows:

- i. the disturbance in the regional and intermediate flow paths very likely has reduced groundwater replenishment in the areas where degradation of groundwater-dependent terrestrial vegetation occurred in the reach of Kangeenarina Creek.
- ii. the disturbance in Weelumurra Creek appears to be more serious on the local and intermediate flow paths, very likely resulting in a falling groundwater table in the three valleys of Weelumurra Creek to the northwest of the SHP.
- iii. It is difficult to assess any changes to the connectivity of surface flows due to a lack of surface water monitoring data. However, given that the creeks only flow episodically, surface water connections are maintained by shallow groundwater-dependent pools (or waterholes). It is very likely that the SHP has changed connectivity of surface flows as well due to its impacts on shallow groundwater inferred from degraded terrestrial GDEs; and

(c) I would expect that groundwater levels have decreased at the locations where degradation of groundwater-dependent terrestrial vegetation has occurred. These changes have very likely resulted from dewatering in the SHP area.

46Based on what I have examined, I can also comment on Paragraph #74 of Affidavit of Christopher Ian Leonard Oppenheim (2023) in which a decreasing trend of Warp 16 water level was considered to be “a reflection of naturally declining water level associated with a reduced rainfall since 2014”.

(d) The decreasing water level of Warp 16 in 2014-2018 is also reflected in the decreasing NDVI of vegetation quadrat #222 during almost the same period (the inset graph in Figure 18). However, in the same period, no NDVI decreasing trend is observed for nearby groundwater-dependent vegetation (polygon #2 and 3). Thus, the decreasing trend in Warp 16 water level is least likely to have resulted from a change of rainfall because any effect of a change of rainfall amount would cover a large area. In my opinion, it is most likely due to dewatering in the SHP area.

References

AQ2 (2019). Solomon Ecohydrology.

Bertrand, G., Goldscheider, N., Gobat, J. M., & Hunkeler, D. (2011). Review: From multi-scale conceptualization to a classification system for inland groundwater-dependent ecosystems. In *Hydrogeology Journal* (Vol. 20, Issue 1, pp. 5–25). <https://doi.org/10.1007/s10040-011-0791-5>

Brim Box, J., Leiper, I., Nano, C., Stokeld, D., Jobson, P., Tomlinson, A., Cobban, D., Bond, T., Randall, D., & Box, P. (2022). Mapping terrestrial groundwater-dependent ecosystems in arid Australia using Landsat-8 time-series data and singular value decomposition. *Remote Sensing in Ecology and Conservation*, 8(4), 464–476. <https://doi.org/10.1002/rse2.254>

Bureau of Meteorology. (Retrieved in November 2023). Groundwater-dependent Ecosystems Atlas. <http://www.bom.gov.au/water/groundwater/gde/>

CSIRO (2015). Pilbara Water Resource Assessment: Lower Fortescue Hedland region, An overview report to the Government of Western Australia and industry partners from the CSIRO Pilbara Water Resource Assessment.

Doody, T. M., Barron, O. V., Dowsley, K., Emelyanova, I., Fawcett, J., Overton, I. C., Pritchard, J. L., Van Dijk, A. I. J. M., & Warren, G. (2017). Continental mapping of groundwater dependent ecosystems: A methodological framework to integrate diverse data and expert opinion. *Journal of Hydrology: Regional Studies*, 10, 61–81. <https://doi.org/10.1016/j.ejrh.2017.01.003>

Ecologia (2015). Solomon Hub Flora and Vegetation Assessment

Fildes, S. G., Doody, T. M., Bruce, D., Clark, I. F., & Batelaan, O. (2023). Mapping groundwater dependent ecosystem potential in a semi-arid environment using a remote sensing-based multiple-lines-of-evidence approach. *International Journal of Digital Earth*, 16(1), 375–407. <https://doi.org/10.1080/17538947.2023.2176557>

Fortescue 2014. Solomon Triennial Aquifer Review - 1 August 2011 to 31 July 2014, SO-RP-HY-0003

Fortescue 2017. Solomon Triennial Aquifer Review: 1 August 2014 to 31 July 2017

Fortescue 2020. Solomon Triennial Aquifer Review to 31 December 2019

Fortescue 2021. Solomon Mining Area: Updated H3 Hydrogeological Assessment

Fortescue 2023. Solomon Triennial Groundwater Monitoring Review 2022

Golder Associates (2012). H3 Hydrogeological Assessment. Report No. 117646036-052-R-Rev2

Liu, W., H. Guan, H.A. Gutierrez-Jurado, E.W. Banks, X. He, X. Zhang (2022). Modeling quasi-three-dimension distribution of solar irradiance on complex terrain, *Environmental Modelling and Software* 149. DOI: 10.1016/j.envsoft.2021.105293

Murray, B. R., Hose, G. C., Eamus, D., & Licari, D. (2006). Valuation of groundwater-dependent ecosystems: A functional methodology incorporating ecosystem services. *Australian Journal of Botany*, 54(2), 221–229. <https://doi.org/10.1071/BT05018>

MWH (2010). Hydrogeological Assessment of the Solomon Project.

Oppenheim (2023). Affidavit of Christopher Ian Leonard Oppenheim sworn 4 August 2023

Wilson, J.L., and H. Guan (2004). Mountain-block hydrology and mountain-front recharge, in Groundwater Recharge in a Desert Environment: The Southwestern United States, edited by J.F. Hogan, F.M. Phillips, and B.R. Scanlon, Water Science and Applications Series, vol. 9, American Geophysical Union, Washington, D.C., 113-137.

Zhou, X., H. Guan, H. Xie, and J.L. Wilson (2009). Analysis and optimization of NDVI definitions and areal fraction models in remote sensing of vegetation, International Journal of Remote Sensing, 30(3), 721-751.

Appendices

A1: The Brief

A2: Huade Guan's Resume

A3: A list of materials which were provided to Huade Guan with the brief

A4a: Pilbara Water Resource Assessment: Lower Fortescue Hedland region

A4b: Mountain-Block Hydrology and Mountain Front Recharge

Appendix 1a

Resume of Associate Professor Huade Guan

College of Science and Engineering
Flinders University
GPO Box 2100, Adelaide, SA 5001
Australia

Phone: + 61 8 82012319
Email: huade.guan@flinders.edu.au
<http://www.flinders.edu.au/people/huade.guan>

Education

B.S. in geochemistry, Peking University, China, 1990
M.S. in geology (groundwater), University of Texas at El Paso, USA, 2001
Ph.D. in hydrology, New Mexico Institute of Mining and Technology, USA, 2005

Professional Positions

Associate Professor, College of Science & Engineering, Flinders University, 2015-
Senior Lecturer, School of the Environment, Flinders University, 2010-2015
Lecturer, School of Chemistry, Physics & Earth Science, Flinders University, 2006-2010
Postdoctoral Research Associate, Earth & Environmental Science, UT San Antonio, 2005-2006

Chief Investigator, National Centre for Groundwater Research and Training, 2009-
Adjunct Professor, Hunan Normal University, 2011-2015
Associate Editor, Journal of Hydrology 2015-
Associate Editor, Frontiers in Climate (Climate, Ecology and People) 2021-

Research grants

1. Skrzypek, G., Dogramaci, S., McCallum, J., Leopold, Guan, H., M., Gibson, J. & Shanafield, M. Unsaturated zone functioning in semi-arid flash flood driven climate (\$830,288). ARC LP21R3, 2022-2026
2. Guan, H., Bruce, D., Clay, R., Moffat, I., Environmental and microclimate benefits of WSUD structures in City of Mitcham (\$74k), The Green Adelaide Board and Mitcham Council, 2022-2024.
3. Gutierrez-Jurado, K., Guan, H., Banks, E., Batelaan, O., and Falzon, G. Solar-powered enhanced evaporation pond system for in-situ salt extraction (\$100k), Australian Government Department of Agriculture, Water and the Environment, 2022-2023
4. Guan, H., Batelaan, O., Bruce, D., Estimation of flood plain understory evapotranspiration based on the maximum entropy production method (\$186k), Murray-Darling Basin Authority, 2021-2023
5. Dittmann, S., Stangoulis, J., Guan, H., Blue carbon opportunities through tidal restoration and avoided disturbance (\$40k), The Green Adelaide Board, 2021-2022
6. Guan, H., Urban water-tree-microclimate relationships at different settings to support WSUD implementation (\$52k + 20k), The Green Adelaide Board and Mitcham Council, 2021

7. Guan, H., Bruce D., Lee, G., Batelaan O., Towards an adaptive woody vegetation management for reducing bushfire risks (\$25k), Flinders University Climate Response Seed Grant Scheme, 2020-2021
8. Guan, H., Deng, Z., Clay, R., Effects of stormwater harvesting on street trees' amelioration of summer microclimate in Adelaide (\$25k), The Adelaide and Mount Lofty Ranges NRMB and Mitcham Council, 2020
9. Guan, H., Effects of enhanced stormwater infiltration on urban trees functioning in dry season (\$15k), The Adelaide and Mount Lofty Ranges NRMB and Mitcham Council, 2019
10. Guan, H., Bestland E., Hua, Q., and Zawadzki A., Hidden carbon sinks in the dry rangelands of South Australia: A pilot study (equivalent \$27k), ANSTO, 2019
11. Sabine Dittmann, Luke Mosley, Paul Sutton, Erick Bestland, Huade Guan, Stephen Crooks, Robert Costanza, James Stangoulis From Salt to C; carbon sequestration through ecological restoration at the Dry Creek Salt Field (\$336k), Goyder Institute, 2017-2019
12. Guan, H., S. Beecham, G. Ingleton, Optimal balance between cooling energy use and green infrastructure irrigation in dry-summer Adelaide (\$48k), State Government (DEWNR) and SA Water, 2014-2016
13. Andrew, R., O. Batelaan, and H. Guan, Natural and managed hydrological changes and the implications for urban planning and water management (\$30k), Goyder Institute, 2013-2015
14. Gharib, S. and H. Guan, Optimisation of natural (sea breeze) and managed (parkland irrigation) summer cooling effects in the Adelaide metropolitan area (\$30k), Goyder Institute, 2013-2015
15. Dittmann, S., E. Bestland, M. Whalen, J. Stangoulis, H. Guan, A. McGrath, J. Hacker, Investigation of field methodologies for measuring coastal wetland carbon capture and storage values (\$48k), Adelaide and Mount Lofty Ranges Natural Resources Management Board, 2012-2013
16. Gillanders, B., S. Robinson, S. Walker, M. Kennedy, J. Watling, K. Soole, J. Tibby, H. Guan, A. Cooper, A. Ball. Stable isotope analysis of environmental and physiological samples (\$420k), ARC, 2012
17. Guan, H., J. Bennett, C. Ewenz, A. McGrath, S. Bengner, V. Soebarto, R. Clay, K. Bellette, and Adelaide City Council, City of Adelaide urban heat island micro-climate study (\$70k), Department of the Premier and Cabinet University Sector Agreement Fund on Climate Change, and Adelaide City Council, 2011-2012
18. Simmons, C. T., ... H. Guan, ... National Centre for Groundwater Research and Training (\$30M), Program 4: Groundwater-vegetation-atmosphere interactions, ARC and National Water Commission, 2009-2014
19. Guan, H., C. T. Simmons, J. Bennett, C. Ewenz, R. Clay, G. Hopkins, The effects of parkland on mitigating urban heat island intensity (\$93K), SA Government, 2009-2010
20. Guan, H., Using modified zeolite to prevent biological clogging of artificial recharge structures (\$5K), Water Quality Research Australia, 2008-2009
21. Guan, H., Investigation of the parkland belt impacts on the urban heat island effect in the Adelaide metropolitan area, (\$5K), Flinders University, 2008

Peer-review publications (* first author primarily under my supervision)

1. *Liu, W., H. Guan, P. Hesp, O. Batelaan (2023). Remote sensing delineation of wildfire spatial extents and post-fire recovery along a semi-arid climate gradient. *Ecological Informatics* 78. <https://doi.org/10.1016/j.ecoinf.2023.102304>
2. *Gou, J., S. Qu, P. Shi, H. Guan, H. Yang, Z. Zhang, J. Liu, Z. Su (2023). Comparison of transit time models for exploring seasonal variation of preferential flow in a Moso bamboo watershed. *Journal of Hydrology*. <https://doi.org/10.1016/j.jhydrol.2023.130308>
3. Huang, X., H. Guan, L. Bo, Z. Xu, X. Mao (2023). Hyperspectral proximal sensing of leaf chlorophyll content of spring maize based on a hybrid of physically based modelling and ensemble stacking. *Computers and Electronics in Agriculture* 208. <https://doi.org/10.1016/j.compag.2023.107745>
4. Luo, Z., Y. Nie, H. Chen, H. Guan, X. Zhang, K. Wang (2023). Water age dynamics in plant transpiration: The effects of climate patterns and rooting depth. *Water Resources Research*. <https://doi.org/10.1029/2022WR033566>
5. *Chen, A., Guan, H. and Batelaan, O. (2022). Spatially differentiated effects of local moisture deficit and increased global temperature on hot extreme occurrences. *Journal of Hydrology*. <https://doi.org/10.1016/j.jhydrol.2022.128720>.
6. *Chen, A., Guan, H., Batelaan, O. (2022). Non-linear interactions between vegetation and terrestrial water storage in Australia. *Journal of Hydrology*, 613. DOI: 10.1016/j.jhydrol.2022.128336.
7. Luo, Z., Nie, Y., Guan, H., Chen, H., Zhang X., Wang, K. (2022). Widespread root-zone water bypass for various climates and species: Implications for the ecohydrological separation understanding. *Agricultural and Forest Meteorology* 324. DOI: 10.1016/j.agrformet.2022.109107
8. Dai J., Zhang X., Wang L., Luo Z., Wang, R., Liu, Z., He, X., Rao, Z., Guan, H. (2022). Seasonal isotopic cycles used to identify transit times and the young water fraction within the critical zone in a subtropical catchment in China. *Journal of Hydrology*, 612. DOI: 10.1016/j.jhydrol.2022.128138
9. Dittmann, S., Mosley, L., Stangoulis, J., Nguyen, V.L., Beaumont, K., Dang, T., Guan, H., Gutierrez-Jurado, K., Lam-Gordillo, O., and McGrath, A. (2022). Effects of extreme salinity stress on a temperate mangrove ecosystem. *Frontiers in Forests and Global Change*. DOI: 10.3389/ffgc.2022.859283 (a new journal)
10. Zhu, J., Wallis, I., Guan, H., Ross, K., Whiley, H., Fallowfield, H. (2022). *Juncus sarophorus*, a native Australian species, tolerates and accumulates PFOS, PFOA and PFHxS in a glasshouse experiment. *Science of The Total Environment*, 826. <https://doi.org/10.1016/j.scitotenv.2022.154184>

11. *Gleeson, X., Johnson, T., Lee, G., Zhou, Y., Guan, H. (2022). Enhanced passive stormwater infiltration improves urban Melia Azedarach functioning in dry season. *Frontiers in Climate*, 4, DOI: 10.3389/fclim.2022.783905 (a new journal)
12. *Xu, X., Guan, H., Skrzypek, G., Williams, D.G. (2022). Topographical influences on foliar nitrogen concentration and stable isotope composition in a Mediterranean-climate catchment, *Ecological Informatics* 68. DOI: 10.1016/j.ecoinf.2022.101569.
13. *Liu, W., Guan, H., Gutierrez-Jurado, H.A., Banks, E.W., He, X., Zhang, X. (2022) Modeling quasi-three-dimension distribution of solar irradiance on complex terrain, *Environmental Modelling and Software* 149. DOI: 10.1016/j.envsoft.2021.105293
14. *Guo, J., Qu, S., Guan, H., Shi, P., Su, Z., Lin, Z., Liu, J., Zhu, J..(2022) Relationship between precipitation isotopic compositions and synoptic atmospheric circulation patterns in the lower reach of the Yangtze River. *Journal of Hydrology* 605 (2022) 127289. DOI: 10.1016/j.jhydrol.2021.127289
15. *Chen, A., Guan, H., Batelaan O. (2021) Seesaw terrestrial wetting and drying between eastern and western Australia. *Earth's Future*. DOI: 10.1029/2020EF001893
16. *Zhou, Y., Guan, H., Gharib, S., Batelaan, O., and Simmons C.T. (2021) Cooling power on sea breezes and its inland penetration in dry-summer Adelaide, Australia. *Atmospheric Research*. 250, 105409. 10.1016/j.atmosres.2020.105409
17. Du, J., Wang, X., Huo, Z., Guan, H., Xiong, Y., Huang, G. (2021) Response of shelterbelt transpiration to shallow groundwater in an arid area. *Journal of Hydrology*. <https://doi.org/10.1016/j.jhydrol.2020.125611>
18. Anderson, T., Bestland, E., Wallis, I., Kretschmer, P., Soloninka, L., Banks, E., Werner, A., Cendon, D., Pichler, M., Guan, H. (2021). Catchment-scale groundwater flow and recharge paradox revealed from base-flow analysis during the Australian Millennium Drought (Mt Lofty Ranges, South Australia), *Hydrogeology Journal*, <https://doi.org/10.1007/s10040-020-02281-0>.
19. Mollehuara-Canalesa, R., Kozlovskayaa, E., Lunkkaa, J.P., Guan H., Banks, E., Moisiao, K. (2020) Geoelectric interpretation of petrophysical and hydrogeological parameters in reclaimed mine tailings areas, *Journal of Applied Geophysics*, <https://doi.org/10.1016/j.jappgeo.2020.104139>
20. *Fan, L., Guan, H., Cai, W., Rofe, K., Xu, J. (2020). A seven-year lag precipitation teleconnection in South Australia and its possible mechanism. *Frontier in Earth Science*. <https://doi.org/10.3389/feart.2020.553506>.
21. *Liu, N., Deng, Z., Wang, H., Luo, Z., Gutierrez-Jurado, H., He, X., Guan, H. (2020). Thermal remote sensing of plant water stress in natural ecosystems. *Forest Ecology and Management*. 476, 118433. 10.1016/j.foreco.2020.118433
22. Dai, J., Zhang, X., Luo, Z., Wang, R., Liu, Z., He, X., Rao, Z., Guan, H. (2020). Variation of the stable isotopes of water in the soil-plant-atmosphere continuum of a Cinnamomum camphora woodland in the East Asian monsoon region. *Journal of Hydrology*. 589, 125199.
23. *Luo, Z., Deng, Z., Singha K., Zhang, X., Liu, N., Zhou, Y., He, X., and Guan, H. (2020). Temporal and spatial variation in water content within living tree stems determined by electrical resistivity tomography. *Agricultural & Forest Meteorology*. 291. <https://doi.org/10.1016/j.agrformet.2020.108058>

24. Wang, H., Guan, H., Liu, N., Soulsby, C., Tetzlaff, D., Zhang, X.(2020) Improving the Jarvis-type model with modified temperature and radiation functions for sap flow simulations. *Journal of Hydrology*. 587. <https://doi.org/10.1016/j.jhydrol.2020.124981>
25. Clay, R., Guan, H. (2020). The urban-parkland nocturnal temperature interface. *Urban Climate*. 31 (2020) 100585. DOI: 10.1016/j.uclim.2020.100585.
26. Wang, X., Guan, H., Huo, Z., Guo, P., Du, J., Wang, W. (2020). Maize transpiration and water productivity of two irrigated fields with varying groundwater depths in an arid area. *Agricultural and Forest Meteorology*. 281(2020) 107849.
27. *Zhou, Y., Guan, H., Huang, C., Fan, L., Gharib, S., Batelaan, O. & Simmons, C. T. (2019) Sea breeze cooling capacity and its influencing factors in a coastal city. *Building and Environment*. 166, 106408.
28. *Liu, N., Wang, H., He, X., Deng, Z., Zhang, C., Zhang, X. & Guan, H. (2019) A hybrid transpiration model for water-limited conditions. *Journal of Hydrology*. 578, 124104.
29. *Luo, Z., Guan, H. & Zhang, X. (2019). The temperature effect and correction models for using electrical resistivity to estimate wood moisture variations, *Journal of Hydrology*, 578, 10 p., 124022.
30. *Xu, X., Guan, H., Skrzypek, G. & Simmons, C. T. (2019). Root-zone moisture replenishment in a native vegetated catchment under Mediterranean climate. *Hydrological Processes*, 33, 18, p. 2394-2407. <https://doi.org/10.1002/hyp.13475>
31. Anderson, T., Bestland, E., Wallis, I. & Guan, H.,(2019). Salinity balance and historical flushing quantified in a high-rainfall catchment (Mount Lofty Ranges, South Australia), *Hydrogeology Journal*, p. 1229-1244.
32. Chen, A., He, X., Guan, H. & Zhang, X. (2019) Variability of seasonal precipitation extremes over China and their associations with large-scale ocean-atmosphere oscillations. *International Journal of Climatology*, 39, 2, p. 613-628.
33. *Chen, A., Guan, H., Batelaan, O., Zhang, X. & He, X. (2019). Global Soil Moisture-Air Temperature Coupling Based on GRACE-Derived Terrestrial Water Storage, *Journal of Geophysical Research: Atmospheres*, 124, 14, p. 7786-7796.
34. *Luo, Z., Guan, H., Zhang, X. and Xu, X. (2019). Examination of the ecohydrological separation hypothesis in a humid subtropical area: Comparison of three methods. *Journal of Hydrology*, 571 pp. 642-650.
35. Xu, H., Hu, X., Guan, H., Zhang, B., Wang, M., Chen, S., et al. (2019). A Remote Sensing Based Method to Detect Soil Erosion in Forests. *Remote Sensing*, 11(5).
36. *Long, X., Guan, H., Sinclair, R., Batelaan, O., Facelli, J.M., Andrew, R., et al. (2019). Response of vegetation cover to climate variability in protected and grazed arid rangelands of South Australia. *Journal of Arid Environments*, 161 pp. 64-71.
37. *Liu, N., Guan, H., Buckley, T., He, X., Zhang, X., Zhang, C., et al. (2019). Improvement of a simplified process-based model for estimating transpiration under water-limited conditions. *Hydrological Processes*.
38. Wang, X., Huo, Z., Guan, H., Guo, P. and Qu, Z. (2018). Drip irrigation enhances shallow groundwater contribution to crop water consumption in an arid area. *Hydrological Processes*, 32(6) pp. 747-758.

39. Yao, T., Zhang, X., Guan, H., Zhou, H., Hua, M. and Wang, X. (2018). Climatic and environmental controls on stable isotopes in atmospheric water vapor near the surface observed in Changsha, China. *Atmospheric Environment*, 189 pp. 252-263.
40. Xu, H., Wang, M., Shi, T., Guan, H., Fang, C. and Lin, Z. (2018). Prediction of ecological effects of potential population and impervious surface increases using a remote sensing based ecological index (RSEI) *Ecological Indicators*, 93 pp. 730-740.
41. Abiodun, O.O., Guan, H., Post, V.E. and Batelaan, O. (2018). Comparison of MODIS and SWAT evapotranspiration over a complex terrain at different spatial scales. *Hydrology and Earth System Sciences*, 22 pp. 2275-2794.
42. Chen, A., He, X., Guan, H., and Cai, Y. (2018). Trends and periodicity of daily temperature and precipitation extremes during 1960–2013 in Hunan Province, central south China. *Theoretical and Applied Climatology*, DOI 10.1007/s00704-017-2069-x.
43. *Andrew, R., Guan, H. and Batelaan, O. (2017). Large-scale vegetation responses to terrestrial moisture storage changes. *Hydrology and Earth System Sciences*, 21 pp. 4469-4478.
44. *Andrew, R., Guan, H. and Batelaan, O. (2017). Estimation of GRACE water storage components by temporal decomposition. *Journal of Hydrology*, 552 pp. 341-350. (Q1, top
45. *Luo, Z., Guan, H., Zhang, X. and Liu, N. (2017). Photosynthetic capacity of senescent leaves for a subtropical broadleaf deciduous tree species *Liquidambar formosana* Hance. *Scientific Reports*, DOI:10.1038/s41598-017-06629-7.
46. Xu, H., Hu, X., Guan, H. and He, G. (2017). Development of a fine-scale discomfort index map and its application in measuring living environments using remotely-sensed thermal infrared imagery. *Energy and Buildings*, 150 pp. 598-607.
<http://dx.doi.org/10.1016/j.enbuild.2017.06.003>
47. *Xu, X., Guan, H., Skrzypek, G. and Simmons, C.T. (2017). Response of leaf stable carbon isotope composition to temporal and spatial variabilities of aridity index on two opposite hillslopes in a native vegetated catchment. *Journal of Hydrology*, 553 pp. 214-223.
<http://dx.doi.org/10.1016/j.jhydrol.2017.05.062> (Q1, top 10%, 4.94)
48. *Deng, Z., Guan, H., Hutson, J.L., Forster, M., Wang, Y. and Simmons, C.T. (2017). A vegetation focused soil-plant-atmosphere continuum model to study hydrodynamic soil-plant water relations. *Water Resources Research*, 53 pp. 4965-4983. DOI:10.1002/2017WR020467
49. Xue, J., Guan, H., Huo, Z., Wang, F., Wang, G. and Boll, J. (2017). Water saving practices enhance regional efficiency of water consumption and water productivity in an arid agricultural area with shallow groundwater. *Agricultural Water Management*, 194 pp. 78-89.
<http://dx.doi.org/10.1016/j.agwat.2017.09.003>
50. Guan, H., Beecham, S., Xu, H. and Ingleton, G. (2017). Incorporating residual temperature and specific humidity in predicting weather-dependent warm-season electricity consumption. *Environmental Research Letters*, 12(2) pp. Art: 024021.
51. *Liu, B., Guan, H., Zhao, W., Yang, Y. and Li, S. (2017). Groundwater facilitated water-use efficiency along a gradient of groundwater depth in arid northwestern China. *Agricultural and Forest Meteorology*, 233 pp. 235-241.
52. *Liu, N., Guan, H., Luo, Z., Zhang, C., Wang, H. and Zhang, X. (2017). Examination of a coupled supply- and demand-induced stress function for root water uptake modeling. *Hydrology Research*, 48(1) pp. 66-76.

53. Tie, Q., Hu, H., Tian, F., Guan, H. and Lin, H. (2017). Environmental and physiological controls on sap flow in a subhumid mountainous catchment in North China. *Agricultural and Forest Meteorology*, 240-241 pp. 46-57.
54. Wang, Y., Ma, J., Guan, H. and Zhu, G. (2017). Determination of the saturated film conductivity to improve the EMFX model in describing the soil hydraulic properties over the entire moisture range. *Journal of Hydrology*, 549 pp. 38-49.
55. Clay, R., Guan, H., Wild, N., Bennett, J.M., Vinodkumar, V. and Ewenz, C.M. (2016). Urban Heat Island traverses in the City of Adelaide, South Australia. *Urban Climate*, 17 pp. 89-101.
56. Guan, H., Vinodkumar, V., Clay, R., Kent, C., Bennett, J.M., Ewenz, C.M., et al. (2016). Temporal and spatial patterns of air temperature in a coastal city with a slope base setting. *Journal of Geophysical Research: Atmospheres*, 121(10) pp. 5336-5355.
57. Jiang, L., Shang, S., Yang, Y. and Guan, H. (2016). Mapping interannual variability of maize cover in a large irrigation district using a vegetation index – phenological index classifier. *Computers and Electronics in Agriculture*, 123 pp. 351-361.
58. *Luo, Z., Guan, H., Zhang, X., Zhang, C., Liu, N. and Li, G. (2016). Responses of plant water use to a severe summer drought for two subtropical tree species in the central southern China. *Journal of Hydrology: Regional Studies*, 8 pp. 1-9.
59. *Wang, H., Guan, H. and Simmons, C.T. (2016). Modeling the environmental controls on tree water use at different temporal scales. *Agricultural and Forest Meteorology*, 225 pp. 24-35.
60. *Wang, H., Guan, H., Guyot, A., Simmons, C. and Lockington, D. (2016). Quantifying sapwood width for three Australian native species using electrical resistivity tomography. *Ecohydrology*, 9(1) pp. 83-92.
61. Wang, Y., Ma, J. and Guan, H. (2016). A mathematically continuous model for describing the hydraulic properties of unsaturated porous media over the entire range of matric suctions. *Journal of Hydrology*, 541(Part B) pp. 873-888.
62. *Yang, Y., Guan, H., Batelaan, O., McVicar, M.R., Long, D., Piao, S., et al. (2016). Contrasting responses of water use efficiency to drought across global terrestrial ecosystems. *Scientific Reports*, 6. <https://www.nature.com/articles/srep23284>
63. Zhang, X.P., Guan, H., Zhang, X.Z., Wu, H.W., Li, G. and Huang, Y.M. (2015). Simulation of stable water isotopic composition in the atmosphere using an isotopic Atmospheric Water Balance Model. *International Journal of Climatology*, 35(6) pp. 846-859.
64. Guan, H., He, X. and Zhang, X. (2015). A comprehensive examination of global atmospheric CO2 teleconnections using wavelet-based multi-resolution analysis. *Environmental Earth Sciences*, 74(10) pp. 7239-7253.
65. Guan, H., McGrath, A.J., Clay, R., Ewenz, C.M., Bengert, S.N. and Bennett, J.M. (2015). Effective surface areas for optimal correlations between surface brightness and air temperatures in an urban environment. *Journal of Applied Remote Sensing*, 9(1) pp. 096059.
66. He, X., Guan, H. and Qin, J. (2015). A hybrid wavelet neural network model with mutual information and particle swarm optimization for forecasting monthly rainfall. *Journal of Hydrology*, 527 pp. 88-100.
67. Liang, W., Yang, Y., Fan, D., Guan, H., Zhang, T., Long, D., et al. (2015). Analysis of spatial and temporal patterns of net primary production and their climate controls in China from 1982 to 2010. *Agricultural and Forest Meteorology*, 204 pp. 22-36.


68. *Yang, Y., Guan, H., Long, D., Liu, B., Qin, G., Qin, J., et al. (2015). Estimation of Surface Soil Moisture from Thermal Infrared Remote Sensing Using an Improved Trapezoid Method. *Remote Sensing*, 7 pp. 8250-8270.
69. *Yang, Y., Long, D., Guan, H., Liang, W., Simmons, C.T. and Batelaan, O. (2015). Comparison of three dual-source remote sensing evapotranspiration models during the MUSOEXE-12 campaign: Revisit of model physics. *Water Resources Research*, 51(5) pp. 3145-3165.
70. Zhang, X., Guan, H., Zhang, X., Wu, H., Lia, G. and Huang, Y. (2015). Simulation of stable water isotopic composition in the atmosphere using an isotopic Atmospheric Water Balance Model. *International Journal of Climatology*, 35(6) pp. 846-859.
71. *Yang, Y., Guan, H., Shen, M., Liang, W. and Jiang, L. (2015). Changes in autumn vegetation dormancy onset date and the climate controls across temperate ecosystems in China from 1982 to 2010. *Global Change Biology*, 21(2) pp. 652-665.
72. Guan, H., Soebarto, V., Bennett, J., Clay, R., Andrew, R., Guo, Y., et al. (2014). Response of office building electricity consumption to urban weather in Adelaide, South Australia. *Urban Climate*, 10(Part 1) pp. 42-55.
73. *Yang, Y., Long, D., Guan, H., Scanlon, B., Simmons, C., Jiang, L., et al. (2014). GRACE satellite observed hydrological controls on interannual and seasonal variability in surface greenness over Mainland Australia. *Journal of Geophysical Research: Biogeosciences*, 119(12) pp. 2245-2260.
74. *Yang, Y., Guan, H., Shang, S., Long, D. and Simmons, C. (2014). Toward the Use of the MODIS ET Product to Estimate Terrestrial GPP for Nonforest Ecosystems. *Geoscience and Remote Sensing Letters, IEEE*, 11(9) pp. 1624-1628.
75. *Xu, X., Guan, H. and Deng, Z. (2014). Isotopic composition of throughfall in pine plantation and native eucalyptus forest in South Australia. *Journal of Hydrology*, 514 pp. 150-157.
76. *Wang, H., Guan, H., Gutierrez-Jurado, H. and Simmons, C. (2014). Examination of water budget using satellite products over Australia. *Journal of Hydrology*, 511 pp. 546-554.
77. *Wang, H., Guan, H., Deng, Z. and Simmons, C. (2014). Optimization of canopy conductance models from concurrent measurements of sap flow and stem water potential on Drooping Sheoak in South Australia. *Water Resources Research*, 50(7) pp. 6154-6167.
78. Bresciani, E., Miraldo Ordens, C., Werner, A., Batelaan, O., Guan, H. and Post, V. (2014). Spatial variability of chloride deposition in a vegetated coastal area: Implications for groundwater recharge estimation. *Journal of Hydrology*, 519 pp. 1177-1191.
79. *He, X., and Guan, H. (2013). Multiresolution analysis of precipitation teleconnections with large-scale climate signals: A case study in South Australia, *Water Resources Research*, doi:10.1002/wrcr.20560.
80. *He, X., Guan, H., Zhang, X., C.T. Simmons (2013). A wavelet-based multiple linear regression model for forecasting monthly rainfall, *International Journal of Climatology*, DOI: 10.1002/joc.3809
81. Guan, H., Zhang, X., Skrzypek, G., Sun, Z. and Xu, X. (2013). Deuterium excess variations of rainfall events in a coastal area of South Australia and its relationship with synoptic weather systems and atmospheric moisture sources. *Journal of Geophysical Research*, 118(2) pp. 1123-1138. [10.1002/jgrd.50137].

82. Guan, H., Zhang, X., Makhnin, O. and Sun, Z. (2013). Mapping mean monthly temperatures over a coastal hilly area incorporating terrain aspect effects. *Journal of Hydrometeorology*, 14 pp. 233-250. [10.1175/JHM-D-12-014.1].
83. *Deng, Z., Priestley, S., Guan, H., Love, A. and Simmons, C. (2013). Canopy enhanced chloride deposition in coastal South Australia and its application for the chloride mass balance method. *Journal of Hydrology*, 497 pp. 62-70. [10.1016/j.jhydrol.2013.05.040].
84. Guan, H., Hutson, J., Ding, Z., Love, A., Simmons, C. and Deng, Z. (2013). Principal component analysis of watershed hydrochemical response to forest clearance and its usefulness for chloride mass balance applications. *Water Resources Research*, 49 pp. 1-17. [10.1002/wrcr.20357].
85. Yang, Y., Shang, S., Guan, H. and Jiang, L. (2013). A novel algorithm to assess gross primary production for terrestrial ecosystems from MODIS imagery. *Journal of Geophysical Research*, 118(2) pp. 590-605. [10.1002/jgrg.20056].
86. *Zhu, S., Guan, H., Bennett, J., Clay, R., Ewenz, C., Benger, S., et al. (2013). Influence of sky temperature distribution on sky view factor and its applications in urban heat island. *International Journal of Climatology*, 33(7) pp. 1837-1843. [10.1002/joc.3660].
87. Zhu, S., Guan, H., Millington, A. and Zhang, G. (2013). Disaggregation of land surface temperature over a heterogeneous urban and surrounding suburban area: a case study in Shanghai, China. *International Journal of Remote Sensing*, 34(5) pp. 1707-1723. [10.1080/01431161.2012.725957]
88. *Mollehuara Canales, R.F., Guan, H., Bestland, E.A., Hutson, J.L. and Simmons, C. (2013). Particle-size effects on dissolved arsenic adsorption to an Australian laterite. *Environmental Earth Sciences*, 68(8) pp. 2301-2312. [10.1007/s12665-012-1909-3]
89. Guan, H., Sebben, M. and Bennett, J. (2013). Radiative- and artificial-cooling enhanced dew collection in a coastal area of South Australia. *Urban Water Journal*, pp. 1-10. [10.1080/1573062X.2013.765494]
90. Zhang, X., Zhian, S., Guan, H., Zhang, X., Huawu, W. and Yimin, H. (2012). GCM simulations of stable isotopes in the water cycle in comparison with GNIP observations over East Asia. *Acta Meteorologica Sinica*, 26(4) pp. 420-437. [10.1007/s13351-012-0403-x]
91. Yang, Y., Shang, S. and Guan, H. (2012). Development of a soil-plant-atmosphere continuum model (HDS-SPAC) based on hybrid dual-source approach and its verification in wheat field. *Science China Technological Sciences*, 55(10) pp. 2671-2685. [10.1007/s11431-012-4974-7]
92. *Yang, Y., Guan, H., Hutson, J., Wang, H., Ewenz, C., Shang, S., et al. (2012). Examination and parameterization of the root water uptake model from stem water potential and sap flow measurements. *Hydrological Processes*, [10.1002/hyp.9406]
93. Huang, G., Fallowfield, H., Guan, H. and Liu, F. (2012). Remediation of nitrate-nitrogen contaminated groundwater by a heterotrophic-autotrophic denitrification approach in an aerobic environment. *Water Air and Soil Pollution*, 223(7) pp. 4029-4038.
94. *Jahan, N., Guan, H., & Bestland, E.A., 2011. Arsenic remediation by Australian laterites. *Environmental Earth Sciences*, 64(1), 247-253.
95. Guan, H., Love, A.J., Simmons, C.T., Hutson, J.L., & Ding, Z., 2010. Catchment conceptualisation for examining applicability of chloride mass balance method in an area with historical forest clearance. *Hydrology and Earth System Sciences*, 14, 1233-1245.

96. Guan, H., Love, A.J., Simmons, C.T., Makhnin, O., & Kayaalp, A., 2010. Factors influencing chloride deposition in a coastal hilly area and application to chloride deposition mapping. *Hydrology and Earth System Sciences*, 14, 801-813.
97. Guan, H., Bestland, E.A., Zhu, C., Zhu, H., Albertsdottir, D., Hutson, J.L., Simmons, C.T., Ginic-Markovic, M., Tao, X., & Ellis, A.V., 2010. Variation in performance of surfactant loading and resulting nitrate removal among four selected natural zeolites. *Journal of Hazardous Materials*, 183(1-3), 616-621.
98. Guan, H., J. Simunek, B.D. Newman, and J. L. Wilson, Modeling investigation of water partitioning at a semiarid ponderosa pine hillslope, *Hydrological Processes*, 10.1002/hyp.7571, 2010.
99. Guan, H., and J. Wilson. A hybrid dual-source model for potential evaporation and transpiration partitioning, *Journal of Hydrology*, v. 375, 578-588, doi:10.1016/j.jhydrol 2009.07.007, 2009.
100. Guan, H., J. Wilson, and H. Xie. A cluster-optimizing regression-based approach for precipitation spatial downscaling in mountainous terrain, *Journal of Hydrology*, v. 375, 578-588, doi:10.1016/j.jhydrol 2009.07.007, 2009.
101. Guan, H., C. Simmons, and A. Love. Orographic controls on rain water isotope distribution in the Mount Lofty Ranges, South Australia, *Journal of Hydrology*, v. 372, 255-264, doi:10.1016/j.jhydrol 2009.06.018, 2009.
102. Zhou, X., H. Guan, H. Xie, and J.L. Wilson, Analysis and optimization of NDVI definitions and areal fraction models in remote sensing of vegetation, *International Journal of Remote Sensing*, 30(3), 721-751, 2009.
103. Guan, H., H. Hsu, O. Makhnin, H. Xie, and J. L. Wilson, Examination of selected atmospheric and orographic effects on monthly precipitation of Taiwan using the ASOADEK model, *International Journal of Climatology*, 29, 1171-1181, doi: 10.1002/joc1762, 2009.
104. Xie, H., H. Guan, M. Zhu, M. Thueson, S.F. Ackley, and Z. Yue. A conceptual model for explanation of albedo changes in Martian craters, *Planetary and Space Science* 56, 887-894, 2008.
105. Guan, H., H. Xie, and M. Zhu, Canopy blockage and scattering effects on apparent soil spectral reflectance and its consequence in spectral mixture analysis of vegetated surfaces, *International Journal of Remote Sensing*, v. 29, 3509-3522, 2008.
106. Wang, X., H. Xie, H. Guan, and X. Zhou, Different responses of MODIS-derived NDVI to root-zone soil moisture in semi-arid and humid regions and their implications for root-zone soil moisture estimation, *Journal of Hydrology*, v. 340, iss. 1-2, p. 12-24, 2007.
107. Gutierrez-Jurado, H.A., E. R. Vivoni, B. J. Harrison, and H. Guan, Ecohydrological controls on soil pedogenesis in complex semiarid rangelands, *Hydrological Processes*, 20, 3289-3316, 2006.
108. Guan, H., J.L. Wilson, and O. Makhnin, Geostatistical mapping of mountain precipitation incorporating auto-searched effects of terrain and climatic characteristics, *Journal of Hydrometeorology*, 6(6), 1018-1031, 2005.
109. Guan, H., E. Vivoni, and J.L. Wilson, Effects of atmospheric teleconnections on seasonal precipitation in mountainous regions of the southwestern U.S. -- A case study in northern New Mexico, *Geophysical Research Letters*, 32, L23701, 2005.

110. Wilson, J.L., and H. Guan, Mountain-block hydrology and mountain-front recharge, in *Groundwater Recharge in a Desert Environment: The Southwestern United States*, edited by J.F. Hogan, F.M. Phillips, and B.R. Scanlon, Water Science and Applications Series, vol. 9, American Geophysical Union, Washington, D.C., 113-137, 2004. (Book chapter)
111. Schulze-Makuch, D., H. Guan, and S.D. Pillai, Effects of pH and geological medium on bacteriophage MS2 transport in a model aquifer. *Geomicrobiology*, 20:73-84, 2003.
112. Guan, H., D. Schulze-Makuch, S. Schaffer, and S.D. Pillai, The effect of critical pH on virus fate and transport in saturated porous medium. *Ground Water*, 41(5):701-708, 2003.
113. Schulze-Makuch, D., R. Bowman, S. D. Pillai, and H. Guan, Field evaluation of the effectiveness of surfactant modified zeolite and iron-oxide-coated sand for removing viruses and bacteria from ground water. *Ground Water Monitoring & Remediation* 23(4):68-74, 2003.
114. Schulze-Makuch, D., L.N. Irwin, and H. Guan, Search parameters for the remote detection of extraterrestrial life. *Planetary and Space Science*, 50, 675-683, 2002.

RESUME

| Basic Information | | | | |
|--|--|--|--|---|
| Name | Zhongli Liu | Birth | Feb-1995 |  |
| Sex | Male | Place of Birth | Yuyeyang City | |
| Nationality | China | Nation | Han | |
| Highest Degree | Master Degree | Graduate Date | Jun-2021 | |
| E-mail | Liu1545@Flinders.edu.au | Telephone | 61-0466529234 | |
| Tertiary Education | | | | |
| Date from | Date to | Institution | Major | |
| Jan-2022 | present | Flinders University | Ecohydrology | |
| Sep-2018 | Jun-2021 | Hunan Normal University | Physical Geography | |
| Sep-2013 | Jun-2017 | Guizhou University of Finance and Economics | Physical Geography and Resources Environment | |
| Research Project | | | | |
| Date from | Date to | Project Name | Position and Responsibilities | |
| Jan-2022 | present | “Unsaturated zone functioning in a semi-arid, flash flood driven hydrologic regime” funded by Australian Research Council (LP210300691) | Participation. using remote sensing to investigate climate, water and ecosystem interactions | |
| Sep-2018 | Dec-2019 | “Sampling, simulation and comparison on stable isotopes of water in the Xiangjiang River Basin” funded by National Natural Science Foundation of China (No.41571021) | Participation. Responsible for sampling stable isotopes of water and managing financial reimbursement of the team. | |
| Skills and Certificates | | | | |
| Computer | National Computer Rank Examination Band II; Proficiency in use of Word, Excel, Power Point, GrADS, Origin, SPSS, ArcGIS Pro, Matlab, Python and GEE. | | | |
| Self Evaluation | | | | |
| Hard-working, adapt to long-term investigation, patient, energetic, punctual, responsible, earnest and diligent. | | | | |
| Good at and willing to communicate with others, well-maintained daily routine, keen on sports. | | | | |
| Diverse hobbies such as reading, electronic sports, billiards, hiking, and in particular badminton. | | | | |

Curriculum Vitae for Wenjie Liu

Full name: Wenjie Liu

Date of birth: 1994/06/14

Mobile: 0468942865

Email: liu1385@flinders.edu.au



Academic Qualifications

Bachelor's Degree *2012 - 2016*
Changsha University of Science & Technology, School of Traffic & Transportation Engineering
Master's Degree *2016 - 2019*
Central South University, School of Geosciences and Info-Physics
PhD Candidature *2021 - Present*
Flinders University, College of Science and Engineering

Skills and Expertise

GIS: Experienced in GIS software and coding for data analysis and mapping.

Remote Pilot License: Licensed for drone operation and aerial data collection.

English: Fluent in spoken and written communication.

Published Research and Conference Presentations

1. Liu, W., Zeng, Y., Zhang, M. (2018) Mapping rice paddy distribution by using time series HJ blend data and phenological parameters. *Journal of remote sensing*. 2018, 22(3):381-391.
2. Liu, W., Zeng, Y., Li, S., Pi, X., & Huang, W. (2019). An improved spatiotemporal fusion approach based on multiple endmember spectral mixture analysis. *Sensors*, 19(11), 2443.
3. Liu, W., Zeng, Y., Li, S., & Huang, W. (2020). Spectral unmixing based spatiotemporal downscaling fusion approach. *International Journal of Applied Earth Observation and Geoinformation*, 88, 102054.
4. Liu, W., Guan, H., Gutiérrez-Jurado, H. A., Banks, E. W., He, X., & Zhang, X. (2022). Modelling quasi-three-dimensional distribution of solar irradiance on complex terrain. *Environmental Modelling & Software*, 149, 105293.
5. Liu, W., Guan, H., Hesp, P. A., & Batelaan, O. (2023). Remote sensing delineation of wildfire spatial extents and post-fire recovery along a semi-arid climate gradient. *Ecological Informatics*, 78, 102304.
6. Presenter at AGU Fall Meeting, December 2021
Modelling quasi-three-dimensional distribution of solar irradiance on complex terrain.
7. Presenter at MODSIM, July 2023
Spatial modelling of understorey evapotranspiration based on the Maximum Entropy Production method

Research Experience

June 2021 - Present, research assistant

MDPA Project: Estimation of flood plain understorey evapotranspiration based on the maximum entropy production method.

Hansen Guan

Undergraduate Student

Skills

Conversant in mandarin

Fluent in Python and Excel

*Experience working with
ArcGIS Pro and Google Earth
Engine*

Extracurricular Activities

Debate Team, 2017 - 2019
Was part of the ASMS debate
team, making it to the
quarterfinals in 2018.

*Japan Super Science Fair,
2018*
Created a scientific poster with
the help of Martin Westwell
and Ancret Szapak, which was
then presented at the Japan
Super Science Fair at
Ritsumeikan University.

Internships

*Geochemistry Internship with
Olivier Alard, 2023*
Prepared olivine,
clinopyroxene, orthopyroxene
and spinel samples for analysis
with the electron microprobe.
Also conducted preliminary
analysis of the resultant data.

Hansen Guan

124 Bandjalong Crescent
Aranda, ACT 2614

0435 513 882
hansenguan333@gmail.com

About Me

I am an undergraduate student at ANU, currently pursuing a major
in Earth Science.

I'm currently looking for work experience opportunities or
internships in the Earth Sciences field to further my practical
experiences.

Yum Sing / Waiter

November 2017 - January 2020, Old Reynella SA

Provided customer service, taking orders and delivering food and
drinks. Also handled cash and credit card transactions at the
takeaway counter

KFC / FOH Team Member

October 2020 - February 2023, Fyshwick ACT

Provided customer service at the front counter and drive through,
packed orders and prepared the restaurant for opening at the
start of the day. Functioned as part of a team in a fast paced and
stressful environment.

ASMS / Higher Secondary Certificate

January 2017 - December 2019, Adelaide

English Literary Studies, Maths Methods, Specialist Maths,
Chemistry, University Extension Studies (Physics)

Australian National University / Bachelor of Science

January 2020 - PRESENT, Canberra

Earth Science Major with a Physics Minor

The Brief

13 October 2023

Dr Huade Guan,
Associate Professor in Hydrology, Flinders University
GPO Box 2100
Adelaide SA 5001

By email: huade.guan@flinders.edu.au

Dear Dr Guan

**BRIEF FOR PREPARATION OF AN EXPERT REPORT FOR USE BY THE
APPLICANT IN PROCEEDINGS WAD 37/2022 – Yindjibarndi Ngurra Aboriginal
Corporation Compensation Claim**

Introduction

1. I act for the Yindjibarndi Ngurra Aboriginal Corporation (YNAC) Applicant in this proceeding. Under s 56(3) of the *Native Title Act 1993* (Cth) (NTA) the Applicant, Yindjibarndi Ngurra Aboriginal Corporation (YNAC), holds in trust for the common law holders (**Yindjibarndi People**) the native title rights and interests that were recognised by the determination titled *Warrie (formerly TJ) on behalf of the Yindjibarndi People v State of Western Australia (No. 2)* [2017] FCA 1299; (2017) 366 ALR 467 (**Warrie (No 2)**)).
2. On 18 February 2022, YNAC filed a compensation application in the Federal Court (WAD37/2022) seeking compensation under ss 50(2) and 61(1) of the NTA. The proceeding involves a compensation application for whole or partial suppression and hence significant diminishing and impairment by, the grants of FMG tenements within the areas of those tenements and will remain suppressed, impaired and diminished for however long those tenements remain on foot.
3. Mining operations at FMG’s Solomon Hub Project (**SHP**) commenced in about October 2012. FMG states that the SHP has an “expected life” of about 33 years but realistically

the life of the mine is unknown. Mining leases, exploration licences, prospecting licences, miscellaneous licences and groundwater licences have been granted for mining and auxiliary infrastructure, including gas pipelines and power stations over an area that includes the Kings, Trinity, Firetail North and Firetail South mining areas within the *Warrie (No 2)* area. Some of the SHP is in Eastern Guruma country to the south-west.

4. Miscellaneous licences and groundwater licences have been granted over an area which includes the Kings, Trinity, Firetail North and Firetail South Mine Pits within the SHP. **Attachment 1** contains copies of FMG Respondent's miscellaneous licences annexed to the affidavit of David Crabtree of the Department of Mines, Industry Regulation and Safety dated 16 June 2023. Copies
5. Further, FMG's hydrogeologist, Christopher Oppenheim, has provided two affidavits, both dated 4 August 2023 found at **Attachment 2A and 2B**. I recommend you begin by reading these two affidavits. They provide a succinct outline of FMG's abstraction and supplementation activities in the compensation area. Please note, these affidavits have been provided by an FMG employee. However, they can be relied on for their objective content. Copies of FMG's groundwater licences – which allow the taking of water from within their miscellaneous licences – are annexed to **Attachment 2B**, being the second of Christopher Oppenheim's affidavits.
6. The Compensation Application is brought on behalf of those Aboriginal people who, but for the grant of the mining tenements, hold exclusive possession native title rights and interests in relation to that area (**Compensation Claim Group**) as described in the *Warrie (No 2)* determination. The area of the compensation application (**Compensation Area**) is identical to the area the subject of the approved determination of native title made by the Court in *Warrie (No 2)*. See at **Attachment 3** a map of the determined native title area with exclusive and non-exclusive possession areas. **Attachment 4** contains an overview map of the are impacted by the SHP and 14 enlargement maps. These maps contain coordinates of the area of the compensation area directly impacted by mining construction and infrastructure.

Native Title compensation claims in Australia

7. The entitlement to compensation under the NTA is an entitlement on just terms to compensate the Compensation Claim Group for any loss, diminution, impairment or other effect of the granting of the Compensable Acts on their native title rights and

interests. The Applicant will argue that the entitlement to compensation would extend to and include compensation for any past or future economic loss attributable to the extinguishment (or complete suppression) of the Compensation Claim Group's native title rights and interests.

8. In *Northern Territory v Mr A. Griffiths (deceased) and Lorraine Jones on behalf of the Ngaliwurru and Nungali Peoples* [2019] HCA 7 (**Timber Creek**) the High Court of Australia determined that compensation for loss of native title can be bifurcated to economic and non-economic loss. Non-economic loss includes the loss of spiritual and cultural attachment: see https://www.austlii.edu.au/cgi-bin/viewdoc/au/cases/cth/HCA/2019/7.html?context=1;query=timber%20creek;mask_path=au/cases/cth/HCA.

Impacts to water and groundwater

9. We are instructed that Kangeenarina Creek and Weelumurra Creek (please note, our clients refer to it as Wirlu-Murra Creek and elsewhere it is referred to as Wirlumurra Creek), as well as permanent pools and springs that are connected to the waters of the Fortescue River and underlying aquifers. We are instructed that permanent water holes and pools, such as Millstream, are affected by the de-watering of the SHP and are visibly depleted. FMG is extracting water, utilising bores and pumps and other water extracting methods. Further, a grout wall has been constructed on the Mine site near the Valley of the Queens (in Eastern Guruma country and outside the Compensation Area). I am instructed that the grout wall has been constructed for the purposes of stopping water flowing into the Mine site from Weelumurra Creek (in the compensation claim area but outside of the SHP).
10. **Attachment 5** contains four photos of permanent pools at Kangeenarina Creek taken on 16 August 2023. This creek is one of the water bodies the Yindjibarndi people say is depleted in comparison to historical levels, as a result of the mine.
11. I attach, at **Attachment 6**, documents I consider may assist your report. These documents contain monitoring data, descriptions of management plans, descriptions of the hydrogeological models for the region and observed or predicted impacts of mining activities on ground water and groundwater-dependent vegetation, such as abstraction, de-watering, construction and supplementation. This attachment contains an index of,

and a link to, those documents, including baseline reports. You should also conduct a review of any literature you consider relevant.

Background

12. Also included with this Brief, at **Attachment 7**, is a copy of the Applicant's Further Amended Points of Claim filed on 27 June 2023, which sets out a detailed description of the compensation claim.
13. Under the *Mining Act 1978* (WA), the following Miscellaneous Licences, referred to in these proceedings as "*Water Management Miscellaneous Licences*", have been granted to FMG:
 - L47/302
 - L47/361
 - L47362
 - L47/363
 - L47/367
 - L47/396
 - L47/472
 - L47/697
 - L47/801
 - L47/813
 - L47/814
 - L47/914
 - L47/919
14. Those Miscellaneous Licences permit a range of water management activities, including "taking water". I attach copies of these licences at **Attachment 8**. These are the same licences annexed to **Attachment 1**. I've compiled them separately for ease of reference.

Benefits of a determination of native title

15. By way of background, the recognition of native title rights and interests under the NTA can and do give rise to significant benefits for native title holders. In general terms, the recognition of native title rights and interests provides native title holders with the right to have those rights and interests protected and enforced.

16. Under the NTA, native title holders also have certain statutory rights including a statutory ‘right to negotiate’ before any mineral, petroleum or other tenements/land holdings are granted over their land (but not a right of veto), if the grant would adversely affect their native title rights and interests. In circumstances where the grant of a proposed mineral tenement would damage a significant site, there is potential for the native title holders to protect that site and effectively prevent the grant from taking place. This right, conferred by Subdivision P, Part 2 of the NTA, would be of particular importance to the members of the Compensation Claim Group who are concerned to protect numerous spiritually significant sites that include but are not limited to sites contained in the ceremonial Bundut that includes, but is not limited to, water sources Ganjingaringunha *wundu* (Kangeenarina Creek), Ganjingaringunha *jinbi* (spring), and other water sources that I am instructed are water-related sites off the Mine. These include, but are not limited to, Weelumurra, Bangkangarra, Jindawarina (Millstream) and Ngurrin Harding River (which include important water sources where Yindjibarndi People have camped, hunted and gathered for thousands of years).
17. The certainty associated with a native title determination from the Court can also strengthen the efforts of native title holders to manage their traditional lands, including through the declaration of an Indigenous Protected Area (**IPA**), a project administered by the Commonwealth Government. It can also assist native title holders to obtain secure tenure for their communities, resulting in enhanced certainty and, arguably, promoting government investment in community facilities and infrastructure.
18. A determination of native title also enhances the ability of native title holders to carry out economic activities on their traditional lands with a view towards their financial betterment or social development, including the exploitation of resources (such as water) or the conduct of tourism activities.
19. The benefits of native title do not include alienability but do include (as outlined above at [11]) the right to negotiate with, and receive compensation from, Government or third parties who wish to carry out mining or other development activities on the land concerned. This statutory ‘right to negotiate’ in relation to certain development projects, and in particular mining and petroleum resource exploitation can at times provide significant wealth to common law native title holders. The loss of native title rights and interests and of the concomitant statutory right to negotiate may, depending upon the circumstances, have a significant economic impact on the native title holders.

20. Native title is more than just the sum total of the rights and interests which may be recorded in a determination of native title. In *Yanner v Eaton* (1999) 201 CLR 351 at 372-3 [37], four Justices of the High Court stated in a joint judgment, that native title rights and interests not only find their origin in traditional Aboriginal laws and customs, “*they reflect connection with the land*”. Their Honours quoted with approval the comments of Brennan J in *R v Toohey & Anor, ex parte Meneling Station Pty Ltd* (1983) 158 CLR 327 at 358 that “*Aboriginal ownership is primarily a spiritual affair rather than a bundle of rights*”.
21. Their Honours acknowledged (at 373 [38]) that the spiritual, cultural and social connection of Aboriginal people with the land is an important aspect of native title:¹
- “Native title rights and interests must be understood as what has been called ‘a perception of socially constituted fact’ as well as ‘comprising various assortments of artificially defined jural rights’ and an important aspect of the socially constituted fact of native title rights and interests that is recognised by the common law is the spiritual, cultural and social connection with the land.”*
22. The loss of spiritual and cultural connection has been acknowledged by the High Court of Australia as being part of the non-economic component of compensation for the suppression, impairment, loss and diminishment of native title.

The cultural significance of water to the Compensation Claim Group

23. Understanding the cultural status of water to the Yindjibarndi people is necessary when considering this non-economic component of compensation.
24. The underground flow – from Yaandanyira (Fortescue River) to Millstream – gives Yindjibarndi country life. It is a Dreaming track of crucial significance. Along it is Gregory’s Gorge, the site of their initial creation. At Bilin Bilin, the very first *Bundut* was performed. The Yindjibarndi have *jowi* (songs) at Kangeenarina Creek, Wirlumurra Creek and elsewhere along the waterway. They have *thalu* (increase sites) connected to this waterway. *Thalu* are both sites of religious significance – nodes at which to speak to country – and practical land management, concerned with species conservation and ecosystem health.

¹ These passages from *Yanner v Eaton* were cited with approval by the Full Federal Court in *Northern Territory v Alyawarr* (2005) 145 FCR 442 at 463 [68].

25. The existence of that water flow from Yaandanyira to Millstream is central to their cultural identity. It binds the Yindjibarndi People to their ancestors, their country and their very creation at the hands of Marga, their creator being. Impacts to the flow of water through Yindjibarndi country weaken this bind.
26. Throughout their witness statements, Yindjibarndi people acknowledge their worry, sadness, anxiety and desperation at the way their waterways are being affected by the SHP. These effects, they say, constrict their cultural practice, including the *Bundut*, the songs and dance of which are now “empty” and “broken” where water levels are significantly lowered. They also speak of reduced plant and animal species, restricting traditional hunting practices.
27. Ultimately, as the many groundwater-fed *jinbi* (springs, pools) diminish, the Yindjibarndi report feeling alienated from their country and helpless as to its care. Water management and extraction activities connected with the SHP have resulted in feelings of loss, hurt and failed responsibility to care for their country.
28. **Attachment 9** includes references to water, contained in the Aboriginal lay-witness statements filed in these proceedings.

Assumed Facts

29. In preparing your report, you should adopt the following assumptions:
 - (a) The SHP is an open-cut iron ore mine in the Hamersley Ranges located 60km north of Tom Price.
 - (b) SHP has a production capacity of 72-100 million tonnes per annum (Mtpa) that includes pits outside the *Warrie (No 2)* area.
 - (c) It comprises the Firetail, Valley of the Kings, Trinity and Valley of the Queens pits as well as contour mining of large portions of Gambalana (Hamersley Ranges), which together have a production capacity of 75 million tonnes of iron ore per annum. Mining operations at the Firetail deposit of the mine commenced in October 2012. The expected mine life of SHP is 33 years.
 - (d) The tenements which comprise the SHP are wholly owned by the FMG Respondents and were granted between 2006 and 2020. Applications for mining tenements by FMG are ongoing, including Miscellaneous Licences for taking water.
 - (e) Approximately 75% of the tenements comprising the SHP were in the Yindjibarndi #1 Native Title determination application area (that was filed on 9 July 2003) and,

from when the determination was made on 17 November 2017, the *Warrie (No 2)* area.

- (f) No agreement has been reached between FMG and the Yindjibarndi People when they were claimants or recognised native title holders after 17 November 2017 in relation to the grant of any of the tenements which comprise the SHP.
- (g) FMG has entered into a relationship and agreements with some, but not all, of the common law native title holders without the consent of the registered claimant for the Yindjibarndi #1 native title determination application (prior to 17 November 2017) or of the YNAC (after 17 November 2017). These agreements and relationships are ongoing. The group of people who have a relationship and agreements with FMG are an Aboriginal Corporation called Wirlu-Murra Yindjibarndi Aboriginal Corporation (**WYAC**). This has caused a division in the Yindjibarndi community between supporters of WYAC and YNAC.
- (h) Due to the ongoing agreements and relationships between FMG and WYAC, but not all Yindjibarndi People, between July 2010 and 17 November 2017, FMG did not consult with the registered claimant for the Yindjibarndi #1 native title determination application (prior to 17 November 2017) in relation to heritage surveys or work programme clearances.
- (i) The Yindjibarndi People have a spiritual obligation, embedded in their traditional laws and customs, to protect their country, including from the presence and activities on it of strangers (or *manjangu*) unless the stranger(s) first obtain(s) permission from Yindjibarndi People: *Warrie (formerly TJ) (on behalf of the Yindjibarndi People) v State of Western Australia* [2017] FCA 803 (**Warrie**) at [54]-[55].
- (j) Many Yindjibarndi People live in Roebourne or Karratha and were moved into the area from further south in the 1960 and 1970s after the Equal Wages case provided that Aboriginal people must be paid the same as non-Aboriginal people. Both Roebourne and Karratha are on Ngarluma country.
- (k) Native title has a physical or material aspect (the right to do something in relation to land) and a cultural or spiritual aspect (the connection with the land).
- (l) I cannot find a record of the closure of an open cut iron ore mine in the Pilbara and hence, I cannot provide you with any record of closed, remediated and rehabilitated iron ore mines and whether there is any likelihood that the SHP can ever be properly rehabilitated.

- (m) The Yindjibarndi People value water for their economic benefit of providing them with food. They also have a strong spiritual and cultural connection to water sources (see **Attachment 9** that are extracts of the Yindjibarndi witness' evidence about their spiritual and cultural connection to water on their country.

Yindjibarndi Native Title determinations

30. There have been two fully contested native title claims taken on behalf of the Yindjibarndi People. The first one was commenced in 1996 by Ngarluma and Yindjibarndi elders on behalf of the respective societies in *Daniel v Western Australia* [2003] FCA 666 (*Daniel*) (the State appealed this decision to the Full Federal Court in 2005 and were unsuccessful): see https://www.austlii.edu.au/cgi-bin/viewdoc/au/cases/cth/FCA/2003/666.html?context=1;query=daniel;mask_path=au/cases/cth/FCA. In *Daniel* the Court recognised that the Ngarluma and Yindjibarndi held non-exclusive native title rights and interests. The non-exclusive rights and interests in *Warrie (No 2)* are identical to those now determined in the *Daniel* determination area since the latter was revised in 2020: see http://www.austlii.edu.au/cgi-bin/viewdoc/au/cases/cth/FCA/2020/1416.html?context=1;query=Yindjibarndi;mask_path=au/cases/cth/FCA.
31. Rares J recognised native title in *Warrie* : see https://www.austlii.edu.au/cgi-bin/viewdoc/au/cases/cth/FCA/2017/803.html?context=1;query=warrie;mask_path=au/cases/cth/FCA. The Court then made a determination of native title on 13 November 2017 over the area that comprises the SHP in *Warrie (No. 2)*: see https://www.austlii.edu.au/cgi-bin/viewdoc/au/cases/cth/FCA/2017/1299.html?context=1;query=warrie;mask_path=au/cases/cth/FCA over the area of **Attachment 3**.
32. Native title has a physical or material aspect (the right to do something in relation to land) and a cultural or spiritual aspect (the connection with the land).
33. You should use defensible and sound methodologies in your report to support your opinions.

Scope of your report

34. The Brief requires you to complete an expert report and provide it in draft form to YNAC by **6 December 2023**.
35. In preparing and compiling your report, you are asked to:

- (a) review and critically assess the material provided with this Brief to the extent that it is relevant;
 - (b) conduct further research, including academic research, or request YNAC to conduct further research, to obtain additional material required to provide a proper and informed basis for any opinions expressed.
36. A broad description of the ecological impacts we are engaging you to interrogate are:
- (a) changes to vegetation richness, extent and any other markers of ecological health you deem appropriate, caused by FMG's mining activities to groundwater-dependent and terrestrial vegetation, through analysis of remote sensing data;
 - (b) changes to connectivity of surface flows, particularly at Kangeenarina and Weelumurra Creeks, and groundwater flows;
 - (c) any observed or predicted impacts to groundwater levels as a result of dewatering, including after mine closure, and associated long-term ecological impacts related to changes in the water table, through a literature review of reports published by FMG; and
 - (d) any other hydrogeological or ecological impacts, at or surrounding the mine, that you consider relevant.
37. This is a slight change from previous discussions we have had. Rather than provide you with field data, we now only require a literature review and analysis of aerial imagery and remote sensing data. We are engaging another expert, who is based in Perth, to cover field data and provide a report which covers dust, light, noise and vibration pollution.
38. You will also have an opportunity to complete a supplementary report once you have read the Perth-based expert's report.

Literature review

39. Please let me know, as soon as possible, if you wish to be provided with any more documents, including baseline documents, published by FMG. Please note that **Attachment 6** – being an index of documents and a link to a Dropbox folder containing those documents – is far more exhaustive than what has already been provided to you. However, we can request further documents from FMG that are within its possession.

40. For the purposes of the literature review, we ask that you review the full range of literature provided to us by FMG and, based on the mining activities therein described – including dewatering, reinjection, pit construction and the construction of grout walls – any observed and/or potential impacts, your expertise and any other materials that you deem relevant, such as academic reports, draw conclusions about the likely impacts of the SHP that have already occur and are likely to occur. Please use the list of impacts at Paragraph 35 as a guide.

Remote sensing

41. Regarding the remote sensing task, please review Landsat imagery, and any other aerial or satellite imagery that we provide to you, to establish a baseline of vegetation health based on pre-mining levels and compare it to recent vegetation health parameters to determine the impact of FMG’s mining activities on vegetation. Please draw any conclusions, based on your expertise, regarding what are the likely causes of reduced vegetation extent and health and what are the likely outcomes in the short and long-term over the life of the mine and after mine closure.

Timeline

42. You are then, based upon the material provided and further research conducted, to:
- (a) provide YNAC with a draft of your Report by **6 December 2023**, prepared in accordance with the Federal Court’s *Expert Evidence Practice Note (GPN-EXPT)* dated 25 October 2016 annexing the Harmonised Expert Code of Conduct (a copy is **Attachment 10** to this Brief), in which your expert opinion about the extent to which the mining operations by the FMG Respondents at the SHP, including abstraction, de-watering, construction and supplementation has affected, and will continue to affect, the ground water on the claim area and any other part of the Yindjibarndi country;
 - (b) consider any comments or feedback by YNAC on the draft report which may be provided to you on or before **10 December 2023**;
 - (c) having reviewed the comments / feedback provided by YNAC, provide a final Report to YNAC, by no later than **15 December 2023**;

- (d) attend a conference of experts, if required, during the week of 18-24 March 2024 with any expert or experts that may be engaged by the State or FMG and where you will be asked to identify:
 - (i) the matters upon which the experts agree;
 - (ii) the matters upon which the experts do not agree; and
 - (iii) the reasons for any disagreement; and
 - (e) attend at the Federal Court in Perth, if required, in the weeks of 8-19 April 2024, to give expert evidence on the issues addressed in your report.
43. FMG or the State may brief and provide an expert report from their own hydrogeology experts in February 2024. Part of your Brief, therefore, may be to consider and provide comments to YNAC on any such reports relevant to your expertise and background within a timeframe to be agreed (but in any event before your attendance at any experts' conference). Equally, we are engaging another expert ecohydrologist/hydrogeologist to interpret field data, including plant tissue samples, and conduct a literature review adjacent to your own.

The form and content of the Report

44. In compliance with *GPN-EXPT* your report must:
- (a) give details of your qualifications and experience, and of the literature and other materials used in writing the report;
 - (b) clearly and fully state all assumptions of fact which you have made in arriving at the conclusions expressed in your report;
 - (c) identify with precision the factual premises upon which your opinions are based;
 - (d) explain the process of reasoning by which you reached the opinions expressed in your report; and
 - (e) clearly differentiate between the facts upon which your opinions are based and the opinions themselves.
45. If you are assisted by any others in the preparation of the report, the nature of that assistance must be identified with details given of the work carried out by, and the qualifications of, each such person who has assisted.

46. The report should be set out in numbered paragraphs and should append a copy of this Brief. It would also be desirable if you could set out very early in the report, a short description of the materials that you have had regard to and the methodology employed in the preparation and the writing of the report.
47. You should also provide an explanation of the way in which your specialised knowledge, based upon your training, study and experience, has equipped you to provide expert opinion evidence on the issues that are addressed in your report.

Rules governing materials provided to you

48. I understand there have been discussions about data collection for purposes of the compensation claim also being used for a s 46 application to vary FMG's conditions of approval. However, there are strict rules that limit how information gleaned from this litigation can be used in other proceedings.
49. As part of the brief, we will likely provide you with documents that are not in the public domain and were provided by FMG or the State of Western Australia. Information that is not in the public domain and was obtained by discovery or subpoena cannot be used for a collateral or ulterior purpose unrelated to the proceedings in which the information was obtained. This is called an implied or "*Harman*" undertaking after *Harman v Secretary of State for the Home Department* [1983] 1 AC 280. It is a substantive legal obligation owed to the party who produces the documents and to the court: *Hearne v Street* (2008) 235 CLR 125 (*Hearne*) at [107]-[108].
50. The rationale for the undertaking is that the compulsion to produce material violates a party's right to confidentiality, and it would be inequitable for that material to be used for purposes other than that which compelled its production.
51. The *Harman* undertaking binds the litigants in proceedings and also any third party who receives documents and is aware that they have come from legal proceedings: *Hearne* at [109]-[112]. The third party does *not* need to know about the undertaking to be bound by it. Nevertheless, we consider it is important that you are aware that you cannot utilise any documents or data provided to you obtained from FMG as part of the YNAC compensation claim discovery process with FMG unless we indicate otherwise.
52. Using information for "a collateral or ulterior purpose" includes using information from one proceeding to maintain a different proceeding, even if the parties and causes of action are identical: *Crest Homes plc v Marks* [1987] 1 AC 829 at 837.

53. Information can be disclosed among a litigant's solicitors, counsel and advisers, as well as to actual and prospective witnesses and to the directors and officers of a corporate litigant. In all cases, those receiving the information are themselves bound by the undertaking.
54. Breach is a contempt of court, and therefore very serious for litigants, third party recipients and legal practitioners. A person can be guilty of contempt of court if they do not comply with a lawful direction of the court such as a "*Harman*" undertaking. There is no "public interest" defence to a breach of the *Harman* undertaking.

Conclusion

55. All attachments to this Brief can be found at this link:
<https://www.dropbox.com/scl/fo/15ycv16xjix83jct4733/h?rlkey=peqk29ahzzdv7m41k2kaolupw&dl=0>
56. If you have any questions in relation to this Brief, please contact Sophie Kilpatrick on 0412 411 023 or at sophie.kilpatrick@crosscountrynts.com.au

Yours sincerely

Simon Blackshield

Appendix 3

COMPLETE INDEX OF MATERIALS PROVIDED TO ME

| No. | Document | Attachment No. to Brief |
|-----|--|-------------------------|
| 1. | Affidavit of David Crabtree affirmed 16 June 2023 | 1 |
| 2. | Affidavit of Christopher Ian Leonard Oppenheim sworn 4 August 2023 | 2A |
| 3. | Second Affidavit of Christopher Ian Leonard Oppenheim sworn 4 August 2023 | 2B |
| 4. | Map of Compensation Area | 3 |
| 5. | Map 1 Overview Map and 14 enlargements | 4 |
| 6. | Photographs of Kangeenarina Creek | 5 |
| 7. | Solomon Operations Annual Monitoring Summary: 1 August 2012 – 31 July 2013 (FMG 2013) | 6.1 |
| 8. | Solomon Triennial Aquifer Review: 1 August 2011 to 31 July 2014 (FMG 2014) | 6.2 |
| 9. | Solomon Life of Mine Hydrogeological Assessment (FMG 2015) | 6.3 |
| 10. | Solomon Pool Census Report (FMG 2015) | 6.4 |
| 11. | Solomon Groundwater Operating Strategy (FMG 2015) | 6.5 |
| 12. | Solomon Groundwater Monitoring Summary: August 2014 to July 2015 (FMG 2015) | 6.6 |
| 13. | Solomon Groundwater Monitoring Summary: August 2015 to July 2016 (FMG 2016) | 6.7 |
| 14. | Solomon Triennial Aquifer Review: 1 August 2014 to 31 July 2017 (FMG 2017) | 6.8 |
| 15. | Weelumurra Creek Condition Environmental Management Plan (FMG 2018) | 6.9 |
| 16. | Solomon Groundwater Monitoring Summary: 1 August 2017 to 31 December 2018 (FMG 2019) | 6.10 |
| 17. | Kangeenarina Pools Supplementation Plan (FMG 2020) | 6.11 |
| 18. | Solomon Triennial Aquifer Review to 31 December 2019 (FMG 2020) | 6.12 |
| 19. | Solomon Groundwater Monitoring Summary: 1 January 2020 to 31 December 2020 (FMG 2021) | 6.13 |
| 20. | Weelumurra Creek Supplementation Plan (FMG 2021) | 6.14 |
| 21. | Technical Report Baseline Survey: Groundwater and Surface Water Pool Systems (October 2019) (FMG 2021) | 6.15 |

Appendix 3

| | | |
|-----|---|------|
| 22. | Solomon Mining Area: Updated H3 Hydrogeological Assessment (FMG 2021) | 6.16 |
| 23. | Solomon Combined Groundwater Operating Strategy (FMG 2021) | 6.17 |
| 24. | Solomon Groundwater Monitoring Summary: 1 January 2021 to 31 December 2021 (FMG 2022) | 6.18 |
| 25. | Stockyards Borefield Expansion: H3 Hydrogeological Assessment (FMG 2022) | 6.19 |
| 26. | Solomon Triennial Groundwater Monitoring Review 2022 (FMG 2023) | 6.20 |
| 27. | Solomon Project: Public Environmental Review (FMG 2010) | 6.21 |
| 28. | Hydrogeological Assessment of the Solomon Project (MWH 2010) | 6.22 |
| 29. | H3 Hydrogeological Assessment (Golder Associates 2012) | 6.23 |
| 30. | Solomon Operations Annual Aquifer Review: 1 August 2011 – 31 July 2012 (FMG 2012) | 6.24 |
| 31. | Kangeenarina Creek and Zalamea Creek Riparian Vegetation Monitoring, Solomon (Coffey Environments 2014) | 6.25 |
| 32. | Kangeenarina Creek and Zalamea Gorge Riparian Vegetation Monitoring (Ecoscape 2015) | 6.26 |
| 33. | Solomon Restricted Vegetation Assessment Supplementary Report (Ecologia 2015) | 6.27 |
| 34. | Solomon Hub Flora and Vegetation Assessment (Ecologia 2015) | 6.28 |
| 35. | Solomon Riparian Vegetation Monitoring 2015 (Ecoscape 2016) | 6.29 |
| 36. | Baseline Survey Plan – Groundwater and Surface Water Dependent Vegetation and Permanent Pools (FMG 2019) | 6.30 |
| 37. | Solomon Ecohydrology (AQ2 2020) | 6.31 |
| 38. | Solomon Ecohydrology Stage 2: Overview Assessment of Analogue Sites (AQ2 2020) | 6.32 |
| 39. | Kangeenarina Creek Ecohydrological Optimisation of Supplementation (AQ2 2021) | 6.33 |
| 40. | Vegetation Health Monitoring Program 2021 (Ecoscape 2022) | 6.34 |
| 41. | Solomon [Redacted] Vegetation Health Monitoring Program 2022 (Ecoscape 2023) | 6.35 |
| 42. | Solomon Iron Ore Project: Report and recommendations of the Environmental Protection Authority (EPA 2011) | 6.36 |

Appendix 3

| | | |
|-----|--|-------------------------------------|
| 43. | Robe Pisolite Assessment and Targeted Gompholobium Karijini (P2) Survey, Solomon Mine Project (Coffey Environments 2011) | 6.37 |
| 44. | Riparian Vegetation Assessment Portion of the Kangeenarina Creek Solomon Project Area (Coffey Environments 2011) | 6.38 |
| 45. | Baseline Aquatic Assessment and Aquatic Fauna Survey of Kangeenarina Creek, Solomon Project (Coffey Environments 2012) | 6.39 |
| 46. | Applicant's Further Amended Points of Claim | 7 |
| 47. | Active Water-related Miscellaneous Licences | 8 |
| 48. | References to Water Loss in YNAC Affidavits and Witness Statements | 9 |
| 49. | Expert Evidence Practice Note (GPN-EXT) | 10 |
| 50. | Yindjibarndi Compensation Claim Map 3 – Regional Overview | Provided supplementary to the brief |
| 51. | WAD 37/2022 Yindjibarndi Ngurra Aboriginal Corporation RNTBC WP2022/001 Topographic Map | Provided supplementary to the brief |
| 52. | Shapefile of Solomon Clearing Extended Area | Provided supplementary to the brief |
| 53. | Shapefile of Solomon Disturbed Areas Extended | Provided supplementary to the brief |
| 54. | Shapefile of Yindjibarndi #1 Determination Area Boundary | Provided supplementary to the brief |
| 55. | Hard Drive containing LIDAR and Aerial Images provided by FMG | Provided supplementary to the brief |



Pilbara Water Resource Assessment: Lower Fortescue Hedland region

An overview report to the Government of Western Australia and industry partners from the CSIRO Pilbara Water Resource Assessment



The Pilbara Water Resource Assessment

CSIRO has completed, for the Government of Western Australia and industry partners, an overview of the current and future climate and water resources of the Pilbara to aid water planning and management, and place local studies into a wider context.

The Assessment covers an area of 288,479 km², which is about 11% of the state of Western Australia. This is one of the world's most important resource regions because of high-grade deposits of iron ore and offshore gas reserves.

The Assessment examined surface water and groundwater resources and their environmental significance in detail for four regions within the Assessment area: Ashburton Robe, Upper Fortescue, Lower Fortescue Hedland and De Grey Canning (Figure 1). There is also a technical report, *Hydroclimate of the Pilbara: past, present and future*. These reports can be downloaded from www.csiro.au/Pilbara-water-assessment.



Figure 1 Reporting regions in the Pilbara Water Resource Assessment area

KEY POINTS

- Only 2% to 13% (6 to 50 mm) of mean annual rainfall becomes **runoff** in the Pilbara. Between 8 and 30 mm of rain is required to initiate runoff. While the number of events that produce runoff may decrease under a dry future climate scenario, the rainfall threshold is not expected to substantially change. Soils dry rapidly between most events because potential evaporation greatly exceeds rainfall across the area.
- **Rainfall** in the Pilbara results from both tropical and more temperate meteorological processes, making projections of future changes difficult because they vary in their response to raised greenhouse gases. The 2030 and 2050 climates almost certainly will be hotter. While global climate models project both wetter and drier conditions, the drier projections are more extreme.
- **Streamflow** exceeds **recharge** volumes by 5 to 6 times. This difference is the result of very large flows during cyclonic events and tropical depressions exceeding the amount of water that can infiltrate during these events.
- **Groundwater** is currently the main water resource in the Pilbara. Most aquifers are recharged by water infiltrating through streambeds during large rainfall events. Alluvial coastal aquifers, an important local drinking water supply, appear capable of withstanding a hotter and drier climate because the proposed reduction in recharge is much less than the reduction in runoff and number of flow days.
- Groundwater resources in the Pilbara have important environmental value in supporting multiple terrestrial ecosystems. **Groundwater-dependent terrestrial vegetation** and river pools, marking groundwater discharge zones, occupy less than 0.5% of the Assessment area.
- Within the Assessment, **provinces** were defined so that discrete, local information on climate, surface water hydrology, groundwater hydrology and groundwater-dependent ecosystems could be integrated, enabling trends and patterns to be identified, analysed and discussed across the entire area.

66

CITATION

CSIRO (2015) Pilbara Water Resource Assessment: Lower Fortescue Hedland region. An overview report to the Government of Western Australia and industry partners from the CSIRO Pilbara Water Resource Assessment. CSIRO Land and Water, Australia.

This report is an overview of the following report: McFarlane DJ (ed.) (2015) Pilbara Water Resource Assessment: Lower Fortescue Hedland region. A report to the Government of Western Australia and industry partners from the CSIRO Pilbara Water Resource Assessment. CSIRO Land and Water, Australia.

Cover: Harding Dam, the most important surface water resource in the Assessment area, supplies water to the West Pilbara Water Supply Scheme © CSIRO

Key findings for the Lower Fortescue Hedland region

- Groundwater is the main water resource in the Lower Fortescue Hedland region (Figure 2). It is contained within coastal alluvial aquifers, the Millstream calcrete, dolomite of the Wittenoom Formation and deeper paleochannel aquifers. Some of the latter are associated with channel iron deposits (CIDs).
- The Lower Fortescue Hedland region has an extreme climate, characterised by extremely hot summers, high potential evaporation and intermittent intense rainfall.
- Future climates are expected to become 1.3 to 2.2 °C hotter (by 2030 and 2050, respectively) than the 1961 to 2012 climate, but it is not clear whether it will be wetter or drier. In general, an ensemble of 18 global climate models (GCMs) suggests that a drier future climate is more probable than a wetter one. Recent decades have experienced above-average rainfalls, but it is not clear how factors such as increased aerosol concentrations in the atmosphere around South-East Asia, and climate change resulting in sea surface

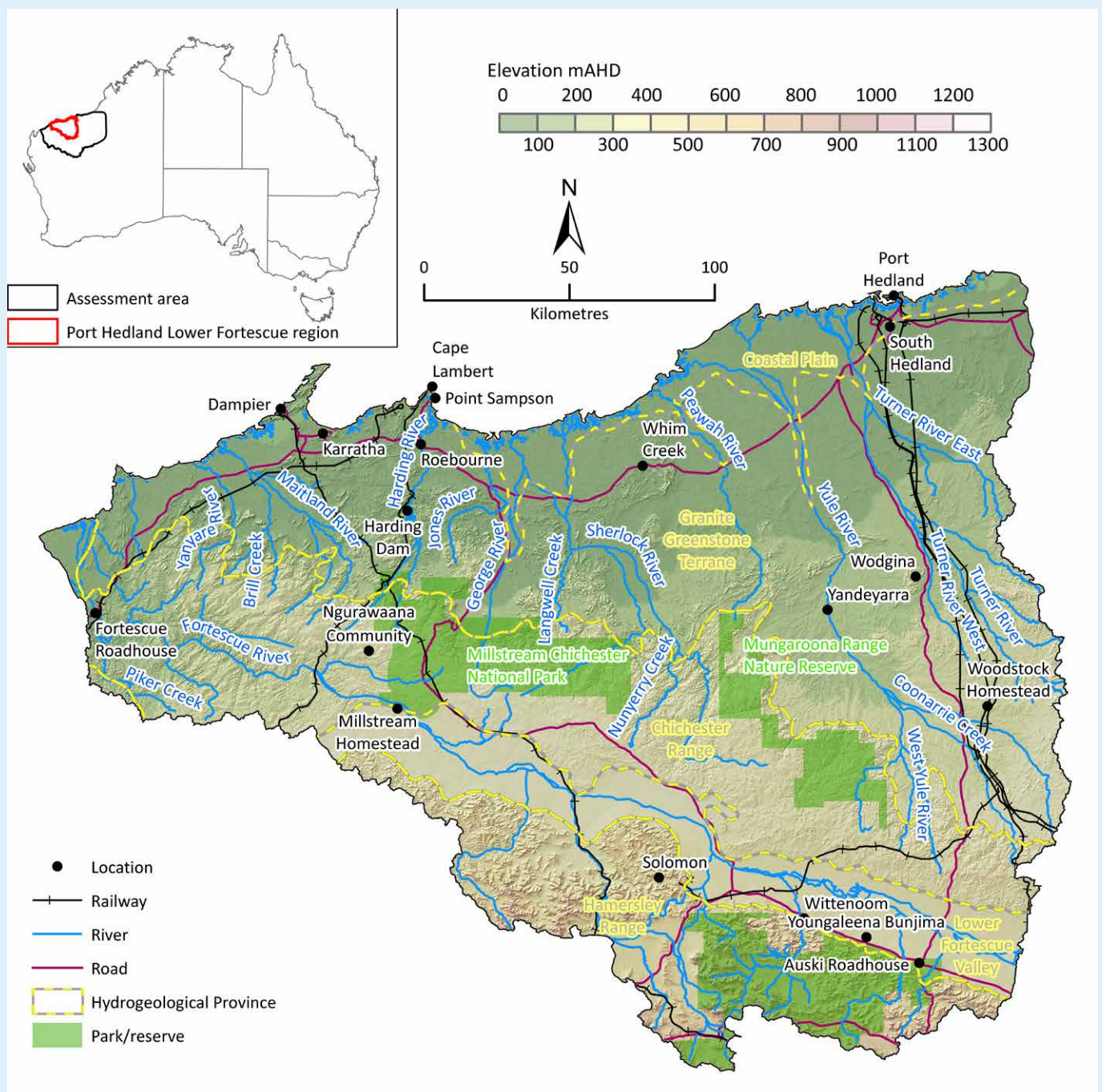


Figure 2 The Lower Fortescue Hedland region's relief, rivers, settlements, national parks and nature reserves, and hydrogeological provinces

temperature changes in surrounding or remote oceans contribute, or whether it is natural variability.

- Streamflow is initiated after rainfall exceeds 19 to 30 mm per event. Only 11 to 41 mm of annual rainfall (2% to 13%) becomes runoff in most years.
- Leakage from streambeds (localised recharge) is the main mechanism for recharging alluvial and underlying aquifers. The area and duration of riverbed inundation largely determine the amount of localised recharge.
- Net annual recharge estimated from rainfall–runoff models is between 1.7 and 5.1 mm, which represents 8 to 54 GL/year when calculated for all hydrogeological provinces. Mean recharge volumes are only about 12% of mean streamflow volumes because large events result in large runoff that occurs in a short period of time and does not allow time for water to recharge aquifers. If the aquifer near the stream is already full, little recharge can occur.
- Much of the Lower Fortescue Hedland region is underlain by fractured rock formations, which can form local aquifers. Previous work has found that recharge to these aquifers is mainly associated with rainfall infiltration (diffuse recharge), which varies between 1% and 5% of annual rainfall, mainly associated with rainfall events greater than 20 mm/day. This is a similar-sized event to initiative runoff.

- Runoff increases by up to 18% in 2050 under a wet future climate scenario but decreases by up to 45% under a dry future climate scenario, relative to the historical baseline period of 1961 to 2012. For each 1% change in rainfall, runoff changes by about 3%. A dry future climate may impact Harding Dam, which is a water source for the West Pilbara Water Supply Scheme.
- Because of climatic conditions, groundwater resources in the Pilbara

have an important environmental value, supporting multiple terrestrial ecosystems.

- Groundwater-dependent ecosystems (GDEs), including springs and groundwater-dependent terrestrial vegetation, comprise less than 0.5% of the region but have important environmental, social and cultural values (Figure 3). Analysis of satellite remote sensing over a 24-year period



Figure 3 Pool supported by groundwater discharging from the Millstream calcrete

(1988 to 2011) indicates that GDEs generally showed limited variability.

- GDEs are ultimately groundwater discharge zones and can be supported by various groundwater systems, which could form aquifers (e.g. karstified dolomites or paleochannels, such as Millstream or pools supported by coastal aquifers) or not (e.g. shallow alluvial systems, or fractured zones along faults or dykes).

- When they rely on localised discharge from regional or local aquifers, GDEs can withstand prolonged dry periods with limited impact.

- GDEs supported by groundwater systems that do not form aquifers (e.g. shallow alluvial aquifers that can be filled by streamflow leakage during most years, such as in the Granite Greenstone Terrane) are more sensitive to climate variability. GDEs formed over groundwater

discharges within seepage zones on scree slopes are the most sensitive to climate variability.

- The strong interdependence of geology, topography, soil and vegetation associations, hydrology and aquifers has enabled five main hydrogeological provinces to be defined to help identify repeating patterns in the water resources of the region (Figure 4).
- Most water resources in the region have a low salinity, and there is sufficient fresh to marginal-quality water in this region to meet residential, mining, dust suppression and stock watering needs. The availability of water in coastal alluvial aquifers and some paleochannels in the Hamersley Range is of increasing interest for irrigated agriculture as a new industry to support higher populations in the coastal towns of Karratha and Port Hedland.
- The findings are based on limited climate and surface water monitoring, and on intense groundwater investigations associated with regionally important alluvial aquifers, for which groundwater models were made available by the Western Australian Department of Water. Mine sites only occupy a very small proportion of this region. The findings are regional in scope, and schematic cross-sections have been used to depict processes and relationships that are more complex at the local scale.

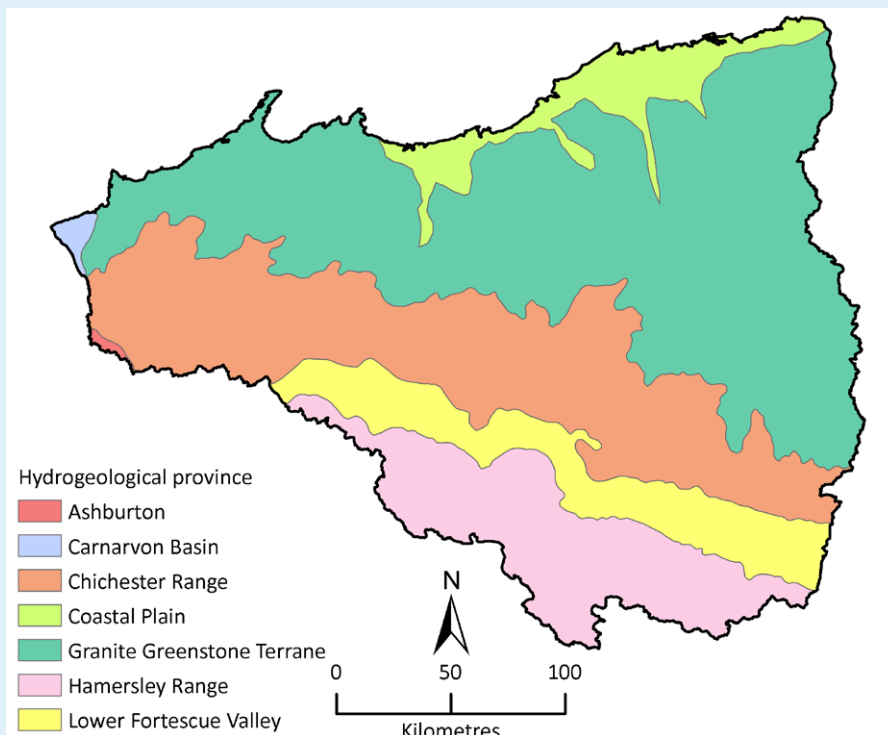


Figure 4 Hydrogeological provinces in the Lower Fortescue Hedland region

Overview of the Lower Fortescue Hedland region

The Lower Fortescue Hedland region has high temperatures for much of the year, and each summer there is a chance that a tropical cyclone will cross the coast and cause wind and flood damage, while bringing widespread rain to replenish aquifers and support flora and fauna.

The region provides major ports and support for much of the iron ore industry in the Pilbara. It is also important for tourism, with a coastal network of attractions, as well as Millstream Chichester and Karijini national parks. It has a resident population of more than 35,000, not including workers who travel to work in the region on a regular basis.

The main physiographic feature is the Hamersley Range. Mount Meharry, the highest peak in Western Australia, with an elevation of 1249 m, is located in the southern part of Karijini National Park just outside the region.

The Hamersley Range has an orographic effect, with some peaks having an annual rainfall almost twice that of adjacent flatter areas. However, the area is semi-arid, with maximum temperatures in summer often exceeding 40 °C. The annual rainfall deficit (rainfall – Class A pan evaporation) ranges from 2400 mm in the range to more than 3100 mm in low-lying areas (Figure 5). Potential evaporation exceeds rainfall by 6 to 11 times, depending largely on elevation.

Rainfall is summer dominant, and is mainly associated with thunderstorms and occasional tropical cyclones and tropical depressions, which result in runoff once infiltration thresholds

are exceeded. Some lower-intensity rainfall can occur in autumn and winter, which can be more effective for plant growth and recharge given the lower temperatures.

The physiography is dominated by its underlying geology. The north and east of the region is underlain by an ancient granite–greenstone terrane, which is usually topographically low with rounded hills, and has few aquifers. The remainder of the region is part of the Archean–Proterozoic Hamersley sedimentary basin, which comprises the Fortescue Group (mainly associated with the Chichester Range) and the Hamersley Group (associated with the Hamersley Range). The Wittenoom Formation, which contains often karstic dolomite, is mainly associated with the Fortescue Valley and underlies some valleys in the Hamersley Range. Erosion and deposition in the Cenozoic formed deep paleochannels, which contain important aquifers and CIDs such as the Solomon Hub. More recent shallow alluvial deposits coincide with the modern stream network. Part of the Carnarvon sedimentary basin extends into the westernmost part of the region. This includes some confined aquifers overlain by recent alluvial deposits. They are more extensive in the Ashburton Robe region.

Soil profiles in the region are weakly developed because of the hot, arid climate and sparse vegetative cover. Upland soils in particular are skeletal, which enhances runoff during high-intensity rainfall events. More developed soil profiles are associated with alluvial deposits in the lower valleys.

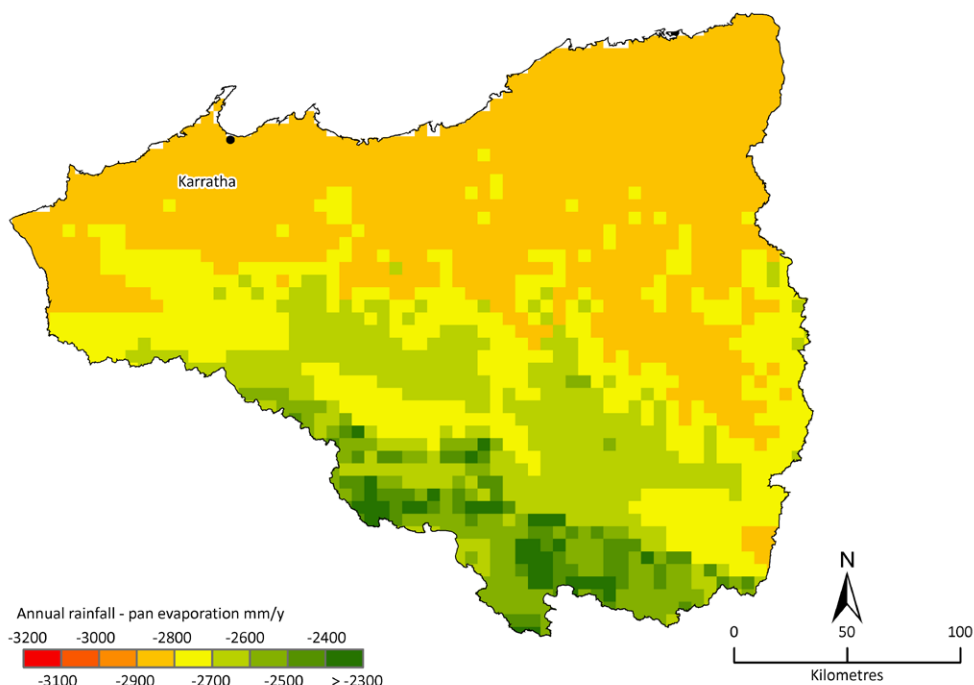


Figure 5 Rainfall deficits for the Lower Fortescue Hedland region

Historical and future climate

A baseline climate (Scenario A, which is a continuation to 2030 and 2050) was defined, against which future climate scenarios may be compared. Water years (1 October to 30 September) between 1961 and 2012 were chosen as the historical baseline, based on the availability of recorded data and representativeness. Annual rainfall during this period averaged 363 mm, almost 10% higher than the 1911 to 2012 mean of 331 mm/year.

There is a trend of increasing annual mean and extreme rainfall, as well as number of rain days, during the 52-year historical period. The 7-year period between 1995 and 2001 was 56% wetter than the historical mean. A larger number of tropical cyclones affected the region during this period, and these years were used to assess the potential impact of a future wetter climate on water resources and GDEs.

Eighteen global climate CMIP5 models from the fifth Intergovernmental Panel on Climate Change report were used to estimate the 2030 and 2050 climate for the Pilbara under two representative concentration pathway (RCP) scenarios: 4.5 and 8.5 W/m². The lower number represents increased emissions of greenhouse gases until about 2040 and then

reductions due to implementation of mitigation, whereas the higher number represents a future with little curbing of emissions and rapidly rising greenhouse gas concentrations. The median projected change (Scenario Cmid) is for little change in annual rainfall for all periods and RCP scenarios (Figure 6).

Wet and dry scenarios were also estimated using 10% and 90% exceedance probabilities based on the 18 models, two periods (2030 and 2050) and two RCPs. The wet scenarios projected mean annual rainfall increases from 3.0% to 8.0%. The absolute magnitudes of these increases are less than those of the projected decreases under the dry scenario: from -3.6% to -16.8%. Mean annual areal potential evaporation (areal PE) is projected to increase by 2.0% to 4.1% by 2030 and by 3.6% to 6.4% by 2050 under the corresponding scenarios. Therefore, even under higher projected rainfall, rainfall deficits (and therefore soil water deficits) are projected to increase under all future scenarios. This is important when considering the effect of future climate scenarios on surface water hydrology and groundwater levels, given the close association between streamflow and localised recharge.

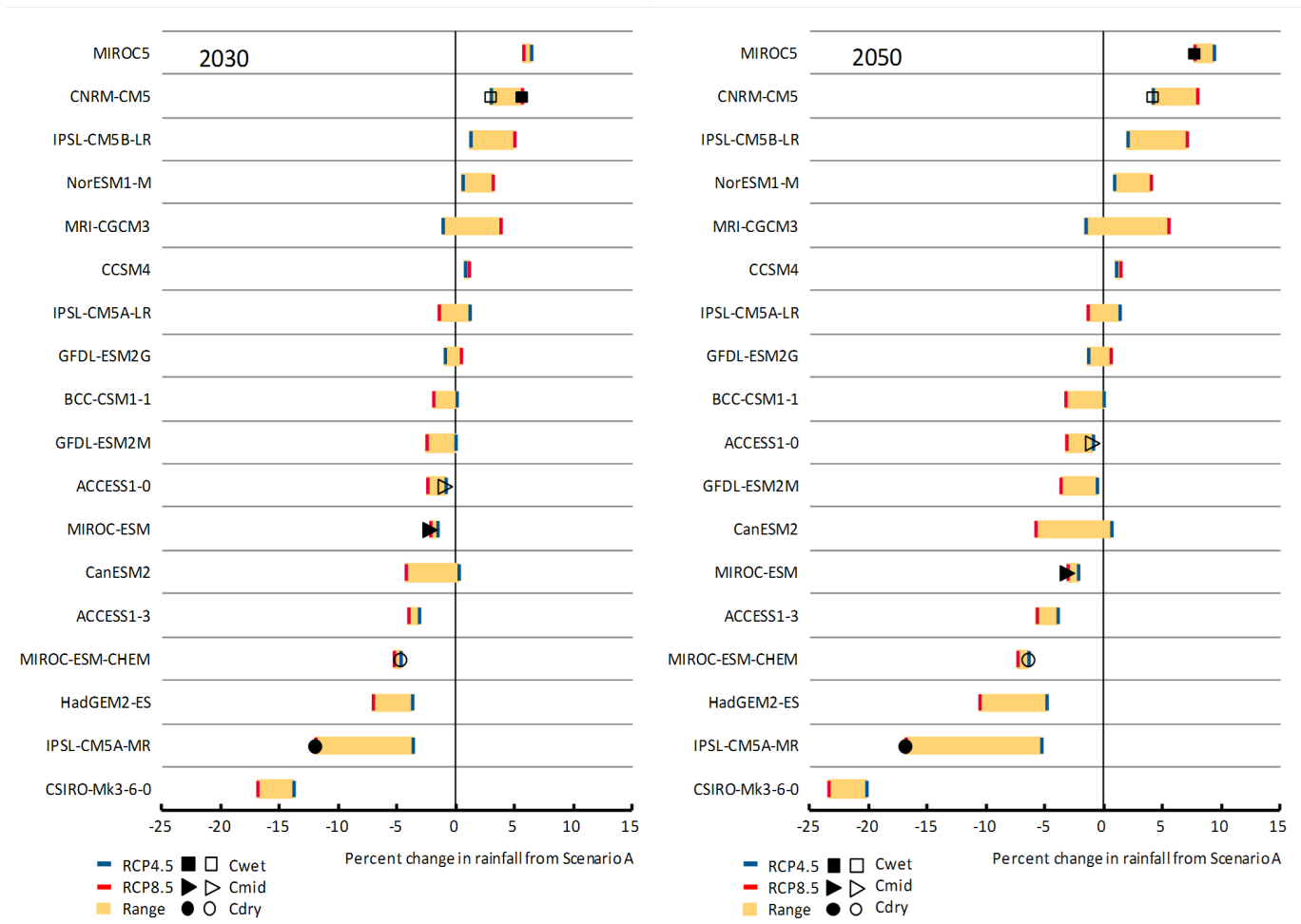


Figure 6 Mean annual rainfall change (percentage, relative to Scenario A) for RCP4.5 and RCP8.5 projections from 18 CMIP5 GCMs for 2030 and 2050 for the Lower Fortescue Hedland region. The second wettest (driest) scenarios from RCP4.5 and RCP8.5 are designated Cwet (Cdry). The median, selected from the 9th and 10th ranked GCM closest to the respective RCP4.5 and RCP8.5 mean, is designated Cmid. Solid symbols are used for RCP8.5, open symbols for RCP4.5. RCP4.5 is a medium scenario, whereas RCP8.5 is a high scenario with continued high levels of emission growth to the end of the century.

Surface water hydrology and resources

The Lower Fortescue Hedland region has 10 gauging stations able to be analysed for the entire historical period. Only about 8% of annual rainfall was recorded as streamflow in these stations, with a range of 3.3% to 13.5% (11 to 41 mm). Runoff in the region can infiltrate further downstream, so these values do not necessarily reflect the streamflows that reached the Indian Ocean, the region’s drainage outlet.

Because streamflow is the main source of recharge and groundwater is the region’s main water resource, the amount of rainfall required to initiate streamflow and how this may change under a future climate are very important. Between 19 and 30 mm of rainfall in a single event has been required in the historical period to initiate streamflow. Modelling indicates that this threshold may not change much by 2030 or 2050. However, the number of events that exceed the threshold changes under the wet and dry scenarios.

Under a wet future climate (C50wet8.5), runoff is projected to increase by about 18%. Under a dry future climate (C50dry8.5),

it decreases by about 45%. This is partly because projected decreases in future rainfall by some GCMs are larger than projected increases, but also because the hotter future climate raises potential evaporation rates, irrespective of changes in rainfall. Catchments are therefore likely to be drier when rainfall starts.

Rainfall intensities exceeding infiltration capacities is probably the main mechanism for runoff initiation in the region, with saturation excess only a factor low in hillslopes, after prolonged events, or in riverbeds and riparian areas.

In general, runoff (measured in mm/year) is highest in the Granite Greenstone Terrane and Chichester Range hydrogeological provinces, reflecting their skeletal soils and low storages (Figure 7). Projected runoff under the median (Cmid) scenarios is less than under the historical period. In general, a 1% change in rainfall can translate into about a 3% change in runoff.

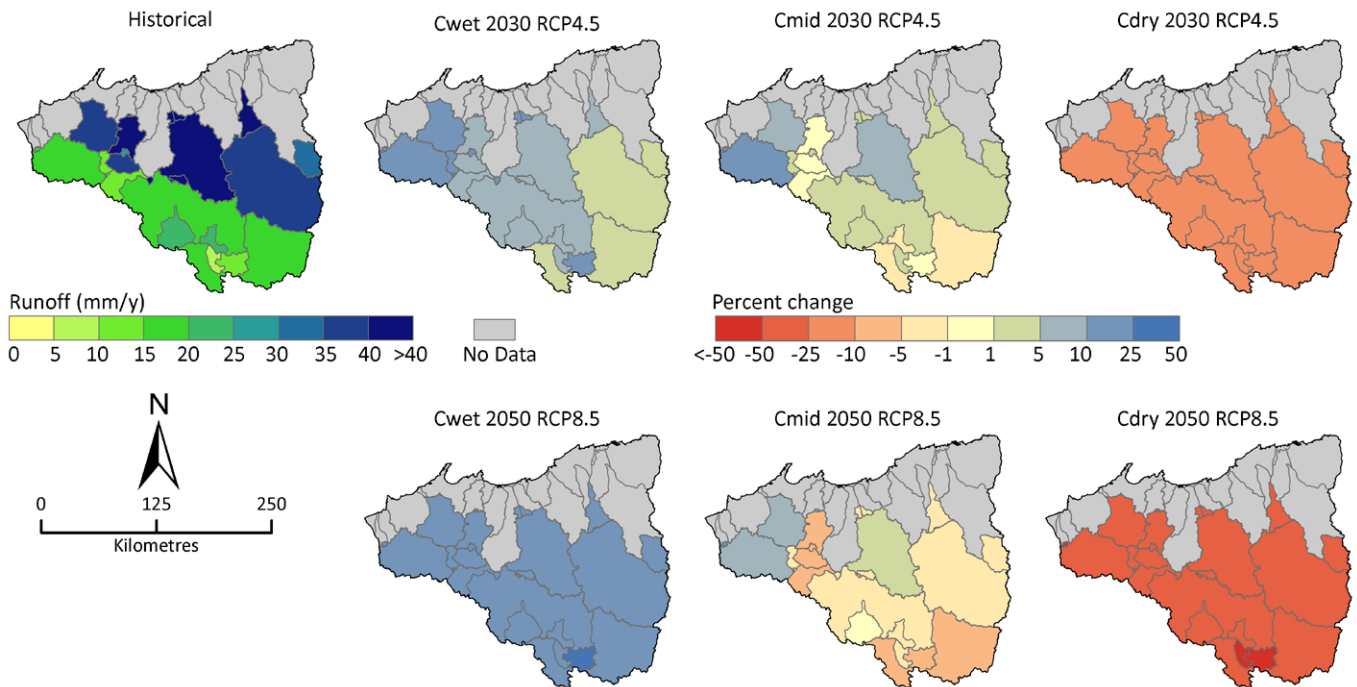


Figure 7 Spatial distribution of annual runoff across the Lower Fortescue Hedland region under the historical period and its change under six climate scenarios

Groundwater hydrology and resources

There are two main types of aquifers capable of providing water in economic quantities in the region:

1. alluvial and paleochannel (Cenozoic) aquifers
2. calcrete aquifers in the main Fortescue Valley.

Karst dolomite of the Wittenoom Formation and CIDs have potential as aquifers when hydraulically connected with overlying alluvial aquifers and where located beneath the present-time stream network. Other formations include low-permeability fractured rocks with limited groundwater storage, which include non-economic banded iron formations.

Groundwater resources are mostly shallow and renewable in the region. Aquifers are largely unconfined except where semi-confined conditions are observed in the main Fortescue Valley.

Localised recharge during streamflow is the main recharge mechanism. Historical stream leakage (for periods varying between 1968 and 2009) was calibrated in three specific areas, namely, Millstream aquifer, Lower Fortescue River aquifer, and Lower Yule River aquifer, and varies between 12 and approximately 20 GL/year. Diffuse recharge in these areas has been estimated to be between 1 and 5 GL/year, taking place predominantly where outcrops of the main aquifers occur.

The main discharge mechanisms identified for the aquifers that were analysed correspond to direct aquifer discharge through springs supporting perennial pools (Figure 8) and direct evaporation of groundwater in the coastal plain aquifers. Calibrated historical spring discharges in the Millstream aquifer range between 6 GL/year for the period 1968 to 1994 and about 19 GL/year for the period 1995 to 2012. Both periods may provide an indication of the range of variation for spring discharges for drier and wetter than average conditions in the Millstream area. Calibrated historical evaporation in the aquifers located in the coastal plain ranges between 13.3 and 14 GL/year.

Based on historical conditions, at least 70 ML/day of streamflow for at least 6 consecutive days is required to generate much recharge in the Millstream aquifer for the climate scenarios evaluated.

For all aquifers analysed, simulated streamflow leakage rates vary between 11 and 29 GL/year under dry and wet scenarios, respectively. At the same time, for aquifers located in the coastal plain (Lower Fortescue and Lower Yule), simulated evaporation rates vary between 13 and 18 GL/year under dry and wet scenarios, respectively; for the Millstream aquifer, spring discharges to perennial pools range between 21 and 27 GL/year under dry and wet scenarios, respectively.

For the monthly mean aquifer level in Millstream, projected differences between dry and wet scenarios can reach up to 0.2 to 0.25 m. In very restricted areas, however, and relative to the historical scenario, decreases can reach up to 0.5 m under a dry scenario, whereas increases can reach up to 0.2 m under a wet scenario. This highlights the resilience of the simulated aquifer to extreme climatic fluctuations. This is most likely linked to the high transmissivity of the main calcrete aquifer.

For the Lower Fortescue aquifer and relative to the historical scenario, local watertable decreases under a dry scenario can reach up to 0.7 m, whereas increases up to 0.3 m are expected under a wet scenario. Spatially, these increases/decreases concentrate along a north–south axis, highlighting the relevance of the north channel of the Fortescue River in the recharge mechanism. There seems to be, as well, a spatial propagation pattern for increases/decreases along eastern tributaries, where alluvial gravels are defined in the main floodplain valley and relatively low conductivity bedrocks are defined in the eastern areas.

For the lower Yule aquifer and relative to the historical scenario, local watertable decreases under a dry scenario can reach up to 1 m, with smaller increases of up to 0.25 m expected under a wet scenario. An apparent spatial pattern for the decreases and increases is observed for both climate scenarios around a central area where the main Yule River splits into north and west channels. This area coincides with a recharge zone associated with large flood events, where the river stage rises over 3 m. Over long periods, two-thirds of the incoming recharge is lost as evaporation and one-third is storage gain.

For all aquifers analysed, simulated groundwater heads and water balance components show a higher sensitivity to the dry scenario than to the wet scenario, indicating that a drier climate may have more substantial impacts on available groundwater resources.



Figure 8 A waterhole used for stock

Groundwater-dependent ecosystems

GDEs comprise less than 0.5% of the Lower Fortescue Hedland region but have very important environmental, social and cultural values. Many wetlands are classified as nationally important. Tanberry Creek is listed as a Priority 1 Wild River; one of two in the Pilbara. As in other regions, protection of groundwater-dependent assets is an important consideration in developing groundwater resources, including development by water service providers (e.g. Water Corporation) or by mining companies.

GDE habitats were mapped based on consideration of geological, hydrogeological and hydrological settings; available information on mapped vegetation and its typical ecohydrological characteristics; and remotely sensed data analysis. Vegetation was classified on the likelihood of its groundwater dependency: from highly dependent (i.e. high likelihood of GDE occurrence), to partly dependent (i.e. medium likelihood of GDE occurrence), to non-groundwater dependent riparian vegetation (i.e. lowest likelihood of GDE occurrence). Some GDEs, particularly those with a high level of groundwater dependency (high likelihood), were also associated with a persistent presence of water.

Those areas were also classified according to the likelihood of water occurrence (Figure 10).

In the Lower Fortescue Hedland region, the following GDE types are associated with groundwater systems of significant ecological function:

Type 1 – Ecosystems dependent on groundwater discharge from regional aquifers: consistent groundwater discharge associated with such systems and controlled by regional groundwater gradients supports the most persistent and spatially substantial GDEs (Figure 9a). These GDEs are characterised by minimal temporal and spatial variability as they are supported by large (or relatively large) groundwater resources for which groundwater recharge and discharge zones are spatially separated. This group includes GDEs associated with groundwater discharge zones from bedrock aquifers hosted in karstified dolomite within the Wittenoom Formation. Millstream is an example of a GDE that is dependent on groundwater discharge from a regional aquifer.

Type 2 – Ecosystems dependent on groundwater discharge from local aquifers, mainly associated with secondary



(a) Type 1: dependence on localised discharge from the regional aquifers or paleochannels (e.g. Millstream) or expression of groundwater table (e.g. river)



(b) Type 2: dependence on localised discharge from the local aquifer (e.g. coastal alluvial systems)



(c) Type 3: dependence on small alluvial systems or fractured rocks (e.g. Hamersley Gorge)



(d) Type 3: dependence on fractured zone along faults

Figure 9 Types of groundwater-dependent ecosystems in the Lower Fortescue Hedland region

deposited formations: these include localised or diffuse discharge associated with CIDs or with other types of paleochannels (Figure 9b). Localised groundwater discharge in such groundwater systems is controlled by catchment-scale groundwater gradients, and supported GDEs (river pools and groundwater-dependent riparian vegetation) are spatially smaller than those dependent on regional aquifers.

Type 3 – Ecosystems dependent on groundwater that does not form an aquifer: at some locations, groundwater resources are not sufficient to be classified as aquifers but nevertheless are important for meeting ecological water requirements. GDEs associated with this group include GDEs dependent on groundwater discharge from fractured rock formations (with a subset of this type associated with localised faults/dyke zones) (Figure 9c and 9d); GDEs associated with shallow alluvial systems (these are more often associated with vegetation with little or no surface expression of water); and GDEs related to groundwater discharge zones towards the base of hillslopes, which in the Pilbara can be found along the edges of colluvial deposits and alluvial fans. These GDE types are associated with terrestrial vegetation while persistent presence of water is not detected.

The GDEs' sensitivity to observed climate variability in this region was minimal. The sensitivity of GDEs in hydrogeological provinces (highest to lowest) is Hamersley Range, Lower Fortescue Valley, Chichester Range, Granite Greenstone Terrane and Coastal Plains.

In the area of the Millstream borefield, groundwater levels deeper than 7–10 m did not have a significant effect on vegetation greenness (as measured using remote sensing).

Furthermore, there was no effect of groundwater abstraction on vegetation greenness detected in this area between 1988 and 2011.

Temperature, solar radiation and potential evaporation have more immediate effects on greenness, while seasonal rainfall variability has a significant effect on vegetation. Seasonal variations in rainfall affected greenness more than individual rain events.

Vegetation greenness in Type 1 GDEs (downstream from Millstream) shows no sensitivity to seasonal variations in river flow. However, vegetation at the river banks (floodplains) is sensitive to seasonal changes in river flow rather than to individual events.

Projected changes in rainfall, streamflow and groundwater levels under future climate scenarios are within the historical range of recorded values. Future 'extremes' may persist for decades compared with these periods. Also, future climates are expected to be hotter, with both higher vegetation stress and soil water deficits.

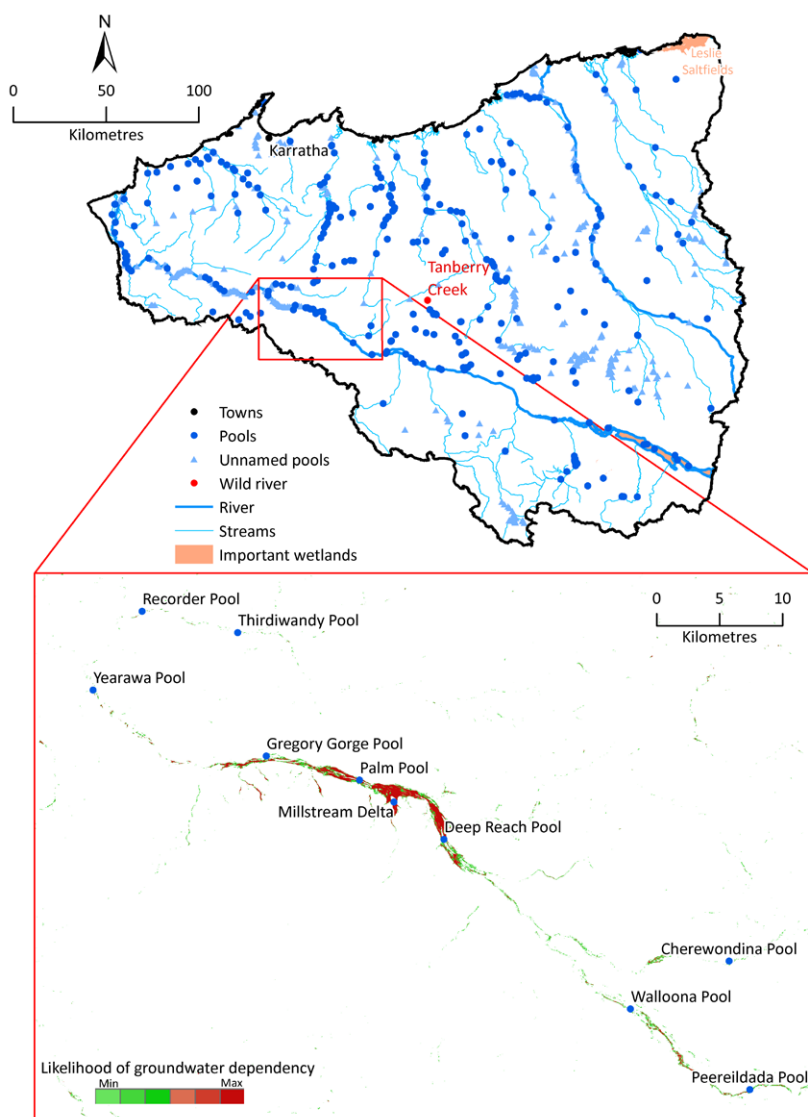


Figure 10 Likelihood of groundwater dependency in the Lower Fortescue Hedland region

Hydrogeological provinces and their projected responses to future climate scenarios

Hamersley Range

This province has the highest elevation and highest rainfall in the region, resulting in a milder climate (25% lower rainfall deficit than surrounding provinces). River valleys within the Hamersley Range contain alluvial aquifers with varying thickness, depending upon the history of landscape erosion or eroded material deposition. They are also crossed by paleochannels, including some with very highly transmissive CIDs, which constitute major iron ore deposits.

Runoff in this province can be generated when daily rainfall exceeds 38 mm; however, average annual runoff is only 8 mm. These estimates are similar to those obtained from gauged catchments in the Upper Fortescue region.

Fractured rock aquifers are important hydrogeological units, particularly when associated with the dolomite of the Wittenoom Formation (Figure 11). They also provide a reliable discharge to support ecosystems in gorges in the Hamersley Range.

Important aquifers are associated with paleochannels and the dolomite of the Wittenoom Formation. Predominantly skeletal soils can result in diffuse recharge to fractured rock aquifers, which has been mainly associated with daily rainfall events in excess of about 20 mm.

Under projected climate changes, mean runoff could increase by about 16% under a wet future climate or decrease by about 43% under a dry future climate. Very low runoff years (<10th percentile) could more than double, indicating that recharge to alluvial aquifers and their GDEs could be impacted were this climate to eventuate.

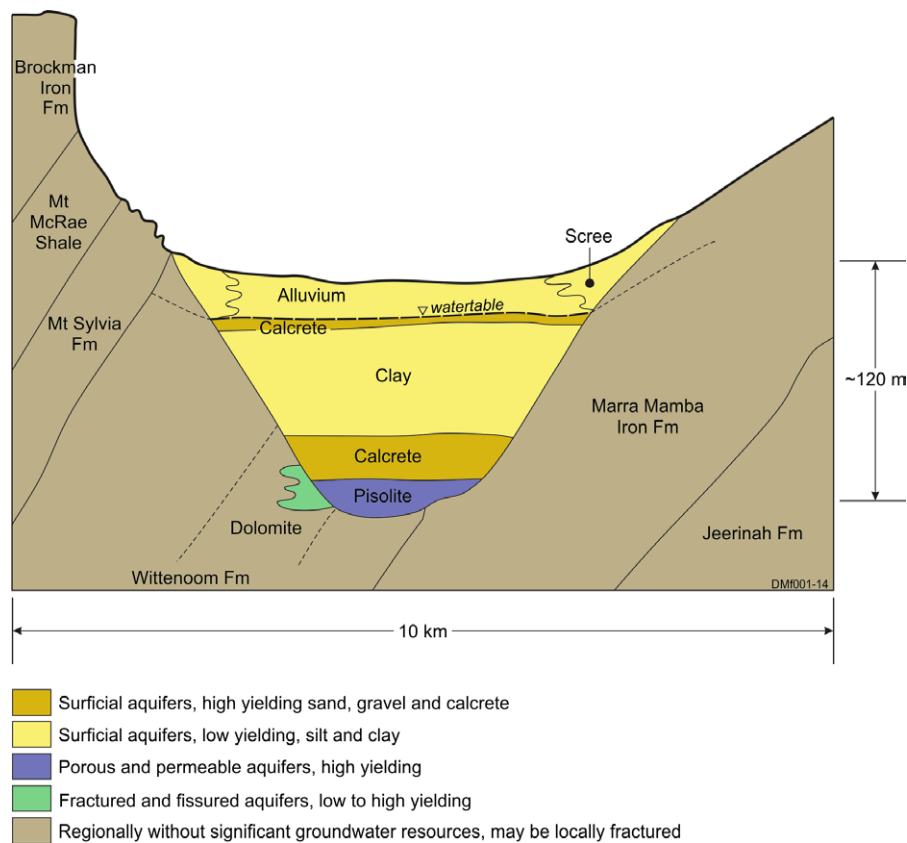


Figure 11 Schematic cross-section across a valley in the Hamersley Range Hydrogeological Province

Lower Fortescue Valley

The Lower Fortescue Valley is contained between the Hamersley and Chichester ranges, and overlying the Wittenoom Formation and Marra Mamba Iron Formation (Figure 12). The Oakover Formation has in places undergone calcretisation, which has formed calcrete with a very high hydraulic conductivity just below the watertable, resulting in a flat watertable that responds in a limited way to climate and pumping. A paleochannel indicates that, west of Millstream, the Fortescue River used to flow parallel to the Hamersley Range and enter what is now the Robe River.

Aquifers in the valley receive recharge from the river as well as from valleys in the Hamersley Range. How much water from the CIDs recharges aquifers in the valley is unclear.

The projected change in runoff under a dry future climate is -39% , which is much larger than the projected increase under a wet future climate ($+15\%$).

Chichester Range

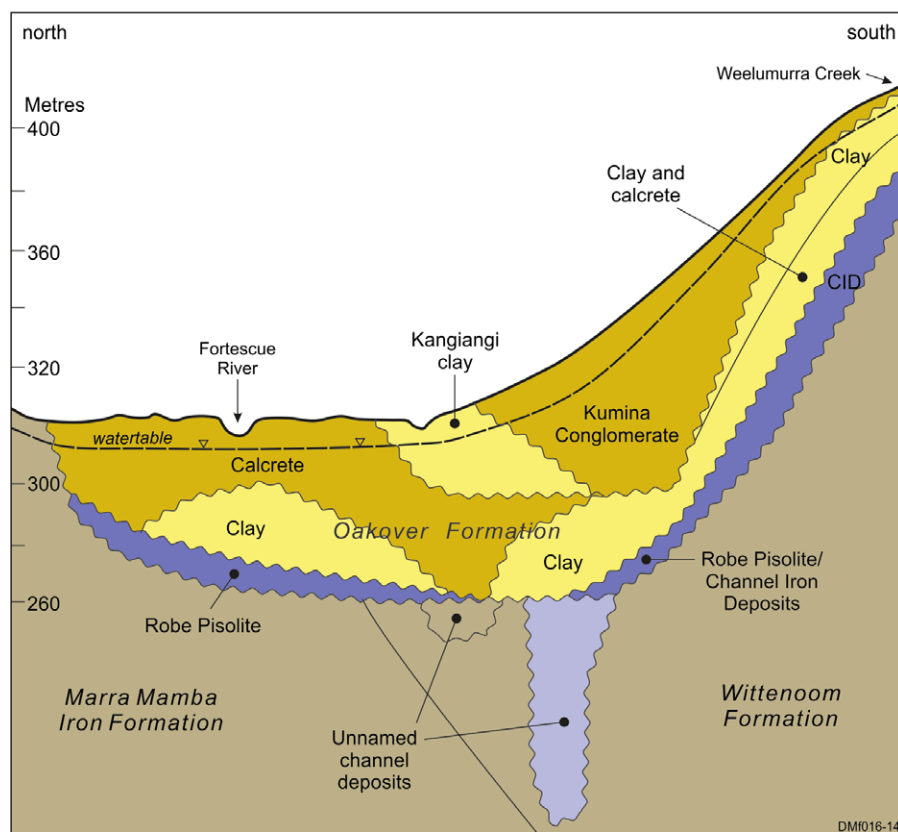
Having a much lower elevation than the Hamersley Range, the Chichester Range only has a small orographic effect on rainfall. Catchments flowing to the south are small, and alluvial deposits can be clayey, having formed from volcanic bedrock. The potential to recharge aquifers is therefore limited.

Most rivers in the Lower Fortescue Hedland region arise from this province. The projected change in runoff under a dry future climate is -38% , which is more than double the projected increase under a wet future climate ($+15\%$).

Granite Greenstone Terrane

Large areas of granite and greenstone lie to the north of the Chichester Range. Being weakly weathered and comprising crystalline bedrock, they contain few aquifers (Figure 13). Most of the rivers that arise in the Chichester Range cross the terrane, including the Harding River, which is used as a major water source for the West Pilbara Water Supply Scheme.

Weathered material from the granite plutons form sandy soils and alluvium downstream, compared with the clayey soils formed from greenstone. Under a dry future climate, runoff is projected to decrease by about 36% . Under a wet future climate, it is projected to



- Surficial aquifers, high yielding sand, gravel and calcrete
- Surficial aquifers, low yielding, silt and clay
- Porous and permeable aquifers, high yielding
- Porous and permeable aquifers, moderately yielding
- Regionally without significant groundwater resources, may be locally fractured

Figure 12 Schematic cross-section of the Hamersley Range (right) and Lower Fortescue Valley (centre left) hydrogeological provinces in the Millstream area

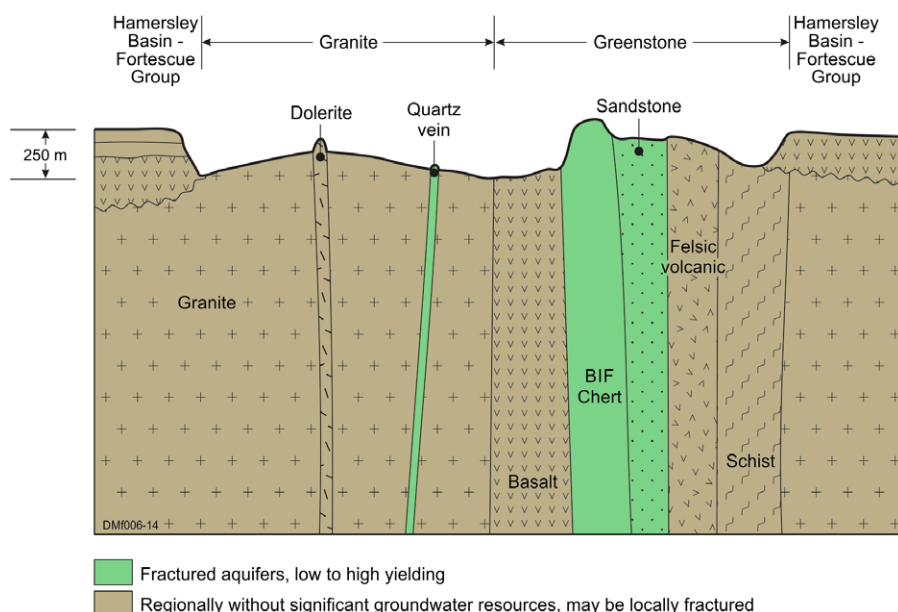


Figure 13 Schematic cross-section of the Granite Greenstone Terrane Hydrogeological Province

increase by about 16% compared with the baseline. Streamflow volumes exceed recharge volumes by about six times, reflecting the large runoff that occurs in major rainfall events. Recharge is much less sensitive than runoff to change in rainfall.

Coastal Plain

The low-lying coastal plain contains important alluvial aquifers near the discharge to the Indian Ocean. These are used to supply drinking water to the East Pilbara Water Supply Scheme (Lower Yule) and to mining operations (Lower Fortescue). Groundwater salinity is low where recharge is received from modern drainage lines and becomes more saline with increasing distance. Little runoff is generated in this province, but it receives water from most of the others.

The Carnarvon sedimentary basin extends into the province in the west, as shown by the Trealla Limestone and Yarraloola Conglomerate in Figure 14, but these formations are better represented in the Ashburton Robe region to the south-west. Under a wet future climate, the runoff in this province may increase by about 27%, but it may decrease by about 40% under a dry future climate.

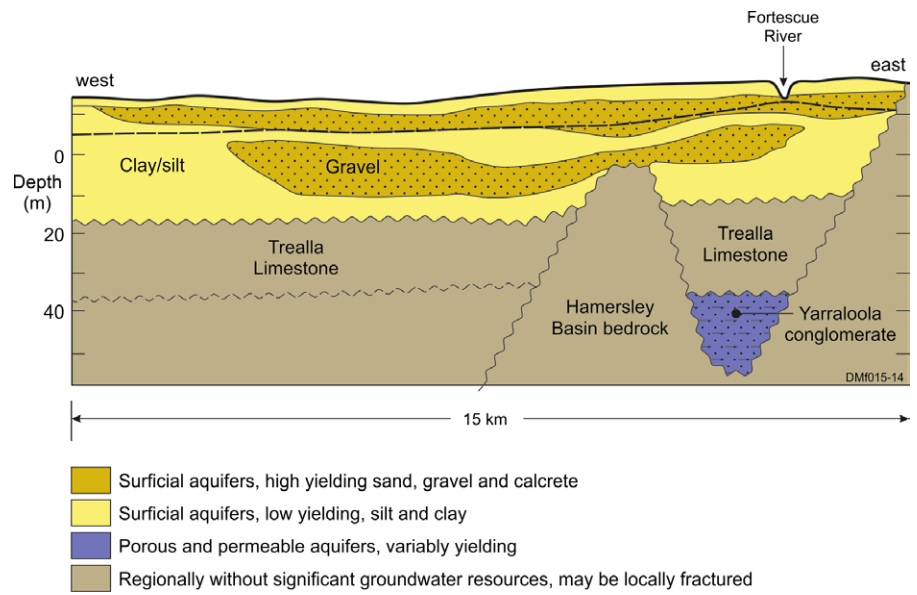


Figure 14 Schematic cross-section of the Coastal Plain Hydrogeological Province



Iron ore transport by rail

Basis of the Assessment

Weather observations were more plentiful and widespread in the 1950s and 1960s, when there were sheep stations throughout the region. More recently, iron ore mining companies have been recording climate data and streamflows at mine sites. However, these latter monitoring data are not yet long term and may not have the longevity of past gauging if they cease when mining moves or ends. Long-term surface water gauging is especially limited.

Groundwater and GDE investigations are intensive where there are valuable drinking water resources associated with alluvial aquifers and at mine locations. The Assessment has used the available long-term data and specific studies to draw a regional picture, which hopefully puts the more intensive studies into a broader context.

Water discharging from fractured rock into a gorge in the Hamersley Range



CONTACT US

t 1300 363 400
 +61 3 9545 2176
e csiroenquiries@csiro.au
w www.csiro.au

FOR FURTHER INFORMATION

Don McFarlane
 Groundwater Hydrology Team Leader,
 Land and Water
t +61 8 9333 6215
e don.mcfarlane@csiro.au
w www.csiro.au/Pilbara-water-assessment

This report was prepared by CSIRO for the Western Australian Government and industry partners – BHP Billiton, Western Australian Department of Water, Water Corporation, Pilbara Development Commission and Western Australian Department of Regional Development. Funding for the project was provided through the Western Australian Government's Royalties for Regions program, BHP Billiton and CSIRO.

COPYRIGHT

© Commonwealth Scientific and Industrial Research Organisation 2015. To the extent permitted by law, all rights are reserved and no part of this publication covered by copyright may be reproduced or copied in any form or by any means except with the written permission of CSIRO.

IMPORTANT DISCLAIMER

CSIRO advises that the information contained in this publication comprises general statements based on scientific research. The reader is advised and needs to be aware that such information may be incomplete or unable to be used in any specific situation. No reliance or actions must therefore be made on that information without seeking prior expert professional, scientific and technical advice. To the extent permitted by law, CSIRO (including its employees and consultants) excludes all liability to any person for any consequences, including but not limited to all losses, damages, costs, expenses and any other compensation, arising directly or indirectly from using this publication (in part or in whole) and any information or material contained in it.



Appendix 4b

Mountain-Block Hydrology and Mountain-Front Recharge*

John L. Wilson and Huade Guan

New Mexico Institute of Mining and Technology, Socorro, New Mexico

In semiarid climates, a significant component of recharge to basin aquifers occurs along the mountain front. Traditionally called “mountain-front recharge” (MFR), this process has been treated by modelers of basins as a boundary condition. In general, mountain-front recharge estimates are based on the general precipitation characteristics of the mountain (as estimated, e.g., by the chloride mass balance and water balance methods), or by calibration of a basin groundwater model. These methods avoid altogether the complexities of the hydrologic system above the mountain front, or at best consider only traditional runoff process. Consequently hydrology above the mountain front is an area ripe for significant scientific advancement. A complete view would consider the entire mountain block system and examine hydrologic processes from the slope of the highest peak to the depth of the deepest circulating groundwater. Important aspects above the mountain front include the partitioning of rainfall and snowmelt into vegetation-controlled evapotranspiration, surface runoff, and deep infiltration through bedrock, especially its fractures and faults. Focused flow along mountain stream channels and the diffuse movement of groundwater through the underlying mountain block would both be considered. This paper first defines some key terms, then reviews methods of studying MFR in arid and semiarid regions, discusses hydrological processes in the mountain block, and finally addresses some of the basic questions raised by the new mountain-block hydrology approach, as well as future directions for mountain-block hydrology research.

1. INTRODUCTION

The term “mountain-front recharge” (MFR) is generally used in arid and semiarid climates to describe the contribution of mountains regions to the recharge of aquifers in adjacent basins. Basin aquifer recharge is typically focused along stream channels and the mountain front; in many cases MFR is the dominant source of replenishment [Hely *et al.*, 1971; Maurer *et al.*, 1999]. Diffuse recharge of basin aquifers, through direct infiltration of precipitation, is limited or absent due to small precipitation volumes, deep vadose zones, and the water scavenging vegetation found in dry climates [Foster and Smith-Carrington, 1980; Phillips, 1994; Izbicki *et al.*, 2000; Flint, 2002a; Walvoord *et al.*, 2002]. Mountains, due to orographic effects, receive more precipitation than the basin floor, with a significant fraction in the form of snow. In addition, mountains have lower temperatures, and sometimes a larger surface albedo due to the snow cover, thus re-

ducing the potential for evapotranspiration (ET). Mountains also have thin soils that can store less water, reducing the amount potentially lost by transpiration. Fast flow along bedrock fractures that underlie the thin soil cover may also limit water loss to ET (Plate 1). A study of 20 selected catchments worldwide shows that the area-weighted mountain contribution to annual river basin discharge is about 4 times that of the basin floor [Viviroli *et al.*, 2003]. In arid and semiarid regions, the mountain contribution can be greater.

MFR has been studied from one of two perspectives: (1) the traditional basin-centered view (Plate 2a), or (2) a mountain-centered view (Plate 2b). With a basin-centered perspective, the mountain front is viewed as a boundary condition for the basin aquifers, thus avoiding the complexities of the hydrologic system above the mountain front. Basin-centered methods include Darcy’s law calculations along the mountain front [Maurer and Berger, 1997] and calibration of groundwater models of the basin aquifer [Tiedeman *et al.*, 1998a; Sanford *et al.*, 2000]. With a mountain-centered

* Preprint of paper to be published in *Groundwater Recharge in A Desert Environment: The Southwestern United States*, edited by Fred M. Phillips, James Hogan, and Bridget Scanlon, 2004, AGU, Washington, DC.

perspective, precipitation amounts over the mountains are crudely related to MFR rates, and do not consider the subsurface hydrologic mechanics in the mountains. Examples of mountain-centered methods include: (1) comparing the geochemical or isotopic characteristics of mountain precipitation with the groundwater at the mountain front (e.g., the chloride mass balance method) [Dettinger, 1989; Maurer and Berger, 1997; Anderholm, 2000]; (2) using locally developed empirical relations between MFR and precipitation [Maxey and Eakin, 1949; Anderson et al., 1992; Maurer et al., 1999; Anderholm, 2000]; and (3) subtracting estimated ET from precipitation [Feth, 1966; Huntley, 1979]. The studies of MFR in either perspective so far neglect detailed hydrologic processes in mountains.

Hydrologic processes in mountains have been studied in detail at the hillslope scale, with a focus on streamflow responses to precipitation in humid regions (e.g., McGlynn et al., 2002; Peters et al., 1995; Tani, 1997). Few of these studies were conducted in arid and semiarid regions [Wilcox et al., 1997; Puigdefabregas et al., 1998]. Hillslope studies typically only examine hydrologic processes in the thin soil layer above the bedrock surface (Plate 1). Studies of semiarid mountain hydrologic processes below the bedrock surface have mostly been limited to Yucca Mountain, the proposed vadose zone nuclear waste repository in Nevada, with an emphasis on solute migration issues.

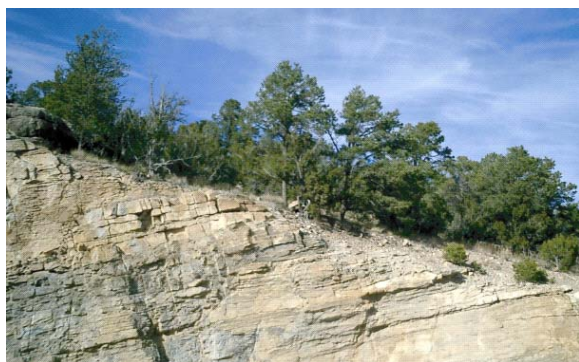


Plate 1. Vegetation, thin soil cover, and limestone bedrock on a hillslope of the eastern Sandia Mountains, New Mexico. The rock is dipping to the north (left). The vegetation is mainly Pinon and Juniper.

Hydrologic science above the mountain front, incorporating a full view of the entire mountain block system and not just the thin soil cover and its vegetation, is an area ripe for significant scientific advancement. This more complete perspective examines hydrologic processes from the slopes of the highest peak to the depths of deepest circulating groundwater. It includes the focused flow of mountain stream channels, and the

diffuse movement of groundwater through the surrounding and underlying mountain blocks. It considers recharge from rainfall, snowmelt, surface runoff, and through fractures and faults, as well as water returned to the atmosphere through vegetation-controlled evapotranspiration. When water is discharged from the mountain block to the adjacent basin, through focused and diffuse surface and subsurface components, it becomes MFR.

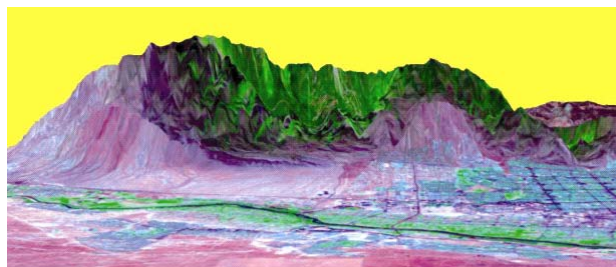


Plate 2. Two different remote sensing perspectives on MFR. (a) The valley-centered perspective is represented by this horizontal view of the Albuquerque Basin bounded by the Sandia Mountains (~25 km visible in this view). The view is east across the city of Albuquerque, with a 5-times vertical exaggeration (TM image 7, 4, 2 bands draping over a DEM). (b) The mountain-centered perspective is represented by this ~130 km wide vertical view of the southern Sangre de Cristo Mountains, New Mexico and part of Rio Grande valley, with a 5-times vertical exaggeration (TM 7, 4, 2 bands draping over a DEM). The east slopes of the Jemez Mountains are on the left.

MFR is an important, if not predominant, source of recharge to basins in arid and semiarid regions, however it is simultaneously the least well quantified. Estimates of the basin-margin recharge to the Middle Rio Grande Basin vary by one order of magnitude [Sanford et al., 2000]. Uncertainty is amplified by climate variability, climate change, and increasing anthropogenic

disturbances that alter mountain environments [Luckman and Kavanagh, 2002], mountain hydrology, and thus mountain-front recharge. Some direct human impacts (e.g., septic systems, transportation, resort development, mine dewatering/contamination) also affect water quality in mountains. A more complete approach to studying MFR in a mountain-centered perspective would provide observations of the temporal and spatial variations of its different components, and improve prediction of how the mountain hydrologic system (including MFR) responds to climate and to local disturbances such as changing vegetation patterns. Mountain-centered observations and predictions are essential for effective groundwater resource management in adjacent basins.

This paper first defines some key terms, then reviews methods of studying MFR in arid and semiarid regions, describes hydrologic processes in the mountain block, and finally addresses some of the basic questions raised by a proposed new mountain-block hydrology approach, as well as future directions for mountain-block hydrology research.

2. MOUNTAIN BLOCK, MOUNTAIN FRONT, AND RECHARGE

A mountain block includes all the mass composing the mountains, including vegetation, soil, bedrock (exposed and unexposed), and water. A mountain block can be formed through a number of geological processes, such as normal faulting in extensional settings, thrust faulting in compressional settings, and volcanic eruption. These processes yield the mountain block's most important characteristic: significant topographic relief. Mountain-block hydrology examines all hydrologic processes in the mountain block, including the temporal and spatial distribution of precipitation, vegetation interception, snow and snowmelt, ET, runoff, interflow (throughflow) in the soil layer, water flow through bedrock matrix and fractures, and surface water and subsurface water interactions.

The term mountain-front recharge is frequently used to describe the contribution from mountains to groundwater recharge of the adjacent basins along the mountain front. The mountain front is positioned somewhere between the mountain block and the basin floor. However, a clear and consistent definition of the mountain front is lacking. Estimates of mountain-front recharge are consequently ambiguous and difficult to compare. Is the mountain front a strict line or a narrow zone? If it is a line, how is it determined? If it is a zone, what criteria are used to identify this zone?

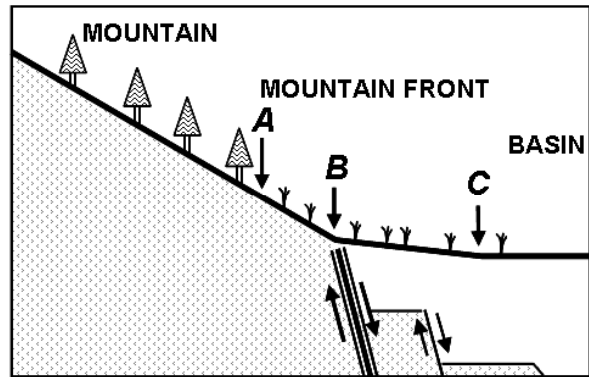


Figure 1. Schematic cross-section showing naturally occurring map lines for potential mountain front definitions. *A* = point of vegetation change, *B* = point of piedmont angle (often a major mountain bounding fault, or master fault, is located in this vicinity), and *C* = point of plinth angle. In extensional settings, like the Rio Grande Rift and Basin and Range, there are a series of normal faults along the mountain front and beneath the alluvial fan leading down into the basin [Russell and Snelson, 1990].

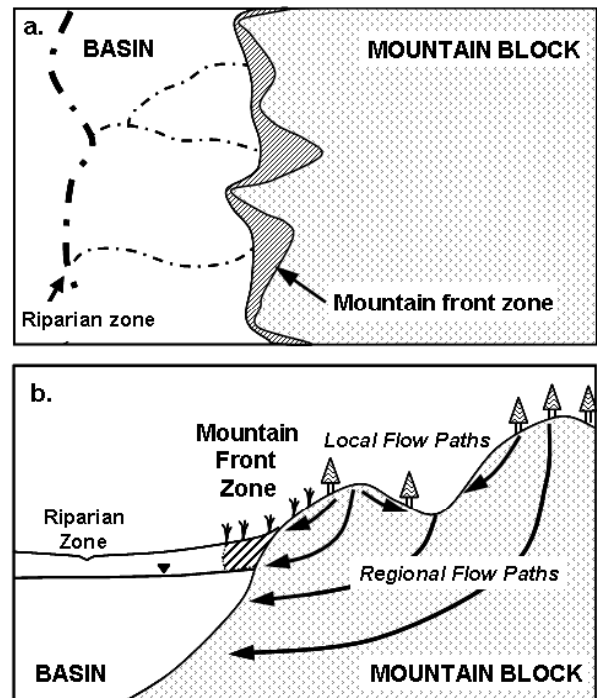


Figure 2. Schematic diagram showing four hydrologically distinctive units of the landscape in map view (a) and in cross-section (b). The cross section also shows various groundwater flow paths in the mountain block (modified from Toth [1963] and Keith, [1980]).

Consider the mountain front defined as a line. Several natural lines could be used, including vegetation boundaries, soil boundaries (e.g., the edge of bare rock), slope boundaries, mountain bounding faults, or

even the snow line. Based on Ruxton and Berry's [1961] description of landforms and weathering profiles in arid regions, we define three alternative definitions of the mountain front boundary: the point where there is a change in vegetation (Figure 1, point A), the point where the mountain abuts the piedmont, often corresponding to a change in soil type and presence of the mountain bounding faults (point B), and the plinth angle where the piedmont meets the edge of the basin floor (point C). Each of these boundaries is a candidate for defining the mountain front because each might represent a distinct hydrologic transition (Table 1).

Suppose instead the mountain front is defined as a transition zone between the mountain and the basin floor. Theoretically, any zone that utilizes the boundaries defined in Figure 1 can be a potential mountain

front zone. For the purpose of studying mountain-front recharge in arid and semiarid areas we believe that the piedmont zone (the area between points B and C) is the best definition of the mountain front. The streamflow at point B represents surface runoff from the mountain block; the stream loss between points B and C reflects the water returned to the atmosphere by ET and by recharge into the mountain front zone (and eventually to the basin aquifer). Mountain bounding faults are typically located within this zone, thus including their hydrologic effect on mountain-front recharge. With this defined as the mountain front zone, the landscape is then divided into four hydrologically distinctive areas: mountain block, mountain front, basin floor, and discharge zones (e.g., phreatic playas and basin riparian areas), illustrated in Figures 2a and 2b.

Table 1 Comparison of three potential boundaries for mountain front determination

| Types of boundaries | Significant change across the boundary | Advantage | Disadvantage |
|---------------------|---|--|--|
| A: Vegetation | Vegetation type, Evapotranspiration. | Good for ecological study. | Varies with climate, slope aspect, etc. Not good for studying mountain front recharge. |
| B: Piedmont angle | Slope, soil, infiltration and runoff characteristics. | Good point to quantify surface runoff from the mountain, generally accompanied with soil change and buried mountain bounding fault zone. | Recharge from surface runoff beyond this point is not included in mountain front recharge. |
| C: Plinth angle | Slope, soil, surface structures. | Surface runoff measured past this point is definitely excluded from mountain front recharge. | May be covered by anthropogenic structures; the point is difficult to identify. |

MFR is defined by Keith [1980] as groundwater recharge to a regional (basin) aquifer at the margin of the aquifer that parallels a mountain area. MFR is often divided into two components [Anderson *et al.*, 1992; Chavez *et al.*, 1994a; Manning, 2002]: (1) subsurface inflow from the adjacent mountains; and (2) infiltration from streams near the mountain front. In this definition, MFR includes the addition of water to the basin aquifer both from the saturated zone under the mountains and through the unsaturated zone at the mountain front. We, and others, call the first component "mountain-block recharge" [Manning, 2002]. Some scientists do not regard this as a component of recharge because it fails their strict definition of recharge as water reaching the water table through the unsaturated zone or

from direct contact with surface water bodies [Flint *et al.*, 2001a]. With this definition, the combined saturated zone of mountain and basin is considered one system, and recharge is the process of adding water from above through the vadose zone. From this perspective, "mountain-block recharge" would perhaps be termed "underflow" between two portions of the system. If instead we consider only the basin aquifer as the system of concern, the broader definition acknowledges that "recharge" occurs when water is added to the aquifer. Meinzer [1923] distinguished these two contributions to aquifer replenishment as direct recharge (from the unsaturated zone) and indirect recharge (from other saturated formations). A recent Na-

tional Research Council [2004] report appears to accept the less strict definition of recharge.

For compatibility with the traditional view of mountain-front recharge in basin hydrologic studies, we suggest that MFR be defined as all water entering the basin aquifer with its source in the mountain block and mountain front (zone). This definition includes direct water-table recharge at the mountain-front zone (direct MFR), and the transfer of subsurface water from the mountain bedrock to the basin aquifer (indirect MFR or mountain-block recharge). In addition to near surface (direct) and subsurface paths (indirect), one can also consider diffuse and focused paths for each, leading to four components of MFR (Figure 3).

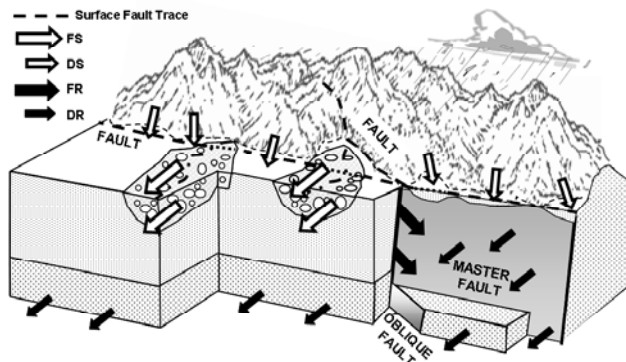


Figure 3. Schematic diagram illustrating MFR components. FS = focused near-surface recharge, DS = diffuse near-surface recharge, FR = focused subsurface recharge, DR = diffuse subsurface recharge.

1) *Focused near surface component (FS)*. This represents MFR contributions at the mountain front from surface stream runoff (FS_1 , easy to measure) and shallow subsurface water transmitted by streambed sediments (FS_2 , difficult to measure). We emphasize FS_2 here because it is sometimes neglected when MFR is estimated solely from the surface runoff. While the stream channel may be dry, there is often significant subsurface discharge in the sediments underlying the stream and above the bedrock surface. This subsurface flow includes the hyporheic zone beneath the stream, but it can be deeper and wider, especially at the mountain front. Theoretically, the surface runoff FS_1 is the amount of stream water runoff (RO) that crosses the piedmont angle (Point B in Figure 1) and enters the mountain front zone. In reality, FS_1 is always less than RO , because of ET losses, and because some surface runoff manages to flow past the downstream boundary of the mountain front zone and into the basin (DRO). In arid regions where streams are mostly ephemeral

and disappear at the mountain front, FS_1 is equal to RO less the loss to ET.

2) *Diffuse near surface component (DS)*. Diffuse near surface flow occurs along steep front slopes via ephemeral surface runoff (in small unmapped channels) and subsurface interflow (through the thin soil layer) originating in small catchments directly above the mountain front. This diffuse component also includes the vertical recharge from precipitation falling directly on the mountain-front zone. Both of these contributions are reduced by the local ET. Given the small area of the mountain front zone compared to the remainder of the mountain block, these contributions provide a relatively small component of MFR.

3) *Focused subsurface component (FR)*. This is subsurface water transmitted along bedrock openings, including fractures (primarily tectonic origin, or due to unloading extension), faults, and pipes (e.g., lava tubes and dissolved openings in carbonates), that connect subsurface water in the mountain block and the basin aquifer. Structural enhancement of rock permeability due to faults and zones of intense fracturing within the bedrock are especially important factors in creating focused subsurface flowpaths, which Feth [1964] calls the ‘hidden path’. Groundwater transmission is mostly by focused flow FR in mountain blocks composed of crystalline rock.

4) *Diffuse subsurface component (DR)*. There is also a diffuse component of groundwater transmission along the contact zone between the bedrock of the mountain block and the sediments of the basin aquifer. In a mountain block with high matrix permeability, such as a volcanic tuff, or regular and ubiquitous fracturing, such as a basalt, diffuse flow DR can be an important component of mountain-front recharge.

Based on these definitions, a simple water balance equation,

$$MFR_I = (FS_1 + FS_2) + DS + FR + DR, \quad (1)$$

describes mountain-front recharge. Despite their simplicity, water balance equations are useful tools for conceptualizing mountain-front recharge. Another way of writing the water balance equation for MFR_I is

$$MFR_I = P - ET_b - ET_f - DRO, \quad (2)$$

where P is precipitation input in the mountain block and the mountain-front zone ($P = P_b + P_f$, where $P_b \gg P_f$), ET_b and ET_f are evapotranspiration in the mountain block and mountain-front zone, respectively, and DRO is streamflow at the downstream end of the mountain-front zone into the basin.

In the arid and semi-arid southwest United States a number of simplifications are taken, leading to less comprehensive definitions of mountain-front recharge. First, stream runoff at the mountain front is generally ephemeral, and almost always disappears within the mountain front zone. Therefore, downstream runoff beyond the mountain front is often negligible ($DRO = 0$). In this case, MFR can be defined as

$$MFR_2 = P - ET_b - ET_f . \quad (3)$$

This can be rewritten, in terms of the four components at the mountain front, as

$$MFR_2 = (RO - RET_f + FS_2) + DS + FR + DR \quad (4)$$

where RET_f is the riparian ET along the focused stream channel across the mountain-front zone (there is a small diffuse component of ET_f throughout the rest of the zone, away from the stream channel, that is already accounted for by the DS component).

In some cases the subsurface water transfer from the mountain bedrock to the basin aquifer is neglected. In other words, only direct MFR is considered, with the component formula becomes

$$MFR_3 = FS + DS . \quad (5)$$

Taking this one step further, the diffuse component and FS_2 are also neglected and mountain-front recharge is assumed to be equal to the surface stream flow measured at the mountain front, FS_1 . This leads to a very simple definition of MFR,

$$MFR_4 = RO , \quad (6)$$

where RO is streamflow at the upstream end of the mountain front zone. This model assumes that all stream runoff at the mountain front becomes recharge to the basin aquifer.

As previously defined, mountain-block recharge (MBR) is recharge to a basin aquifer from the mountain bedrock. It is expressed as the sum of subsurface components,

$$MBR_1 = FR + DR . \quad (7)$$

This water balance equation excludes the subsurface water transfer in the streambed. If we broaden the definition of mountain-block recharge to include this component, then we have

$$MBR_2 = FS_2 + FR + DR . \quad (8)$$

This mountain-block water balance equation can be written as

$$MBR_2 = P - ET_b - RO \quad (9)$$

when the front-slope runoff is negligible.

Why bother to write out these various versions of the water balance equation? They illustrate the range of different conditions that apply in nature and the range of assumptions that people make in order to understand and estimate mountain-front and mountain-block recharge. In particular, for methods adopting a particular conceptual water balance model, they show what is being neglected and so point out bias. The assumptions used by analysts and modelers are not always consistent with the appropriate conditions for a particular mountain range and its bounding basins.

3. ESTIMATION METHODS

Various physical, chemical, and numerical methods have been applied to study MFR over the past five decades. Table 2 summarizes the methods used in several studies of MFR in arid and semiarid regions. While Flint et al. [2002b] summarizes methods used at Yucca Mountain for estimating recharge to the mountain block itself, here we review a wide variety of the methods employed to estimate MFR.

3.1 Water Balance Method

Generally, precipitation is the only water input to a mountain block. The amount of mountain-front recharge can be estimated if water loss by ET and surface runoff is known. Which MFR components are estimated is based on where ET and surface runoff are quantified. If ET is estimated in the mountain block, and stream runoff is measured at the upstream end of the mountain front zone, then equation (9) is applied. The resulting estimate is for mountain-block recharge, MBR_2 . If, however, the ET is estimated over the mountain block and the mountain front zone, and the stream runoff is measured at the downstream end of the mountain front zone, equation (2) is applied. The result is an estimate of mountain-front recharge, MFR_1 .

ET in mountains is usually estimated in relation to mean annual precipitation, pan evaporation, or derived from the water balance equation by assuming mountain bedrock impermeability. Huntley [1979] estimated actual ET loss in the Sangre de Cristo and San Juan Mountains of Colorado by multiplying calculated potential ET with an empirical factor, and reported that, respectively, 14% and 38% of annual precipitation becomes mountain-block recharge, MBR_2 (when comparing these numbers it is interesting to note that, among other differences, the Sangre's are crystalline rock whereas the San Juan's are volcanic).

Table 2 Quantitative assessment on mountain front recharge by various methods

| Location | Authors | Methods | MFR or MBR amount in mm/year (percentage of precipitation) | Precipitation mm/year | Notes |
|---|--------------------------|--|---|-----------------------|---|
| Wasatch Range / Weber Delta District, Utah | Feth et al. [1966] | Water balance method, precipitation and ET estimated by increments of elevation. | MBR ₂ = 201 (22%) | 926 | Streamflow at mountain front is 25% annual precipitation in the mountain. |
| San Juan Mtns / San Luis Valley, Colorado | Huntley [1979] | Water balance method, ET estimated from calculated potential, ET multiplied by crop coefficient. | MBR ₂ = (38%) | Not reported | Volcanic rock with high permeability in the mountain. |
| Sangre de Cristo Mtns / San Luis Valley, Colorado | Huntley [1979] | Water balance method, ET estimated from calculated potential, ET multiplied by crop coefficient. | MBR ₂ = (14%) | Not reported | Shists, gneiss, and granitic intrusives, well-cemented sedimentary rocks in the mountain. |
| White River Valley, Nevada | Maxey and Eakin [1949] | Maxey-Eakin method. | Not reported | Not reported | |
| Sandia Mtns / Albuquerque Basin, New Mexico | Anderholm [2000] | Precipitation-runoff regression method, using two empirical equations. | MFR ₄ = 23 (4.6%) (Waltemeyer model) MFR ₄ = 66 (13%) (Hearne and Dewey model) | 510 | Subsurface inflow and ET at mountain front was believed negligible. |
| Carson Mtns, Virginia Mtns / Eagle Valley, Nevada | Maurer et al. [1997] | Chloride mass balance. | MFR ₃ = 27 (7.8%) (data resulted from four subcatchments) | 350 | Weathered and fractured granitic, basaltic and metamorphic rocks. |
| Sandia Mtns / Albuquerque Basin, New Mexico | Anderholm [2000] | Chloride Mass Balance. | MFR ₃ = 31 (6.1%) | 510 | 0.3 mg/l chloride conc. used for bulk precipitation. |
| Santa Catalina Mtns / Tucson Basin, Arizona | Chavez et al. [1994] | Analytical seasonal stream flow model with stochastic estimation procedures. | MBR ₂ = 1.1 (0.2%) | 280-760 | Layered gneiss with folds. |
| Carson Mtns, Virginia Mtns / Eagle Valley, Nevada | Maurer et al. [1997] | Darcy's law. | MFR ₁ = 31 (8.8%) [data resulted from four subcatchments] | 350 | Weathered and fractured granitic, basaltic and metamorphic rocks. |
| Sandia Mtns / Albuquerque Basin, New Mexico | Tiedeman et al. [1998] | Modeling of basin aquifer, calibrated using inverse method. | MFR ₁ = 132 (26%) | 510 | Precipitation data from Anderholm [2000]. |
| Sandia Mtns / Albuquerque Basin, New Mexico | Sanford et al. [2000] | Modeling of basin aquifer, calibrated using ¹⁴ C groundwater age | MFR ₁ = 15 (3%) | 510 | Precipitation data from Anderholm [2000]. |
| Eagle Mtns / Red Light Draw Valley, Texas | Hibbs and Darling [1995] | 2D Numerical modeling of both mtns and valley area, calibrated using groundwater age. | MFR ₁ = 1.8 (0.6%) | 300 | Widespread, well-developed calcic soil horizon in basin. |
| Yucca Mtns, Nevada | Flint et al. [2001] | Modeling in mountains. | MBR ₁ = 4.5 (2.7%) | 170 | Welded and non-welded tuff. |

Feth et al. [1966] calculated MBR_2 from the Wasatch Mountains to the Weber Delta District of Utah using a similar approach. MBR_2 was reported to be 22% of annual precipitation with an ET loss of 53% (Table 2). Hely et al. [1971] estimated MBR_2 for another section of the Wasatch Mountains to be 19% annual precipitation, with an ET loss of 44% (reviewed by Manning [2002]).

The accuracy of a water balance approach depends mainly on the estimation of ET, which is difficult to quantify, especially for the complex terrain and varied vegetation of mountains. In semiarid regions, ET is a dominant water balance component even in mountains [Brandes and Wilcox, 2000]. The uncertainty of the ET estimate is amplified by the uncertainty of other balance components. Take water balance equation (2) as an example. If the actual ET is 60% of P , and MFR_1 is 20% of P , then a 20% uncertainty in the ET estimate leads to a 60% uncertainty in MFR_1 , assuming that P and DRO are measured exactly. This undermines the reliability of MFR quantification using the water balance method.

Due to large uncertainty in ET quantification, ET is often empirically related to the local mean annual precipitation, reflecting a direct function between MFR and the mountain's mean annual precipitation. Maxey and Eakin [1949] considered the high spatial variation of precipitation in mountains and demonstrated an empirical relationship between precipitation zones and the MFR to groundwater basins in Nevada. In the Maxey-Eakin method, MFR is estimated by the following steps [Avon and Durbin, 1994]: (1) identifying several mean annual precipitation zones; (2) assigning each zone a scaling factor to account for the loss of water by ET and runoff; and (3) summing the recharge amount of each zone. Since, both ET and runoff loss is considered in Maxey-Eakin method, the recharge estimate is conceptually either MBR_2 or MFR_1 , depending on the spatial extent of precipitation estimation and the location of runoff estimation (see above). Since the Maxey-Eakin method crudely considers spatially distributed precipitation, it is preferable to other water balance methods that use only a single scaling factor for ET for an entire mountain area. Avon and Durbin [1994] reported that applications of the Maxey-Eakin method in Nevada were generally in fair agreement with estimates from other independent methods.

More recently, Anderson [1992] presented an empirical relationship between the total volume of direct MFR (or MFR_3) and the total volume of mountain precipitation exceeding 203 mm, based on basin-scale water balance estimates in south-central Arizona and

parts of adjacent states. This relation can be approximated by

$$MFR_3 = 0.042 (P_m - 203)^{0.98}, \quad (10)$$

where MFR is direct mountain-front recharge in mm per year, and P_m is mean annual precipitation in mm per year.

Maurer and Berger [1997] gave another empirical regression for mountain water yield (including surface runoff and subsurface flow, approximately equivalent to MFR_2) at Carson Basin, Nevada,

$$MFR_2 = 2.84 \times 10^{-5} P_m^{2.43}, \quad (11)$$

where P_m is the mean annual precipitation in mm per year.

When estimated recharge by the Maxey-Eakin method is plotted against the mid-value of each of four precipitation zones, with $P_m = 8-12$, 12-15, 15-20, and >20 inches, and with scaling factors 0.03, 0.07, 0.15, and 0.25, respectively (for the White River Basin, Nevada [Maxey and Eakin, 1949]), another power law empirical relationship is revealed,

$$MFR = 9 \times 10^{-9} P_m^{3.72}, \quad (12)$$

where P_m is the mean annual precipitation in mm per year. Equation (12) deviates from Maxey-Eakin estimates when $P_m > 600\text{mm} \cong 23.6$ inches.

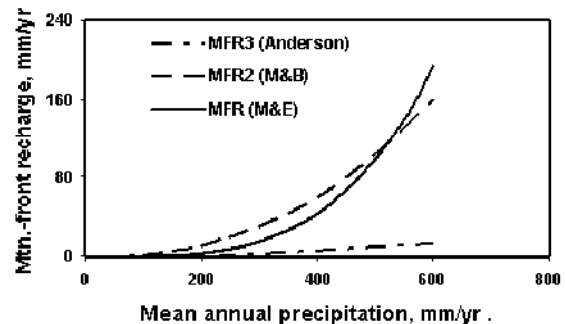


Figure 4. MFR vs. mean annual precipitation for three empirical relations provided by Anderson [1992], Maurer and Berger [1997], and Maxey and Eakin [1949], equations (10)-(12), respectively. Note that Anderson's equation gives direct MFR, while Maurer and Berger's version gives the total water yield [both surface and subsurface] from the mountain.

These three empirical equations (10)-(12) provide substantially different MFR estimates (Figure 4), even though they were all developed for portions of the Basin and Range Province of the southwestern United

States, and have somewhat similar climates. Although different MFR components are quantified in these equations, the large deviation between MFR_3 and MFR_2 , i.e. (10) and (11), suggests that these empirical estimates are likely restricted to the locale where they were developed and should not be transferred to other areas.

3.2 Precipitation-Runoff Regression Method

When subsurface recharge (MBR_2) is negligible, stream runoff at the mountain front (runoff measured at point B in Figure 1, or RO) may be considered the total contribution to MFR [Anderholm, 2000]. The mountain-front recharge estimate is given by MFR_4 in equation (6). Regression analysis can be used to find the relationship between runoff from a mountain area and the mean annual precipitation [Waltemeyer, 1994; Maurer and Berger, 1997] or winter precipitation [Hearne and Dewey, 1988] for that mountain area. Three assumptions are implicit in the application of a precipitation-runoff regression method to estimate MFR: (1) all stream runoff recharges at the mountain front (i.e., RET_f and DRO are negligible); (2) interflow (FS_2) in the stream sediments is negligible compared to the stream runoff; and (3) the bedrock in the mountain block is impermeable.

In arid and semiarid areas, most streams at the mountain front are ephemeral, and most water infiltrates into the underlying basin sediments. Does all this water actually recharge the basin aquifer or is some lost to near channel ET? Stream flow at the mountain front can result from intense convective storms during the summer or spring snowmelt. During the snowmelt period, the stream may flow for a few months and, before the start of the growing season, ET loss may be small in comparison to the water that becomes recharge. In summer, the stream only flows for a few hours or days following a storm and ceases between storms. ET loss can be substantial in this situation. Izbicki [2002] estimates that recharge over the 15-km length of Oro Grande Wash in the Mojave Desert, is about one-tenth the average streamflow as reported by Lines [1996]. This suggests that much of the streamflow along the wash is lost by ET.

Besides the surface runoff at the mountain front, some shallow subsurface flow in the channel sediments may contribute to the focused recharge along the channel. How does this subsurface flow (FS_2) recharge compare to the surface runoff? Wroblicky et al. [1998] used numerical modeling to study the cross-sectional area and temporal variation of the lateral hyporheic zone underlying mountain streams in two geologic

environments. Their results suggest that the hyporheic zone can conduct significant water into the mountain front. At Clear Creek (10,000 acres) of the Carson Range, Nevada, [Maurer and Berger, 1997] subsurface flow in the sediments was about 4% of the annual precipitation, and 23% of the surface runoff.

There are also reports that subsurface flow through mountain bedrock can be important [e.g., Maurer and Berger, 1997]. Thus, the three basic assumptions for precipitation runoff regression method are not always reasonable. The first assumption, neglecting RET_f and DRO , leads to an overestimate of MFR, while the last two assumptions, neglecting FS_2 , FR and DR , result in an underestimate. While these biases may compensate for each other, sometimes yielding reasonable estimates of MFR, the precipitation-runoff regression method is conceptually less reasonable than the water balance method. Its empirical nature and bias makes the precipitation-runoff regression method less useful for predicting the effects of climate and land use change, and non-transferable to other regions.

3.3 Chloride Mass Balance Method

The chloride mass balance method is commonly used to estimate groundwater recharge in arid and semiarid areas. Recharge estimates on the basin floor use the chloride profile in the upper 10-15 meters of the vadose zone [Scanlon et al., 1997, 2002; Walvoord et al., 2002]. A different approach must be used in mountains, which have only a few tens of centimeters of soil cover over the bedrock. To estimate MFR, the chloride concentration of groundwater resulting from MFR is compared to that of bulk precipitation, to give the fraction of precipitation which results in recharge [Dettinger, 1989; Maurer and Berger, 1997; Anderholm, 2000]. When integrated over the entire mountain block, this method ignores the complex hydrologic processes within the mountain block. The chloride mass balance method can be expressed as

$$MFR = \frac{C_p P - C_r R}{C_g} \quad (13)$$

where C_g is the chloride concentration in MFR groundwater, P is the precipitation on the mountain, C_p is chloride concentration in bulk precipitation, and R and C_r are respectively the runoff and its chloride concentration at the mountain front.

Major assumptions include: (1) that the bulk precipitation (dry fall and precipitation) is the only source of chloride in the system, and chloride is inert in the system; (2) that the chloride deposition rate and mean annual precipitation rate are accurately estimated and

have been constant over the period of groundwater residence time within the mountain block; and (3) that the measured chloride concentration of groundwater at the mountain front accurately represents the mean value of total groundwater resulting from MFR. Regarding the first assumption, the chloride mass balance method may not work in mountain blocks that have a chloride source in the rocks (e.g., marine-derived sedimentary rock [Claassen and Halm, 1996]) or a chloride source due to anthropogenic activities (e.g., the application of road salt) [Maurer and Berger, 1997]. Failure to account for additional chloride sources leads to an underestimate of MFR. As for the second assumption, the chloride mass balance method only applies to a mountain hydrologic system in equilibrium with current climate conditions. Changes in the average precipitation rate or chloride deposition rates over the period of groundwater residence time within the mountain block may lead to over- or underestimates depending on the nature of the change. The third assumption may lead to an erroneous MFR estimate when there is significant spatial variation in MFR. For example, if the measured MFR does not include some fast-flow deep MBR (that experiences less ET loss), MFR will be underestimated. Specifically, if the water is sampled at mountain front alluvial aquifer, the chloride mass balance more possibly gives MFR_3 , shown in equation (5).

3.4 Darcy's Law

MFR can be estimated using a simple Darcy's law calculation, provided that water equipotential lines and the hydraulic properties of sediments and rocks at the mountain front are known [Hely et al., 1971; Belan and Matlock, 1973; Maurer and Berger, 1997; NRC, 2004]. This method is based only on observation data at the mountain front, avoiding the complex hydrologic processes in the mountain block but potentially missing MFR contribution from some deep MBR flow paths. The accuracy of this method strongly depends on the estimated aquifer hydraulic parameters. Furthermore, a simple calculation of Darcy's law cannot deal with complex geological structures and heterogeneity of the aquifer materials that are often present at the mountain front [Koltermann and Gorelick, 1996].

3.5 Numerical Modeling of Basin Groundwater

Due to the scarcity of surface and subsurface hydrologic data in mountains, MFR is often estimated based on hydrologic modeling of the adjacent basins. Few basin numerical simulations have been extended to the

mountain block [Hibbs and Darling, 1995; Tiedeman et al., 1998b; Manning, 2002; Keating et al., 2003]. In a basin-centered view, MFR is a boundary condition of the basin aquifer and calibration of a numerical model, based on observed data, is used to estimate the amount of MFR [Tiedeman et al., 1998a; Sanford et al., 2000]. In calibration of a groundwater model, recharge rates and hydraulic conductivity are highly correlated and therefore the accuracy of the recharge estimate strongly depends on the availability of hydraulic conductivity data, a parameter that can range over several orders of magnitude. Keating et al. [2003] show that simulation results also depend on the spatial resolution of the hydrographic units used by the model.

Model calibration uniqueness issues are especially important for this approach. In cases where only basin hydraulic head data are available, the ratio of recharge to hydraulic conductivity can be estimated, but not the conductivity itself [Townley and Wilson, 1989; Sanford, 2002; Scanlon et al., 2002]. The addition of flux observations (e.g., baseflow in streams) or groundwater ages can improve uniqueness and the accuracy of the recharge estimate [Sanford, 2002]. For example, the addition of ^{14}C groundwater age data in calibrating a groundwater model of the Albuquerque Basin provided estimated MFR one order of magnitude less than when calibrated without the data [Sanford et al., 2000]. This complementary data could also be used to estimate how recharge rates have varied over the last 30 kyrs [Sanford, 2002]. Manning [2002] shows that groundwater temperature can be another excellent complement to obtain more unique estimates of mountain-block recharge.

3.6 Hydrologic Modeling in Mountains

There have been extensive field observations and many numerical simulations of water flow and solute transport, in both the unsaturated and saturated zones, at Yucca Mountain [Wittwer et al., 1995; Ho et al., 1995; Bagtzoglou et al., 2000; Doughty, 1999; and Flint et al., 2001a]. This attention on a single geological and climatic setting has helped improve our understanding of subsurface hydrologic processes in mountain blocks, yet that understanding remains primitive. The Yucca Mountain studies have not dynamically coupled surface and subsurface processes, and obviously do not address subsurface flow in more humid, high-elevation mountain blocks common throughout the western U.S., or in different mountain geological settings.

Several other groundwater models focus on groundwater flow within the mountain block itself, taking as a

boundary condition percolation into the bedrock from the surface. These are usually models that extend out into the basin (see previous section). For example, Manning [2002] developed a two-dimensional steady state cross-sectional model of the Wasatch Mountains near Salt Lake City, with prescribed recharge into the mountain block, estimated by model calibration (see previous section). One difficulty with this approach is that, under steady flow conditions, the prescribed recharge rate into the block simply becomes the rate of discharge from the block; that is, it becomes the rate of mountain-block recharge (MBR) to the adjacent basin(s).

The many other studies of mountain hydrology considered near surface hydrologic processes, but give little or no attention to deep percolation into the mountain block or to any other deep subsurface processes within the block. These studies have examined a wide variety of settings, sometimes focused at the hillslope scale, and other times at surface watersheds. For example, Kafri and Ben-Asher (1976) used a numerical model to simulate individual rainfall events resulting in percolation through thin mountain soil cover, without further investigating water flow at depth. An interesting contrast are the papers by Chavez et al. [1994a and 1994b], who developed an analytic model with a stochastic estimation procedure to estimate stream runoff and MBR ($=MBR_1$ or possibly MBR_2). This model applied Eagleson's [1978] vegetal equilibrium hypothesis to estimate ET based on vegetation cover. The increasing availability of remote sensing data (e.g., precipitation, fractional vegetation cover, interception, ET, etc.) and high resolution DEMs, together with improved models of vegetation and the surface energy balance, will substantially improve the feasibility of coupled models of the surface and subsurface of mountain blocks.

3.7 Environmental Tracers

Environmental tracers other than chloride have also been intensively used to study water flow and estimate groundwater recharge [Scanlon, 1992; Phillips, 1994; Unnikrishna et al., 1995; Scanlon et al., 1997]. The vertical concentration profile in the thick vadose zone of basin floor gives clues to its history of water flow and groundwater recharge. This approach is sometimes also applied on the mountain hillslopes with good soil covers. Newman et al. [1996] used profiles of chloride and aqueous stable isotopic composition to estimate the evaporation depth and the downward water flux through the soil layers near Los Alamos, New Mexico. However, thin soil cover, root controlled sub-

horizontal soil macropores [e.g., Wilcox et al., 1997], and fractures in the bedrock make profile methods much less useful in mountains than on basin floors. Instead, integrated tracer measures and ratios are used, in which concentrations in MFR components are examined and compared to each other and to precipitation, as we earlier saw with the chloride mass balance method.

The stable isotopic composition of water ($\delta^2\text{H}$ and $\delta^{18}\text{O}$) is the most frequently used environmental tracer. Stable isotope composition of precipitation varies with altitude and season. In the Southwestern United States this is useful for determining the relative importance of winter and summer (monsoon) precipitation for groundwater recharge [Simpson et al., 1972; Cunningham et al., 1998; Winograd et al., 1998; Newman and Duffy, 2001] and for identifying the location of this recharge (mountain vs. basin) [Eastoe et al, this volume; Plummer et al., this volume]. Its not only used in the southwest, Abbott et al. [2000] identified two distinctive recharge zones in a mountain in Vermont, USA, by comparing the stable isotopic compositions of precipitation and groundwater.

Using multiple conservative environmental tracers it is possible to delineate detailed groundwater recharge paths and quantities at a higher spatial resolution. Adar et al. [1990] used environmental tracers (ions and O/H isotopes) combined with a mixing-cell model to quantitatively assess the spatial distribution of MFR. Some radioactive isotopes can be used to obtain groundwater residence times and thus to estimate recharge rates. Guerin [2001] reported fast fracture flow in Yucca Mountain based on tritium and ^{36}Cl data. Recently, dissolved gases in groundwater have been used to estimate the elevation of mountain-block recharge [Manning and Solomon, this volume].

3.8 Other Methods

Temperature profiles in the near surface have been used to estimate water percolation rates under the ephemeral streambeds along the mountain front [Niswonger and Constantz, 2000]. MFR from stream flow infiltration can be calculated, given that the stream timing and saturated channel width are known. Reiter [2000] used the temperature profile at depth in the basin aquifer to estimate the lateral flow rate due to MFR. While this may not provide a quantitative estimate of MFR, it can show evidence of MFR. Manning [2002] found that a heat and fluid flow model calibrated with temperature data from basin wells could place important constraints on MBR. Together, these studies sug-

gest that temperature data could be very useful in quantification of MFR.

In addition to these physical tools, Duffy and colleagues have used time series analysis tools in order to investigate the multiple paths that water can take from the mountain top to the basin floor, with water moving back and forth between the mountain streams and the underlying mountain block. They combine multichannel, singular-spectrum data analysis with low-dimensional models to understand the temporal and spatial characteristics of hydrologic processes in mountains [Shun and Duffy, 1999; Brandes et al., 1998; Newman and Duffy, 2001].

4. MOUNTAIN BLOCK HYDROLOGY

We have seen that most studies of MFR avoid the complexity of hydrologic processes within and on mountain blocks. While near-surface hydrologic processes have been investigated at the hillslope and watershed scales, these studies almost always assume that the bedrock is impermeable. Likewise, some deep bedrock processes have been investigated for locations like Yucca Mountain and the Wasatch Mountains outside of Salt Lake City, but with an assumed percolation rate at the top of the bedrock surface. There are few integrative studies that bring these two fields together for a full view of the mountain hydrologic system.

Meteorological, hydrologic, and ecological conditions vary considerably across a mountain due to the steep altitude gradient. Compared to the basin floor, a mountain block provides less storage for water, and thus is more sensitive to climatic changes. Small variations in atmospheric forcing on the mountain block may cause detectable hydrologic impacts, including the occurrence of springs, the amount and distribution of snow, vegetative cover, and MFR.

Mountain-block hydrology would address these conditions through the integrated study of processes across a variety of temporal and spatial scales. For example, mountain-block recharge to an adjacent basin requires that water enter the block in the first place. This takes place at the hillslope scale, where precipitation is partitioned into deep percolation that enters the mountain block and to other processes. Upon entering the block some water may then discharge to head-water or higher-order streams, and the block may receive other water from the streams, both occurring along a range of shallow and deep flow paths. Water leaves the mountain block as run-off (*RO*, as defined in Section 2) originated as surface runoff from rain and snowmelt, as interflow through the shallow soil cover, or as intrablock discharge of shallow or deep mountain-block

groundwater. In mountain-block hydrology we expect multiple exchanges of water between these different reservoirs, controlled by topography, geology, soil cover and vegetation, and leading to a confusion of response and residence time scales.

Among the many space scales we believe that the two most important for the study of mountain-block hydrology are the hillslope scale and the scale of the entire mountain block. It is at the hillslope scale that water enters the block, a result of partitioning of precipitation. It is the scale of the mountain block that determines surface, shallow (local), and deep (regional) flow pathways, and how they are linked in time and space.

An integrated mountain-block hydrologic model would allow us to predict changes in MFR in response to climate change and variability, vegetation change (including the effects of fire), and direct human impacts. But a sound understanding of mountain-block hydrology has other benefits, such as the accurate prediction of water-related geological hazards in mountains [Bell, 1998]. In this section the components and processes that comprise mountain-block hydrology are discussed, stressing first the hillslope scale and then the entire mountain block. At first reading this review may appear to be a primer on hydrology, but we use it to point out the processes and problems that are especially important in mountain-block hydrology.

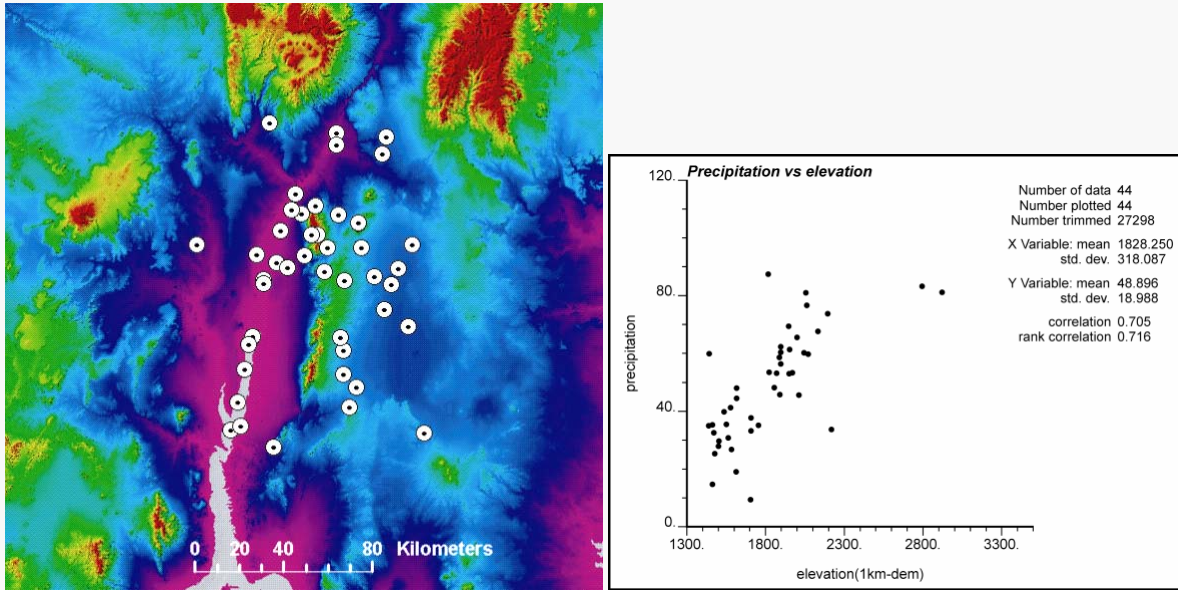
4.1 Precipitation

Precipitation is the only water input to the mountain block. Temporal and spatial variability of precipitation, as well as its effects on hydrologic processes, has been recognized as important [e.g., Goodrich et al., 1995]. Because of topographic complexity and elevation, precipitation varies even more markedly within a mountain block and is difficult to measure. The problem of measurement is exacerbated by a lack of precipitation gauge stations in mountains. Recently, radar has improved the estimation of spatially distributed precipitation; however, beam blockage, underestimation, and non-detection of precipitation are significant problems when radar is used in mountainous terrains [Young et al., 1999].

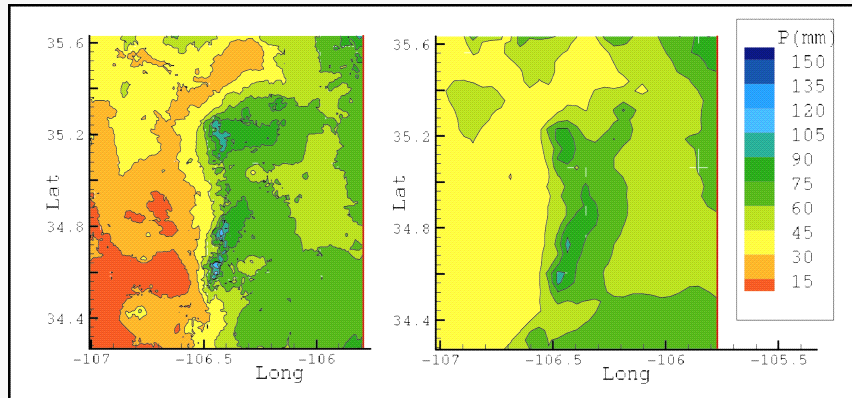
Geostatistics and other tools can be used to synthesize spatial distribution estimates of mountainous precipitation. In addition to rain gauge measurements and radar, secondary variables, such as terrain and atmospheric characteristics that correlate with precipitation, are used to estimate precipitation distribution [Hevesi et al., 1992; Goovaerts, 2000; Kyriakidis et al., 2001].

Box 1 Co-kriging monthly precipitation with terrain altitude

Generally, precipitation in the mountain areas strongly correlates with terrain elevation. The following map shows 44 weather stations in central New Mexico centered on Albuquerque and the Sandia Mountains. Mean July precipitation was obtained from National Climate Data Center, and correlated well with 1 km DEM elevation ($r^2 = 0.71$). Thus, using co-kriging it is possible to use elevation as a secondary variable to better estimate the spatial distribution of precipitation. This method estimates the precipitation distribution with a spatial resolution equal to that of the elevation data used, as evident by comparing the co-kriging estimate using DEM data (shown in the lower left panel) and PRISM estimates [Daly *et al.*, 1994] (lower right panel).



Left: DEM of Sandia Mountains and surrounding areas, and the location of 40 precipitation stations; Right: correlation between the mean July precipitation (mm) with 1km pixel elevation.



Left: Mean July precipitation distribution from co-kriging gauge precipitation and elevation; Right: PrISM precipitation data.

In mountainous terrain precipitation generally correlates well with elevation, providing a strong secondary variable to improve the estimate of spatially distributed precipitation (Box 1).

Accuracy of precipitation gauge measurement is also a significant concern [Goodrich *et al.*, 1995]. Major systematic errors result from the wind's influence on falling precipitation, rain gauge evaporation, and wetting of the walls of rain gauge [Lapin, 1990]. Wind speed is the most important factor in determining gauge error [Nespor and Sevruk, 1999], especially when snow and mixed precipitation falls during the winter [Yang *et al.*, 1999]. Precipitation intensity also contributes to wind-induced measurement error. These problems exist for all gauge measurements but are more challenging in mountains because of complex terrain and extreme weather conditions. Before using rain gauge data it is important to assess the potential magnitude of these errors and make the necessary corrections.

Snow and ice pose another problem to mountain hydrology. In most mountains, winter precipitation falls in the form of snow. Afterwards the snow is redistributed by strong winds and avalanches. This adds to the spatial variability inherited from the snowfall. In western United States, snow water equivalence (SWE) is estimated at over 600 SNOTEL sites, many located in mountainous headwater catchments, but which have poor spatial coverage for any one basin or range. Mountain hydrology requires a more detailed mapping of the spatial statistics and distribution of SWE [Balk and Elder, 2000; Marks *et al.*, 2002], using remote sensing and other tools. Another problem of snow and ice hydrology is the timing of the snowmelt. Solid water is not immediately active in the hydrologic processes; therefore it is necessary to determine when melt occurs and the equivalent liquid volume. In addition to locking water in a solid form, snow cover dramatically changes the surface albedo, altering the energy balance and consequently changing the dynamics of mountain hydrology. Two types of models are currently applied to estimate snowmelt rate: energy-balance models and temperature-index models [Dingman, 1994]. The energy-balance model involves more physical processes and thus requires substantial data [Brock and Arnold, 2000; Marks *et al.*, 2002]. The temperature-index model is less complex, based only on temperature distribution that may be related to topographic data (e.g. DEM).

4.2 Interception

Not all measured precipitation reaches the ground surface; some is lost through interception by the vegetation canopy. In some tropical forests canopy interception may approach 50% of gross precipitation [Schellekens *et al.*, 1999]. In semiarid regions, where vegetation cover is generally sparse, interception is less but may still be as much as 30% of the gross annual rainfall [Llorens and Gallart, 2000; Navar and Bryan, 1990]. Interception losses for the vegetation found in the mountains of the southwestern United States has not been well studied.

A water balance for interception [Crockford and Richardson, 1990] illustrates some of the many processes that must be accounted for before the precipitation reaches the ground,

$$I = E + S = P - TF - SF, \quad (14)$$

where I = interception,
 E = water evaporated during the precipitation event,
 S = water stored in vegetation during the event and evaporated after the event,
 P = gross precipitation,
 TF = throughfall, and
 SF = stem flow.

The magnitude of interception is controlled by vegetation characteristics (areal vegetation density, vegetation type, leaf area index, etc.) and meteorological characteristics (such as precipitation form, intensity and duration, temperature, and wind speed). For continuous precipitation events, water evaporation during the storm is negligible, thus interception approaches the canopy storage capacity. For intermittent events, water evaporated during the storm can be several times the canopy storage capacity, leading to greater interception losses.

4.3 Evapotranspiration

Hydrologically active water (from rainfall and snowmelt) at the ground surface partitions into surface runoff, interflow within the soil and sediments at the surface, ET, and deep percolation through bedrock fractures and matrix. In arid and semiarid mountain environments ET represents the largest water loss from the mountain block [Brandes and Wilcox, 2000]. ET can be estimated from point measurements, as with (1) lysimeters [Gee *et al.*, 1991; Tomlinson, 1996], (2) the Bowen ratio method [Gay, 1991; Stannard, 1991; and Tomlinson, 1996], (3) the eddy-covariance method

[Tanner *et al.*, 1985; Weaver, 1991], or (4) by calculating potential ET derived from point meteorological data or from pan evaporation [Beyazgul *et al.*, 2000; Allen, 2000]. ET can be estimated from areal measurements with instruments such as (5) scintillometers [Meijninger and de Bruin, 2000], or (6) derivation using remote sensing data [Bastiaanssen *et al.*, 1998; Granger *et al.*, 2000; Caparrini and Castelli, 2002; Nishida *et al.*, 2003]. ET can also be derived from (7) hydrologic modeling [Droogers, 2000; Kite, 2000]. Most ET quantification in semiarid and arid regions has been conducted on irrigated agricultural areas. Some ET measurement has been done on naturally vegetated surface areas that are topographically flat and homogenous, or located in lower elevation riparian zones. Few ET quantifications have been attempted in mountainous terrains, partially because measuring ET in complex terrain remains a major technical problem.

Because of the spatial variability of topography, vegetation, and incoming solar radiation in the mountain block, upscaling a few point ET measurements to estimate ET for a whole mountain block makes little sense. However, point data can be synthesized with remote sensing data to provide spatially distributed ET with high spatial resolution at the time remote sensed data is obtained. ET during periods between instantaneous remote sensed events can be estimated by interpolation with the assumption of constant crop coefficients or evaporative fraction [Allen, 2000]. Accuracy of the remote sensing method in the complex terrain of mountainous areas has not been well tested.

Another approach for estimating spatially distributed ET is via distributed hydrologic modeling with system-dependent ET simulations. The ET in the model is constrained by the atmospheric demand (potential ET) and soil water potential (a root-water-uptake model). The root-water-uptake model is a key link to demonstrate the vegetation effects in the hydrologic models. However, little of the data needed to develop these models for natural vegetation exists. A root-water-uptake database of natural vegetation is necessary for rigorous hydrologic modeling of arid and semiarid environments.

4.4 Bedrock Percolation

Seepage into bedrock has been noticed for decades [Chorley, 1978]. However, most hillslope hydrologic studies assume that the bedrock is essentially impermeable and do not allow significant deep percolation. Does much of the water that reaches the soil-bedrock interface partition into deep percolation (into the bedrock), or does it all move down the hillslope, as inter-

flow through the shallow soil that covers the bedrock? That is, under what conditions can we assume essentially impervious bedrock?

We ran some preliminary steady-state numerical simulations of saturated-unsaturated flow on 2-D cross-sections of hypothetical hillslopes. These simulations indicate that bedrock with sufficiently high bulk (fracture and matrix) permeability has the potential to allow for significant deep percolation. For the studied conditions this threshold permeability is 10^{-16} m². Some mountain bedrock, such as a tuff, has a matrix permeability far exceeding this value, whereas intact crystalline rock is essentially impermeable to significant flow through the matrix. When rock is fractured, its permeability can increase by several orders magnitude. For example, Gimmi *et al.* [1997] estimated a permeability of 10^{-18} m² for a crystalline rock that lacks fractures at the investigation scale. Using packer tests, Snow [1979] reported bulk (or composite) permeability at 10^{-14} m² for most of the fractured crystalline rocks he considered. Caine *et al.* [2003] similarly estimated a bulk permeability of 10^{-13} to 10^{-14} m² for intensively fractured crystalline rock in the Turkey Creek Watershed of the Front Range of Colorado. Most of these bulk permeabilities are above the threshold, suggesting that if the water is available, and the rock is fractured, it can accept water at rates high enough to lead to significant deep percolation.

What can prevent water from reaching the soil-bedrock interface? Conditions may be sufficiently arid that not enough water infiltrates into the soil to begin with, or actual ET may be strong enough to remove it before water content at the interface is large enough to cause deep percolation. The main barrier observed in the field [Wilcox *et al.*, 1997], which we have simulated, appears to be the development of strong soil layering. It prevents downward infiltration to the soil-bedrock interface, diverts water to down slope interflow, and stores water for later extraction by transpiration. What can cause water to reach the interface, even in the presence of these conditions? Significant precipitation variability can lead to occasional wet periods with substantial percolation, despite average dry conditions [NRC, 2004]. Surface, soil layer, and bedrock topography can focus water into areas with enhanced flow and enhanced water content at the interface, leading to percolation into the bedrock [Flint *et al.*, 2002b].

Some of the water entering the bedrock may return, mostly via fractures, to streams, the sediments underlying streams, or even to the surface. The rest recharges the bedrock aquifer of the mountain block and eventually becomes MBR. Water in the shallow soil layer that does not percolate into the bedrock will flow in the

soils and sediments toward streams or the mountain front, or be lost to the atmosphere via ET.

4.5 Groundwater Flow in Mountain Blocks

After the water percolates into the bedrock, where does it go and how long does it take to get there? Flow paths with various lengths can occur in mountain blocks (Figure 2b) [Toth, 1963; Keith, 1980]. Local flow paths involve shallow water circulation, transmitting water to nearby streams, or back to the shallow soil cover. Regional flow paths involve deep water circulation in the mountain block, which transmit water to the adjacent basins, i.e., MBR. A study conducted by Tiedeman et al. [1998b] near Mirror Lake, New Hampshire, shows that about 60% of the MFR (or its equivalent) into the basin travels along deeper flow paths in bedrock. Research conducted by Maurer and Berger [1997] in Eagle Valley, Nevada, also showed that more than 40% of water was transmitted through the bedrock in the mountain block to the adjacent basin (Figure 5). Deep water circulation is also evident by persistent water discharge in tunnels and mine openings constructed in some mountains [e.g., Feth, 1964; Marechal, 2000], the drawdown in the overlying aquifer due to the tunnel or mine construction [e.g., Olofsson, 1994], and the geochemical signals in tunnel or mine water [e.g., Olofsson, 1994].

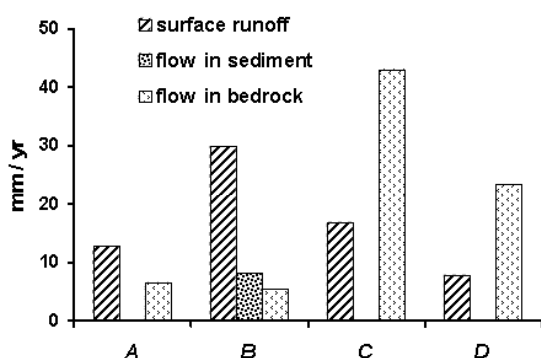


Figure 5. Comparison of water discharge from a mountain block by different paths, summarized from Maurer and Berger [1997] for watersheds tributary to Eagle Valley of western Nevada. The watersheds are: A: C-Hill, B: Kings Canyon, C: Goni, and D: Centennial Park, Carson City, Nevada.

The capacity of a mountain block to transmit subsurface water to the basin depends on the hydrogeological architecture of the mountain block. Heterogeneous and anisotropic hydrologic properties (e.g., permeability), especially those controlled by geologic structural elements like faults, strongly control groundwater flow.

Stratigraphic units with different hydrologic properties may lead to the lateral water movement along some interfaces [Flint et al., 2001b], and even discharge to the surface as springs [Mayo et al., 2003]. In a mountain block with low matrix permeability it is fracture networks, especially zones of intense fractures near faults, that play the major role in transmitting subsurface water. Fractures also connect water in different hydrostratigraphic units, which would otherwise be isolated by lower permeability features [Flint et al., 2001b].

Theoretically, fracture density and aperture, and bedrock matrix porosity, decrease with depth due to an increase of over-burden stress, leading to a decrease of bulk permeability with depth in the mountain block. However, data from some deep boreholes indicates that at least in some cases, fracture distribution does not decrease significantly within the first several thousand meters (Box 2). This presents the possibility that some mountain blocks are permeable to significant depths, allowing deep groundwater circulation and MBR to adjacent basin aquifers. It should be noted that this active deep groundwater circulation can be confined to permeable zones, leaving inactive zones between [Mayo et al., 2003]. In stratified mountain blocks, some low-permeable sub-horizontal formations may impede vertical groundwater movement, and strongly reduce groundwater circulation at depth [Mayo et al., 2003].

Faults play an important role in regulating water flow paths in mountain blocks. Faults are believed to act as both hydraulic conduits and barriers. Faults that developed in brittle crystalline or lithified sedimentary rock have a damage zone and a core zone. Due to intense fracturing, the saturated permeability of the damage zone is several orders of magnitude higher than undamaged rock, whereas the core zone has a permeability several orders of magnitude lower [Evans et al., 1997]. Brittle-rock faults may become a saturated flow hydraulic conduit in a direction parallel to the fault plane, while acting as a hydraulic barrier when perpendicular to the fault. Faults in poorly lithified sediments, including non-welded tuffs, usually develop deformation bands with significantly reduced permeability [Rawling et al., 2001; Ogilvie et al., 2001; Wilson, et al., 2003], instead of fractures, and other features that lead them to become saturated flow hydraulic barriers. The type of deformation also influences the hydraulic effects of faults. For example, brittle-rock faults and fractures developed in structurally extensional domains, like the Basin and Range, may potentially conduct more water than those in structurally contractional domains [Ohlmacher, 1999].

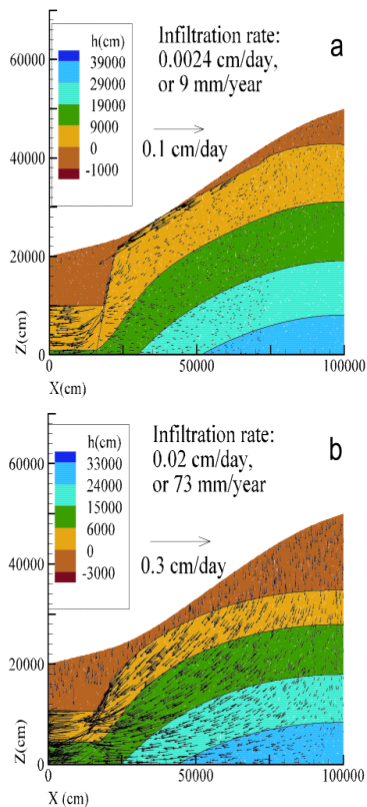


Plate 3. Subsurface saturated-unsaturated flow field within a mountain block bounded by a Basin-and-Range type high-angle normal fault that juxtaposes basin-fill sediments ($k = 4 \times 10^{-12} \text{m}^2$) and the mountain bedrock. (a) A fractured granite (bulk $k = 1 \times 10^{-16} \text{m}^2$) mountain with a 20-meter unloading and weathering zone ($k = 1 \times 10^{-15} \text{m}^2$) at the top. (b) A mountain with highly permeable tuff (bulk $k = 1.6 \times 10^{-15} \text{m}^2$). The magnitude of the vectors is shown next to the legend. These isothermal steady-state simulations have a prescribed uniform infiltration rate at the top boundary (note the different infiltration rates for the two cases), and a constant hydraulic head at the distal end of the basin. Fault internal architecture was not simulated.

Faults may also juxtapose two distinctive hydraulic units and change the groundwater flow field [Titus, 1963; Huntoon, 1983; Haneberg, 1995; Mailloux et al., 1999]. We present simulated subsurface saturated-unsaturated flow fields for two hypothetical mountain blocks in Plate 3. The mountain blocks are juxtaposed with basin-filled sediments by normal faulting. One mountain block is composed of a high (bulk) permeability volcanic tuff and the other of a crystalline granite. The fault zone at the mountain front becomes a focused MFR recharge path for the low-permeability granite mountain block. However, the mountain bounding fault does not have a significant effect on

MFR for a mountain block composed of high-permeability tuff.

In the vadose zone, which comprises a significant portion of many mountain blocks, the presence of capillary forces can dramatically alter the role of faults. Subvertical fractured damage zones still provide enhanced fault-parallel permeability, but only if conditions are sufficiently wet [NRC, 2001]. Instead of barriers, deformation bands enhance fault-parallel permeability under sufficiently dry conditions [Sigda and Wilson, 2003]. Under wetter conditions tilted deformation band [Sigda et al., 2003] and brittle-rock faults redistribute and focus unsaturated flows laterally.

Box 2. Fracture characteristics with depth

Fracture aperture, connectivity, and density are three factors that control the capacity of bedrock to conduct water. Because of unloading and weathering processes, bedrock near the surface tends to have higher fracture density and larger apertures. This unloading fracture zone in granite usually occurs in the top 20 meters and is characterized by fracture planes parallel to the ground surface [Price and Cosgrove, 1990]. Data from 40 bedrock wells at the fractured-rock research site in the Mirror Lake area, New Hampshire indicate that at shallow depths, there appear to be more fractures beneath the hillslope than beneath the valley [Johnson, 1999; Harte, 1997]. Fracture density at this site decreases with depth in the top 100 meters [Johnson, 1999]. However, this trend does not continue with greater depth. Similarly, no decrease in fracturing with depth was observed in the Cajon Pass scientific drill hole, California, at depths between 1800 and 3500 meters [Barton and Zoback, 1992]. Data of hydro-conductive fractures from 227 wells in crystalline rocks in Coastal Maine indicate that there is no evidence that fracture yield or fracture density decrease with depth in at least the upper 180 meters [Loiselle and Evans, 1995]. These studies suggest that for some situations fracture characteristics may not change significantly with depth in mountain blocks, except for the top weathering zone. In fact, fracture flow has been observed at a depth of 2000 meters [Barton et al., 1995]. Fracture networks in the mountain mass may therefore be able to carry water to an elevation below the valley floor and recharge valley aquifer by "hidden paths", as first suggested by Feth [1964].

5. CONCLUSIONS AND FUTURE WORK

MFR is an important and even predominant component of the basin groundwater balance in arid and semiarid areas. Improved understanding of mountain-block hydrology and estimation of MFR is critical for effective basin water management.

MFR is traditionally estimated using basin-centered approaches, such as basin groundwater modeling or by a Darcy's law calculation at mountain fronts. These methods take advantage of data available in the basin, but do not consider the hydrology above the mountain front. Isotopic signatures, temperature, and age of groundwater in basins can improve these basin-centered MFR estimates. Most mountain-centered MFR estimation approaches have been empirical; MFR is estimated by the equations derived from locally instrumented mountain watersheds and the results are difficult to transfer to other areas or to use predictively if climate, vegetation, or land-use changes.

The mountain-block hydrologic system is ripe for new studies that advance understanding, improve observational and synthesis capabilities, and make predictive modeling possible. These studies are currently challenged by the size, complexity, and even the accessibility of mountain systems, as well as the limited availability of historic and paleo hydrologic data. Most recent efforts have been limited to the mountain front or the thin mantle of soil and vegetation overlying the mountains. These studies are insufficient for integrated understanding of hydrologic processes throughout an entire mountain block.

To overcome limited understanding of MFR we propose an integrated mountain-centered approach, yielding high-resolution models and visualization of water movement in mountain blocks. This approach integrates hydrologic processes across time and space scales: water input from precipitation (accounting for snow and interception), surface processes (ET, infiltration, and runoff), interflow through the thin soil layer covering bedrock, deep percolation into fractured bedrock, and water discharged via near-surface and deep flow paths to streams and to the basin at the mountain front. New scientific methods, such as precipitation radar, remote sensing techniques for accessing ET, snow cover, and vegetation cover, and digital elevation models (DEM) and GIS techniques, are all necessary to improve both understanding and characterization. Geophysical techniques for characterizing geology of the mountain block and mountain front, geochemical and paleohydrology approaches (especially environmental tracers) for characterizing water flow paths and residence time distributions, field-sampling campaigns and long-term observations are also required to unravel the complexity of mountain-block hydrologic systems. By reducing the uncertainty of mountain hydrology, and closing the water balance at the hillslope, watershed and mountain block scales, we will move mountain hydrology closer to a predictive science, including predictions of MFR.

Several key questions should be among those pursued in order to develop a better understanding of MFR. These questions are aimed at improved understanding of processes, and the integration of observing strategies and technology with models.

Form, intensity, duration, pattern and redistribution of mountain precipitation. How can better estimates of the space-time distribution of mountain precipitation be obtained? How is hydrologically active water (at the land surface) affected by interception and the redistribution of snow by wind and avalanche? What effect does distribution have on mountain hydrologic processes? In particular, how does precipitation affect deep percolation into bedrock?

Evapotranspiration. What approaches can be most effectively used to improve estimates of the space-time distribution mountain ET? How is mountain ET affected by soil moisture and the nature of soil layering in the thin soil cover? What are appropriate root-water-uptake models and parameterizations for mountain vegetation, soils and rock, and what are appropriate root distributions?

Partitioning to bedrock. At the hillslope scale, how do slope and aspect, bedrock characteristics (matrix and fracture), vegetation cover, and soil cover (type and thickness) affect the partitioning of water between interflow in the thin overlying soil and deep percolation into mountain bedrock?

Water flow through mountain blocks. What is the pattern of shallow and deep flow paths and residence times within typical mountain blocks? How do the hydrogeologic characteristics of mountain blocks, and the stream network geometry, affect these patterns and rates? In particular how do they affect the rates and patterns of flow to streams and to adjacent basins? What is the relative streamflow contribution of surface runoff, the shallow soil cover interflow, and the discharges from shallow to deep subsurface mountain-block flow paths? How does the geologic "architecture" of the mountain block, especially the dominant fracture and fault zones (e.g., mountain bounding faults), influence the relative importance of different pathways to produce MFR, and how does it influence the amount of that recharge? How can we efficiently improve characterization of important hydrogeologic structures within mountain blocks?

Mountain front recharge. What controls the contribution of each component of MFR at the mountain front? In particular, for what conditions is the subsurface (*MBR*) component important? When is flow through streambed sediments (*FS₂*) significant relative to surface runoff (*RO*)? Does all surface runoff arriving at the mountain front actually recharge the adjacent

basin groundwater? If not, what determines the portion of stream runoff at the mountain front that becomes MFR leaving the remainder to ET or downstream flow (DRO)? Which of the existing MFR estimation methods shows the most promise for continued use, when a whole mountain-block hydrology approach is unrealistic or inappropriate? Is there another, simple MFR estimation approach, perhaps relying on new technology, that can be used for these situations?

The integrated mountain-centered hydrologic approach provides estimates of all four components of MFR previously described in equation (1). With varied atmospheric boundary conditions due to climate change or variability, the response of mountain block hydrologic systems to past and potential future conditions can be simulated. Likewise, an improved understanding of how water partitions within the mountain block and mountain front will improve our ability to predict how land use (e.g., grazing, housing developments) and land cover changes (e.g., thickening forests due to fire suppression or fire itself) impact mountain block hydrology and MFR rates. These models can also help detect the impacts of long-term climate change and local disturbances, and help estimate potential hydrogeological hazards due to high-rate snowmelt or intensive summer storms. Although a better understanding of mountain block hydrology has these and other ancillary benefits, our prime motive here is that it will quantify the link between precipitation and recharge to basins bounding the mountain front.

Acknowledgements. Laurel B. Goodwin from New Mexico Institute of Mining and Technology provided assistance in building mountain block archetypes for the simulations in Plate 3. Mary Black and James Hogan provided editorial assistance. Valuable comments from two reviewers are greatly appreciated. This material is based upon work supported by SAHRA (Sustainability of semi-Arid Hydrology and Riparian Areas) under the STC Program of the National Science Foundation, Agreement No. EAR-9876800. PACES, a NASA university research center located at UTEP, provided the remote sensing images.

REFERENCES

- Abbott, M.D., A. Lini, and P.R. Bierman, $\delta^{18}\text{O}$, δD and ^3H measurements constrain groundwater recharge patterns in an upland fractured bedrock aquifer, Vermont, USA, *J. of Hydrology*, 228, 101-112, 2000.
- Adar, E.M., A.S. Issar, and E. Rosenthal, The use of environmental tracers for quantitative assessment of MFRs into an arid basin, in *Water Resources in Mountainous Regions*, vol. 22, edited by A. Parriaux, *MEMOIRES of the 22nd Congress of IAH*, Lausanne, Switzerland, 571-581, 1990.
- Allen, R.G., Using the FAO-56 dual crop coefficient method over an irrigated region as part of an evapotranspiration intercomparison study, *J. of Hydrology*, 229, 27-41, 2000.
- Anderholm, S.K., Mountain-front recharge along the eastern side of the Middle Rio Grande Basin, central New Mexico, *U.S. Geological Survey Water-Resources Investigation Report 00-4010*, 2000.
- Anderson, T.W., G.W. Freethey, and P. Tucci, Geohydrology and water resources of alluvial basins in south central Arizona and parts of adjacent states, *U.S. Geological Survey Professional Paper 1406-B*, 1992.
- Avon, L., and T.J. Durbin, Evaluation of the Maxey-Eakin method for estimating recharge to ground-water basins in Nevada, *Water Resources Bulletin*, 30, 99-111, 1994.
- Bagtzoglou A.C., T.L. Tolley, S.A. Stothoff, and D.R. Turner, Perched aquifers in arid environments and inferences for recharge rates, *IAHS-AISH Publication no.262*, 401-406, 2000.
- Balk, B., and K. Elder, Combining binary decision tree and geostatistical methods to estimate snow distribution in a mountain watershed, *Water Resources Research*, 36, 13-26, 2000.
- Barton, C.A., and M.D. Zoback, Self-similar distribution and properties of macroscopic fractures at depth in crystalline rock in the Cajon Pass Scientific Drill Hole, *J. of Geophysical Research*, 97(B4), 5181-5200, 1992.
- Barton, C.A., M.D. Zoback, and D. Moos, Fluid flow along potentially active faults in crystalline rock, *Geology*, 23, 683-686, 1995.
- Bastiaanssen, W.G.M., M. Menenti, R.A. Feddes, and A.A.M. Holtslag, A remote sensing surface energy balance algorithm for land (SEBAL), *J. of Hydrology*, 212-213, 198-212, 1998.
- Belan, R.A., and W.G. Matlock, Groundwater recharge from a portion of the Santa Catalina Mountains, *Hydrology and Water Resources in Arizona and the Southwest*, 3, 33-40, 1973.
- Bell, F.G., *Environmental Geology: Principles and Practice*, Blackwell Science Ltd, London, 594p, 1998.
- Beyazgul, M., Y. Kayam, and F. Engelsman, F., Estimation methods for crop water requirements in the Gediz Basin of western Turkey, *J. of Hydrology*, 229, 19-26, 2000.
- Brandes D., C. J. Duffy, and J. Cusumano, Stability and damping in a dynamical model of hillslope hydrology, *Water Resources Research*, 34, 3303-3313, 1998.
- Brandes, D., and B.P. Wilcox, Evapotranspiration and soil moisture dynamics on a semiarid ponderosa pine hillslope, *J. of the American Water Resources Association*, 36, 965-974, 2000.
- Brock, B.W. and N.S. Arnold, A spreadsheet-based (Microsoft Excel) point surface energy balance model for glacier and snow melt studies, *Earth Surface Processes and Landforms* 25, 649-658, 2000.
- Caine, J.S., and S.R.A. Tomusiak, Brittle structures of the Turkey Creek Watershed, Colorado Rocky Mountain Front Range: aquifer system characterization and controls on groundwater hydrology, *Geological Society of America Bulletin*, in press, 2003.

- Caparrini, F., and F. Castelli, Remote sensing used to estimate land surface evaporation, *EOS Transactions*, 83(27), 290-291, 2002.
- Chavez, A., S.N. Davis, and S. Sorooshian, Estimation of mountain-front recharge to regional aquifers 1: Development of an analytical hydroclimatic model, *Water Resources Research*, 30(7), 2157-2167, 1994a.
- Chavez, A., S. Sorooshian, and S.N. Davis, Estimation of mountain-front recharge to regional aquifers 2: A maximum likelihood approach incorporation prior information, *Water Resources Research*, 30(7), 2169-2181, 1994b.
- Chorley, R.J., The hillslope hydrological cycle, in *Hillslope Hydrology*, edited by M.J. Kirby, pp. 1-42, John Wiley & Sons, Ltd., New York, 1978.
- Claassen, H.C., and D.R. Halm, Estimation of evapotranspiration or effective moisture in Rocky Mountain watersheds from chloride ion concentrations in stream flow, *Water Resources Research*, 32(2), 363-372, 1996.
- Crockford, R.H., and D.P. Richardson, Partitioning of rainfall in an eucalypt forest and pine plantation in southeastern Australia: III. Determination of the canopy storage capacity of a dry sclerophyll eucalypt forest, *Hydrological Processes*, 4, 157-167, 1990.
- Cunningham, E.E.B., A. Long, C. Eastoe, and R.L. Bassett, Migration of recharge waters downgradient from the Santa Catalina Mountains into the Tucson basin aquifer, Arizona, USA, *Hydrogeology J.*, 6, 94-103, 1998.
- Daly, C., R.P. Neilson, D.L. Phillips, A statistical-topographic model for mapping climatological precipitation over mountain terrain, *J. of Applied Meteorology*, 33, 140-158, 1994.
- Davis, S.N., D.O. Whittemore and J. Fabryka-Martin, Uses of chloride/bromide ratios in studies of potable waters, *Ground Water*, 36, 338-350, 1998.
- Doughty, C., Investigation of conceptual and numerical approaches for evaluating moisture, gas, chemical, and heat transport in fractured unsaturated rock, *J. of Contaminant Hydrology*, 38,(1-3), 69-106, 1999.
- Dettinger, M.D., Reconnaissance estimates of natural recharge to desert basins in Nevada, U.S.A., by using chloride balance calculations, *J. of Hydrology*, 106, 55-78, 1989.
- Dingman, S.L., Snow and snowmelt, in *Physical Hydrology*, edited by S.L. Dingman, pp. 159-209, Prentice Hall, Englewood Cliffs, N.J., 1994.
- Droogers, P., Estimating actual evapotranspiration using a detailed agro-hydrological model, *J. of Hydrology*, 229, 50-58, 2000.
- Eagleson, P.S., Climate, soil and vegetation, 6, Dynamics of the annual water balance, *Water Resources Research*, 4(5), 749-764, 1978.
- Eastoe, C.J., A. Gu and A. Long, The origins, ages and flow paths of groundwater in Tucson Basin: results of a study of multiple isotope systems, this volume.
- Evans, J.P., C.B. Forster, and J.V. Goddard, Permeability of fault-related rocks, and implications for hydraulic structure of fault zones, *J. of Structural Geology*, 19, 1393-1404, 1997.
- Feth, J. H., Hidden recharge, *Ground Water*, 2(4), 14-17, 1964.
- Feth, J.H., D.A. Barker, L.G. Moore, R.J. Brown, and C.E. Veirs, Lake Bonneville: geology and hydrology of the Weber Delta District, including Ogden, Utah, *U. S. Geological Survey Professional Paper 518*, 1966.
- Flint, A.L., L.E. Flint, E.M. Kwicklis, G.S. Bodvarsson, and J.M. Fabryka-Martin, Hydrology of Yucca Mountain, Nevada, *Reviews of Geophysics*, 39, 447-470, 2001a.
- Flint, A.L., L.E. Flint, G.S.W. Bodvarsson, E.M. Kwicklis, and J. Fabryka-Martin, Evolution of the conceptual model of unsaturated zone hydrology at Yucca Mountain, Nevada, *J. of Hydrology*, 247, 1-30, 2001b.
- Flint, A.L., L.E. Flint, J. Blainey, and J.A. Hevesi, Determining regional ground-water recharge in the Great Basin, *Geological Society of America, Rocky Mountain Section, 54th annual Meeting, Abstracts with Programs*, 34(4), 56, 2002a.
- Flint, A.L., L.E. Flint, E. M. Kwicklis, J.T. Fabryka-Martin, and G. S. Bodvarsson, Estimating recharge at Yucca Mountain, Nevada, USA: comparison of methods, *Hydrogeology J.*, 10, 180-204, 2002b.
- Foster, S.S.D., and A. Smith-Carrington, The interpretation of tritium in the Chalk unsaturated zone, *J. of Hydrology*, 46, 343-364, 1980.
- Gay, L.W., Bowen ratio measurements at sites C and L, in *Evapotranspiration measurements of native vegetation, Owens Valley, California, June 1986*, edited by D.H. Wilson, R.J. Reginato, and K.J., Hollet, U.S. Geological Survey Water-Resources Investigation Report 91-4159, 1991.
- Gee, G.W., M.D. Campbell, and S.O. Link, Arid site water balance using monolith weighing lysimeters: Richland, Wash., Battelle, Pacific Northwest Laboratory, *Report PNL-SA-18507*, 1991.
- Gimmi, T., M. Schneebeli, H. Fluhler, H. Wydler, and T. Baer, Field-scale water transport in unsaturated crystalline rock, *Water Resources Research*, 33, 589-598, 1997.
- Goodrich, D.C., J. Faures, D.A. Woolhiser, L.J. Lane, S. Sorooshian, Measurement and analysis of small-scale convective storm rainfall variability, *J. of Hydrology*, 173, 283-308, 1995.
- Goovaerts, P., Geostatistical approaches for incorporating elevation into the spatial interpolation of rainfall, *J. of Hydrology*, 228, 113-129, 2000.
- Granger, R.J., Satellite-derived estimates of evapotranspiration in the Gediz basin, *J. of Hydrology*, 229, 70-76, 2000.
- Guerin, M., Tritium and ³⁶Cl as constraints on fast fracture flow and percolation flux in the unsaturated zone at Yucca Mountain, *J. of Contaminant Hydrology*, 51, 257-288, 2001.
- Haneberg, W.C., Steady state groundwater flow across idealized faults, *Water Resources Research*, 31, 1815-1820, 1995.
- Harte, P.T., Preliminary assessment of the lithologic and hydraulic properties of the glacial drift and shallow bedrock in the Mirror Lake area Grafton County, New Hampshire, *U.S. Geological Survey Open-File Report 96-654A*, 1997.
- Hearne, G.A., and J.D. Dewey, Hydrological analysis of the Rio Grande Basin north of Embudo, New Mexico, Colorado and New Mexico, *U.S. Geological Survey Water-Resources Investigations Report 86-4113*, 1988.
- Hely, A.G., R.W. Mower, and C.A. Harr, Water resources of Salt Lake County, Utah, Utah Dept. of Natural Resour., *Technical Publication No.31*, 1971.

- Hevesi, J.A., J.D. Istok, and A.L. Flint, Precipitation estimation in mountain terrain using multivariate geostatistics, Part I: structure analysis, *J. of Applied Meteorology*, 31 (7), 661-676, 1992.
- Hevesi, J.A., A.L. Flint, and J.D. Istok, Flint, Precipitation estimation in mountain terrain using multivariate geostatistics, Part II: isohyetal maps, *J. of Applied Meteorology*, 31(7), 677-688, 1992.
- Hibbs, B.J., and B.K. Darling, Environmental isotopes and numerical models for understanding aquifer dynamics in southwestern basins, In *Advances in the Development and Use of Models in Water Resources*, edited by T. G. Cleveland, 195-201, Houston, Texas, 1995.
- Ho, C.K., S.J. Altman, and B.W. Arnold, Alternative conceptual models and codes for unsaturated flow in fractured tuff: preliminary assessments for GWTT-95, *Sandia Report Sand 95-1546*, 1995.
- Huntley, D., Groundwater recharge to the aquifers of northern San Luis Valley, Colorado. *Geological Society of America Bulletin*, Part II, 90(8), 1196-1281, 1979.
- Huntoon, P.W., Fault severing of aquifers and other geologically controlled permeability contrasts in the basin-mountain interface, and the implications for ground water recharge to and development from the major artesian basins of Wyoming, Wyoming Water Research Center, *Research Project Technical Completion Report (A-034-WYO)*, 1983.
- Izbicki, J.A., J. Radyk, and R.L. Michel, Water movement through a thick unsaturated zone underlying an intermittent stream in the western Mojave Desert, southern California, USA, *J. of Hydrology*, 238, 194-217, 2000.
- Izbicki, J. A., Geologic and hydrologic controls on the movement of water through a thick, heterogeneous unsaturated zone underlying an intermittent stream in the western Mojave Desert, southern California, *Water Resources Research*, 38, 21-214, 2002.
- Johnson, C.D., Effects of lithology and fracture characteristics on hydraulic properties in crystalline rock: Mirror Lake Research Site, Grafton County, New Hampshire, in U.S. Geological Survey Toxic Substances Hydrology Program, Proceedings of the Technical Meeting, *U.S. Geological Survey Water-Resources Investigations 99-4018c*, Vol 3 of 3, pp. 795-802. 1999.
- Kafri, U., and J. Ben-Asher, Evaluation of recharge through soils in a mountain region: a case study on the Empire and the Sonoita basins, *Hydrology and Water Resources in Arizona and the Southwest*, 6, 203-213, 1976.
- Keating, E.H., V.V. Vesselinov, E. Kwicklis, and Z.Lu, Coupling basin-and site-scale inverse models of the Espanola aquifer, *Ground Water*, 41(2), 200-211, 2003.
- Keith, S.J., Mountain front recharge, in *Regional Recharge Research for Southwest Alluvial Basins*, edited by L.G. Wilson et al., pp. 4-1 to 4-44, Chapter 4, Tucson, University of Arizona, 1980.
- Kite, G.W., Using a basin-scale hydrological model to estimate crop transpiration and soil evaporation, *J. of Hydrology*, 229, 59-69, 2000.
- Koltermann, C.E., and S.M. Gorelick, Heterogeneity in sedimentary deposits: A review of structure-imitating, process-imitating, and descriptive approaches, *Water Resources Research*, 32, 2617-2658, 1996.
- Kyriakidis P.C., J. Kim, and N.L. Miller, Geostatistical mapping of precipitation from rain gauge data using atmospheric and terrain characteristics, *J. of Applied Meteorology*, 40, 1855-1877, 2001.
- Lapin, M., Measurement and processing of atmospheric precipitation in mountainous areas of Slovakia, in *Hydrology of Mountainous Areas*, edited by L. Molnar, pp. 47-56, International Association of Hydrological Sciences, Publication no. 190, 1990.
- Lines, G.C., Ground-water and surface-water relations along the Mojave River, Southern California, *U.S. Geol. Surv. Water Resource Investigation Report 95-4189*, 1996.
- Llorens, P., and F. Gallart, A simplified method for forest water storage capacity measurement, *J. of Hydrology*, 240, 131-144, 2000.
- Loiselle, M., and D. Evans, Fracture density distributions and well yields in Coastal Maine, *Ground Water*, 33, 190-196, 1995.
- Luckman, B., and T. Kavanagh, Impact of climate fluctuations on mountain environments in the Canadian Rockies, *AMBIO*, 29, 371-380, 2002.
- Mailloux, B.J., M. Person, S. Kelley, N. Dunbar, S. Cather, L. Strayer, and P. Hudleston, P., Tectonic controls on the hydrogeology of the Rio Grande Rift, New Mexico, *Water Resources Research*, 35, 2641-2659, 1999.
- Manning, A.H., Using noble gas tracer to investigate mountain-block recharge to an intermountain basin, Dissertation, University of Utah, 2002.
- Manning, A.H., and D.K. Solomon, , Constraining mountain-block recharge to the eastern Salt Lake Valley, Utah with dissolved noble gas and tritium data, this volume.
- Marechal, J.C., The Mont-Blanc massif: identification of a water-bearing important structure, *Houille Blanche-Revue Internationale De Leau*, (2000), no.6, 78-86, 2000.
- Marks, D., A. Winstral, and M. Seyfried, Simulation of terrain and forest shelter effects on patterns of snow deposition, snowmelt and runoff over a semi-arid mountain catchment, *Hydrological Processes*, 16, 3605-3626, 2002.
- Maurer, D.K., and D. L. Berger, Subsurface flow and water yield from watersheds tributary to Eagle Valley hydrographic area, west-central Nevada, *U.S. Geological Survey Water-Resources Investigation Report 97-4191*, 1997.
- Maurer, D.K., D.E. Prudic, D.L. Berger, and C.E. Thodal, Sources of water flowing into basin-fill aquifers underlying Carson City, Nevada, *Geological Society of America, 1999 Annual Meeting, Abstracts with Programs*, 31(7), 87, 1999.
- Maxey, G.B., and T.E. Eakin, Ground water in White River Valley, White Pine, Nye, and Lincoln Counties, Nevada, *Nevada Department of Conservation and Natural Resources Water Resources Bulletin*, no. 8, 1949.
- Mayo, A.L., T.H. Morris, S. Peltier, E.C. Petersen, K. Payne, L.S. Holman, D. Tingey, T. Fogel, B.J. Black, and T.D. Gibbs, Active and inactive groundwater flow systems: Evidence from a stratified, mountainous terrain, *Geological Society of America Bulletin*, 115, 1456-1472, 2003.

- McGlynn, B.L., J.J. McDonnell, and D.D. Brammer, A review of the evolving perceptual model of hillslope flowpaths at the Maimai catchments, New Zealand, *J. of Hydrology*, 257, 1-26, 2002.
- Meijninger, W.M.L., and H.A.R. de Bruin, The sensible heat fluxes over irrigated areas in western Turkey determined with a large aperture scintillometer, *J. of Hydrology*, 229, 42-49, 2000.
- Meinzer, O.E., Outline of ground-water hydrology with definitions, *US Geological Survey Water Supply Paper 494*, 1923.
- National Research Council, *Conceptual Models of Flow and Transport in the Fractured Vadose Zone*, National Research Council, Washington, DC, 382 p., 2001.
- National Research Council, *Groundwater Fluxes Across Interfaces*, National Research Council, Washington, DC, 84 p., 2004.
- Navar, J., and R. Bryan, Interception loss and rainfall redistribution by three semi-arid growing shrubs in northeastern Mexico, *J. of Hydrology*, 115, 51-63, 1990.
- Nespor V., and B. Sevruk, Estimation of wind-induced error of rainfall gauge measurements using a numerical simulation, *J. Atmospheric and Oceanic Technology*, 16(4), 450-464, 1999.
- Newman, B.D., A.R. Campbell, and B.P. Wilcox, Tracer-based studies of soil water movement in semi-arid forest of New Mexico, *J. of Hydrology*, 196, 251-270, 1997.
- Newman, B.D., and C.J. Duffy, Evaluating the hydrogeochemical response of springs using singular spectrum analysis and phase-plane plots, in *New Approaches Characterizing Groundwater Flow*, edited by K.P. Seiler and S. Wöhnlich, v.2, pp. 763-767, A.A. Balkema Publishers, Rotterdam, 2001.
- Nishida, K., R.R. Nemani, S.W. Running, and J.M. Glassy, Remote sensing of land surface evaporation (I) theoretical basis for an operational algorithm, *J. of Geophysical Research D (Atmosphere)*, 108(9), ACL5-1 to -14, 2003.
- Niswonger, R.G., and J. Constantz, Using heat as a tracer to estimate mountain-front recharge at Bear Canyon, Sandia Mountains, New Mexico, *U.S. Geological Survey Middle Rio Grande Basin Study—Proceedings of the Third Annual Workshop, Albuquerque, New Mexico*, 19.76:99-203, 71-72, 2000.
- Ogilvie, S.R., J.M. Orribo, and P.W.J. Glover, The influence of deformation bands upon fluid flow using profile permeametry and positron emission tomography, *Geophysical Research Letters*, 28, 61-64, 2001.
- Ohlmacher, G.C., Structural domains and their potential impact on recharge to intermontane-basin aquifers, *Environmental & Engineering Geoscience*, 5(1), 61-71, 1999.
- Olofsson, B., Flow of groundwater from soil to crystalline rock, *Applied Hydrogeology*, 2(3), 71-83, 1994.
- Peter, D.L., J.M. Buttle, C.H. Taylor, and B.D. LaZerte, Runoff production in a forested, shallow soil, Canadian Shield basin, *Water Resources Research*, 31, 1291-1304, 1995.
- Phillips, F.M., Environmental tracers for water movement in desert soils of the American Southwest, *Soil Science Society of America J.*, 58, 15-24, 1994.
- Plummer L.N., W.E. Sanford, L.M. Bexfield, S.K. Anderholm and E Busenberg, Using geochemical data and aquifer simulation to characterize recharge and groundwater flow in the Middle Rio Grande Basin, New Mexico, this volume.
- Price, N.J., and J.W. Cosgrove, Diapirs, related structures and circular features, in *Analysis of Geological Structures*, pp. 89-122, Cambridge University Press, 1990.
- Puigdefabregas, J., G. del Barrio, M.M. Bore, L. Gutierrez, and A. Sole, Differential responses of hillslope and channel elements to rainfall events in a semi-arid area, *Geomorphology*, 23, 337-351, 1998.
- Rawling, G.C., L.B. Goodwin, and J.L. Wilson, Internal architecture, permeability structure, and hydrologic significance of contrasting fault-zone types, *Geology*, 29, 43-46, 2001.
- Reiter, M., Hydrogeothermal studies in the Albuquerque Basin—preliminary results, *U.S. Geological Survey Open-file Report 00-488*, 44, 2000.
- Russell, L. R., and S. Snelson, Structural style and tectonic evolution of the Albuquerque Basin segment of the Rio Grande rift, in *The Potential of Deep Seismic Profiling for Hydrocarbon Exploration*, edited by B. Pinet and C. Bois, Institut Francais Petrole Research Conference Proceedings, Editions Technip, Paris, 1990.
- Ruxton, B.P., and L. Berry, Weathering profiles and geomorphic position on granite in two tropical regions, *Rev. Geomorphologic Dynamics*, 12, 16-31, 1961.
- Sanford, W.E., L.N. Plummer, D.P. McAda, L.M. Bexfield, and S.K. Anderholm, Estimation of hydrologic parameters for the ground-water model of the Middle Rio Grande Basin using carbon-14 and water-level data. *U.S. Geological Survey Open-file Report 00-488*, 4-6, 2000.
- Sanford, W.E. Recharge and groundwater model: an overview. *Hydrogeology J.*, 10, 110-120, 2002.
- Scanlon, B.R., Evaluation of liquid and vapor water flow in desert soils based on chlorine 36 and tritium tracers and non-isothermal flow simulations, *Water Resources Research*, 28, 285-297, 1992.
- Scanlon, B.R., S.W. Tyler, and P.J. Wierenga, Hydrologic issues in arid, unsaturated systems and implications for contaminant transport, *Reviews of Geophysics*, 35, 461-490, 1997.
- Scanlon, B.R., R.W. Healy and P.G. Cook, Choosing appropriate techniques for quantifying groundwater recharge, *Hydrogeology J.*, 10, 18-39, 2002.
- Schellekens, J., F.N. Scatena, L.A. Bruijnzeel, and A.J. Wickel, Modelling rainfall interception by a lowland tropical rain forest in northeastern Puerto Rico, *J. of Hydrology*, 225, 168-184, 1999.
- Shun, T., and C.J. Duffy, Low-frequency oscillations in precipitation, temperature, and runoff on a west facing mountain front: A hydrogeologic interpretation, *Water Resources Research*, 35, 191-201, 1999.
- Sigda, J.M., and J.L. Wilson, Are faults preferential flow paths through semiarid and arid vadose zone?, *Water Resources Research*, 39, 1225-1240, 2003.
- Sigda, J.M., J. L. Wilson, L.B. Goodwin, and J.L. Conca, J, Conduits to catchments: deformation band faults in arid and semi-arid vadose zone sands, *EOS Transactions*, Abstract T12G-11, 83(47), 2002.

- Simpson, E.S., D.B. Thorud, and I. Friedman, Distinguishing seasonal recharge to groundwater by deuterium analysis in southern Arizona, in *World water balance, Proceedings of the 1970 Reading Symposium*, International Association of Scientific Hydrology – UNESCO-WMO, pp. 623-633, 1972.
- Snow, D.T., Packer injection test data from sites on fractured rock, *LBL (Lawrence Berkeley Laboratory, Energy and Environment Division) Rpt. No. 10080* (197911), 15p., 1979.
- Stannard, D.I., Bowen ratio measurements at sites C and F, in *Evapotranspiration measurements of native vegetation, Owens Valley, California, June 1986*, edited by Wilson, D.H., Reginato, R.J., Hollet, K.J., *U.S. Geological Survey Water-Resources Investigation Report 91-4159*, 1991.
- Tani, M., Runoff generation processes estimated from hydrological observations on a steep forested hillslope with a thin soil layer, *J. of Hydrology*, 200, 84-109, 1997.
- Tanner, B.D., M.S. Tanner, W.A. Dugas, E.C. Campbell, and B.L. Bland, Evaluation of and operational eddy correlation system for evapotranspiration measurements, in *Advances in Evapotranspiration*, American Society of Agricultural Engineers, Publication 14-85, pp 87-99, 1985.
- Tiedeman, C.R., J.M. Kernodle, and D P. McAda, Application of nonlinear-regression methods to a ground-water flow model of the Albuquerque Basin, New Mexico. *U.S. Geological Survey Water-Resources Investigation Report 98-4172*, 90p. 1998a.
- Tiedeman, C.R., D.J. Goode, and P.A. Hsieh, Characterizing a ground water basin in a New England mountain and valley terrain, *Ground Water*, 36, 611-620, 1998b.
- Titus, F.B., Jr., Geology and ground-water conditions in eastern Valencia County, New Mexico, *New Mexico Bureau of Mines and Mineral Resources Ground Water Report*, 7, 1963.
- Tomlinson, S.A., Comparison of Bowen-ratio, eddy-correlation, and weighing–lysimeter evapotranspiration for two sparse-canopy sites in Eastern Washington, *U.S. Geological Survey Water-Resources Investigation Report 96-4081*, 1996.
- Toth, J., A theoretical analysis of groundwater flow in small drainage basins, *J. of Geophysical Research*, 68(16), 4795-4812, 1963.
- Townley, L.R. and J.L. Wilson, Estimation of boundary values and identification of boundary types, *Transport in Porous Media*, 4(6), 567-584, 1989
- Unnikrishna, P.V., J.J. McDonnell, D.G. Tarboton, and C. Kendall, Isotopic analysis of hydrologic processes in a small semiarid catchment, paper presented at International Union of Geodesy and Geophysics; XXI general assembly, Colorado, 237-238, 1995.
- Viviroli, D., R. Weingartner, and B. Messerli, Assessing the hydrological significance of the world's mountains, *Mountain Research and Development*, 23, 32-40, 2003.
- Waltemeyer, S.D., Methods for estimating streamflow at mountain fronts in southern New Mexico, *U.S. Geological Survey Water Resources Investigations Report 93-4213*, 1994.
- Walvoord, M.A. M.A., Plummer, F.M. Phillips, and A.V. Wolfsberg, Deep arid system hydrodynamics 1. Equilibrium states and response times in thick desert vadose zones, *Water Resources Research*, 38(12), 1291-1302, doi:10.1029/2001WR000824, 2002.
- Weaver, H.L., Eddy-correlation measurements at sites C and F, in *Evapotranspiration measurements of native vegetation, Owens Valley, California, June 1986*, edited by D.H. Wilson, R.J. Reginato, and K.J. Hollet, *U.S. Geological Survey Water-Resources Investigation Report 91-4159*, 1991.
- Wilcox, B.P., B.D. Newman, D. Brandes, D.W. Davenport, and K. Reid, Runoff from a semiarid ponderosa pine hillslope in New Mexico, *Water Resources Research*, 33, 2301-2314, 1997.
- Wilson, J.E., L.B. Goodwin, and C.J. Lewis, Deformation bands in nonwelded ignimbrites: Petrophysical controls on fault-zone deformation and evidence of preferential fluid flow, *Geology*, 31(10), 837-840, 2003.
- Winograd, I.J., A.C. Riggs, A.C., and T.B. Coplen, The relative contribution of summer and cool-season precipitation to groundwater recharge, Spring Mountains, Nevada, USA, *Hydrogeology J.*, 6, 77-93, 1998.
- Wittwer, C., G. Chen, G. Bodvarsson, M. Chornack, A. Flint, L. Flint, E. Kwicklis, and R. Spengler, Preliminary development of the LBL/USGS three-dimensional site-scale model of Yucca Mountain, Nevada, U.S. Department of Energy, Rpt. Lawrence Berkeley National Laboratory, LBL 37356, UC0814, 69p., 1995.
- Wroblicky, G.J., M.E. Campana, H.M. Valett, and C.N. Dahm, Seasonal variation in surface-subsurface water exchange and lateral hyporheic area of two stream-aquifer systems, *Water Resources Research*, 34, 317-328, 1998.
- Yang, D., E. Elomaa, A. Tuominen, A. Aaltonen, B. Goodison, T. Gunther, V. Golubev, B. Sevruk, H. Madsen, and J. Milkovic, Wind-induced precipitation undercatch of the Hellmann gauges, *Nordic Hydrology*, 30, 57-80, 1999.
- Young, C. B., C.D. Peters-Lidard, A. Kruger, M.L. Baeck, B. R. Nelson, A.A. Bradley, and J.A. Smith, An evaluation of NEXRAD precipitation estimates in complex terrain. *J. of Geophysical Research*, 104 (D16), 19691-19703, 1999.

Mr. Huade Guan, Dept. of Earth & Environmental Science, New Mexico Tech, Socorro, NM 87801.

Prof. John L. Wilson, Dept. of Earth & Environmental Science, New Mexico Tech, Socorro, NM 87801.